Numerical Option Pricing in CARMA Models

by

Anders Engan

THESIS

for the degree of

MASTER OF SCIENCE

(Master i Modellering og Dataanalyse)

Faculty of Mathematics and Natural Sciences
University of Oslo

December 2013

Det matematisk-naturvitenskapelige fakultet
Universitetet i Oslo

Abstract

This thesis investigates numerical methods for pricing options and forward contracts in Continuous Autoregressive Moving Average (CARMA) models. Via the Feynman-Kac connection between Markovian processes and Partial Differential Equations (PDEs), option and forward prices are obtained as solutions to their respective backward pricing PDEs. Our objective is to devise efficient numerical procedures that accommodate the possibly multi-dimensional CARMA state dynamics. We consider finite difference schemes and propose an Alternating Direction Implicit (ADI) method to deal with two or more spatial dimensions. The schemes are tested in a series of applications to the electricity and temperature markets for various spot models driven by CARMA processes. We discuss specifically CAR(1) and CARMA(2,1) processes, and illustrate how to adapt the finite difference schemes to solve so-called Partial Integro Differential Equations (PIDEs) to obtain forward prices in a jump-diffusion spot electricity model. Analytical results and Monte Carlo are used to benchmark the numerical approximations.

Acknowledgements

I would like to thank Prof. Fred Espen Benth for providing me with an interesting project and directing me towards energy finance. His research has been a profound source of inspiration throughout my studies, and in particular during the writing of this thesis. I am also indebted to my family for their endless support, and to my girlfriend for her unfaltering patience.

Anders Engan
December 2013, Oslo

Contents

Chapter 1

Introduction

The electricity market has experienced a vast deregulation over the past few decades, resulting in organized trade in a variety of contracts. Whereas traditional commodity markets allow trading in the underlying spot, there are no analogous buy-and-hold strategies in electricity, since electric power cannot be stored. Forward type contracts and other derivatives effectively become the primary assets for risk management. Another distinct feature of the electricity market is the intimate connection to weather. Volumes will be heavily temperature dependent and generating hydro and wind power rely on favourable weather conditions. Hydro power production requires sufficient amounts of water in the reservoirs to last through cold winters, and wind power generation is feasible only for a certain range of wind-speeds. Nevertheless, hedging adverse weather in an economical sense was until recently an exclusive insurance affair. The organized trade in weather derivatives has produced a new breed of financial contracts providing protection against prescribed weather events. In contrast to standard insurance agreements, an actual weather-related loss need to be incurred, making the weather contracts a vital contribution to energy risk management. Of course, these contracts can be used to hedge any exposure to weather risk, or merely serve as an independent asset class and an opportunity to speculate. Over-The-Counter (OTC) trading in futures and options on weather variables was established in 1999 at the Chicago Mercantile Exchange (CME), which is still the only established market for weather derivatives. The CME offers a product suite based on temperature, precipitation and hurricane indices. Despite several attempts, there is yet no market place for trading in wind speed derivatives. Wind speed modeling is nonetheless subject to research at the prospects of a shift towards renewable energy sources.

Much work has been done in order to capture the *stylized facts* of electricity markets. The most notable characteristics are mean-reversion, extreme volatility, frequent abrupt price spikes and seasonality. In a modeling framework, sudden jumps followed by a fast mean-reversion can be attributed a Lévy-driven Ornstein-Uhlenbeck process, or more generally a Lévy-driven CARMA process. In this thesis, we propose to model spot electricity as the sum of a Gaussian and a non-Gaussian Ornstein-Uhlenbeck process. Such a specification is not necessarily an optimal statistical

description, but has sufficient generality and forward prices in closed-form, so we can validate our numerical scheme in the presence of jumps. Weather variables such as temperature and wind also exhibit mean-reversion and can be modeled by the class of Gaussian CARMA processes. We give a summary on temperature modeling and pricing for contracts traded at the CME. However, our primary interest is in solving PDEs for European and American options on spot temperature in a Gaussian CARMA model. Such options do not exist as exchange-traded contracts, but may be of interest as OTC agreements.

Solving PDEs in CARMA models is (to the best of our knowledge) uncharted territory. Our contribution in this thesis is to highlight apparent numerical difficulties stemming from the multi-dimensional CARMA state dynamics. The thesis is organized as follows. Chapter 2 recapitulates finite difference methods with emphasis on two dimensional parabolic PDEs; in chapter 3 we give an introduction to American options and review the numerical algorithms due to Longstaff and Schwartz and Brennan and Schwartz; chapter 4 provides the necessary background on Lévy driven CARMA processes; chapter 5 discusses electricity and temperature markets, whereupon we present the numerical results; finally, in chapter 6 we provide concluding remarks on the numerical results. Some mathematical arguments and selected Matlab code are given in the appendix.

Chapter 2

Finite Difference Methods

In this chapter we review the finite difference method (FDM) for solving PDEs. This includes a brief account of central notions and theoretical properties. We introduce some basic schemes and present the alternating direction implicit (ADI) method devised for solving multi-dimensional problems.

2.1 General Theory

PDEs are widespread in theoretical and applied mathematics. Unfortunately, most equations encountered in practice do not allow for closed-form solutions and extensive research has resulted in numerous numerical remedies. One of the prevailing techniques is the finite difference method, which is probably the simplest and most intuitive approach. By truncating Taylor series, we can approximate the differential quotients in the PDEs by their corresponding finite difference quotients. The discretized equation is reduced to an algebraic system that can be solved by techniques from numerical linear algebra.

The objective in this thesis is to numerically solve multi-dimensional linear parabolic PDEs of the form

$$\frac{\partial u}{\partial t} = \sum_{i=1}^{n} b_i(t,\mathbf{x})\frac{\partial u}{\partial x_i} + \sum_{i,j=1}^{n} a_{i,j}(t,\mathbf{x})\frac{\partial^2 u}{\partial x_i \partial x_j} + c(t,\mathbf{x})u, \quad t > 0, \tag{2.1}$$

for $n = 1, 2$. This type of equations arise naturally in option pricing problems due to the intimate connection between moments of Markovian diffusions and second-order parabolic PDEs, which is verified by the Feynman-Kac formula[1]. The physical problem is often posed in an infinite spatial domain, in which case it must be localized to a finite region $\Omega \in \mathbb{R}^n$ with boundary $\partial\Omega$, where numerical computations are conducted. When localizing the domain we need to impose artificial boundary

[1] There exist generalizations of the Feynman-Kac formula establishing connections between more general stochastic processes and PIDEs.

conditions to make computations feasible. These are usually of one or a mixture of the following types:

- *Dirichlet*: $u(t, \mathbf{x}) = g(t, \mathbf{x})$
- *Neumann*: $\frac{\partial u(t,\mathbf{x})}{\partial \mathbf{n}} = g(t, \mathbf{x})$
- *Linear*: $\frac{\partial^2 u(t,\mathbf{x})}{\partial \mathbf{n}^2} = 0$

for $\mathbf{x} \in \partial\Omega$ and $t > 0$, where $\mathbf{n}$ is the unit vector normal to the boundary[2]. In the sequel we study the following initial boundary value problem (IBVP)

$$\begin{cases} \frac{\partial u}{\partial t} = \mathcal{L}u, \quad \forall (t, \mathbf{x}) \in (0, T] \times \Omega \\ u(0, \mathbf{x}) = f(\mathbf{x}), \quad \forall \mathbf{x} \in \overline{\Omega}. \\ u(t, \mathbf{x}) = g(t, \mathbf{x}), \quad \forall \mathbf{x} \in (0, T] \times \partial\Omega. \end{cases} \tag{2.2}$$

For simplicity of exposition we will assume homogeneous Dirichlet boundary conditions, that is $g \equiv 0$. Here $\mathcal{L}$ is the differential operator $\mathcal{L} : C^{1,2} \to \mathbb{R}$

$$(\mathcal{L}u)(t, \mathbf{x}) = \sum_{i=1}^{n} b_i(t, \mathbf{x}) \frac{\partial u}{\partial x_i} + \sum_{i,j=1}^{n} a_{i,j}(t, \mathbf{x}) \frac{\partial^2 u}{\partial x_i \partial x_j} + c(t, \mathbf{x})u, \tag{2.3}$$

where the diffusion coefficients $a_{i,j}$ are restricted to the set of positive functions, c is a negative function and the convection coefficients b_i can take any sign.

2.1.1 Finite Differences

We are particularly interested in the two-dimensional IBVP with time-independent coefficients

$$\begin{cases} \frac{\partial u}{\partial t} = b_1(x, y) \frac{\partial u}{\partial x} + b_2(x, y) \frac{\partial u}{\partial y} + a_1(x, y) \frac{\partial^2 u}{\partial x^2} + a_2(x, y) \frac{\partial^2 u}{\partial y^2} + c(x, y)u, \\ \quad \forall (t, x, y) \in (0, T] \times \Omega \\ u(0, x, y) = f(x, y), \quad \forall x, y \in \overline{\Omega}, \\ u(t, x, y) = 0, \quad \forall x, y \in (0, T] \times \partial\Omega, \end{cases} \tag{2.4}$$

which will serve as a model problem for multi-dimensional PDEs. We suppose that our problem is confined to the finite spatial domain

$$\Omega = (X_{min}, X_{max}) \times (Y_{min}, Y_{max}) .$$

[2]

$$\frac{\partial u}{\partial \mathbf{n}} = \mathbf{n} \cdot \nabla u$$

The domain is discretized in time and space to form a computational grid

$$\{(t_n, x_i, y_j), \quad n = 0, ..., N,\ i = 0, ..., I,\ j = 0, ..., J\},$$

on which we want to obtain approximations to the unknown function. Here

$$\begin{aligned} t_n &= n\Delta t, & \Delta t &= \frac{T}{N}, \\ x_i &= x_0 + i\Delta x, & \Delta x &= \frac{x_I - x_0}{I}, \\ y_j &= y_0 + j\Delta y, & \Delta y &= \frac{y_J - y_0}{J}, \end{aligned}$$

and $(X_{min}, X_{max}) \times (Y_{min}, Y_{max}) = (x_0, x_I) \times (y_0, y_J)$. We will occasionally employ the following difference operators to facilitate a compact notation (x denotes a generic spatial variable):

Forward Differences

$$\Delta_{+t} u(t, x) \triangleq u(t + \Delta t, x) - u(t, x) \tag{2.5}$$

$$\Delta_{+x} u(t, x) \triangleq u(t, x + \Delta x) - u(t, x) \tag{2.6}$$

Backward Differences

$$\Delta_{-t} u(t, x) \triangleq u(t, x) - u(t - \Delta t, x) \tag{2.7}$$

$$\Delta_{-x} u(t, x) \triangleq u(t, x, y) - u(t, x - \Delta x) \tag{2.8}$$

Central Differences

$$\delta_t u(t, x) \triangleq u(t + \frac{1}{2}\Delta t, x) - u(t - \frac{1}{2}\Delta t, x) \tag{2.9}$$

$$\delta_x u(t, x) \triangleq u(t, x + \frac{1}{2}\Delta x) - u(t, x - \frac{1}{2}\Delta x) \tag{2.10}$$

Double Interval Central Differences

$$\begin{aligned} \Delta_{0x} u(t, x) &\triangleq \frac{1}{2} \left[\Delta_{+x} u(t, x) + \Delta_{-x} u(t, x)\right] \\ &= \frac{1}{2} \left[u(t, x + \Delta x) - u(t, x - \Delta x))\right] \end{aligned} \tag{2.11}$$

Second order Central Differences

$$\delta_x^2 u(t, x) \triangleq u(t, x + \Delta x) - 2u(t, x) + u(t, x - \Delta x) \tag{2.12}$$

Note that the second-order central difference operator is obtained by operating the central difference operator twice.

Assuming that the unknown function is smooth, Taylor expansions read

$$\begin{aligned}\Delta_{+t}u(t,x) &= u(t+\Delta t,x)-u(t,x)\\ &= u_t\Delta t+\frac{1}{2}u_{tt}(\Delta t)^2+\frac{1}{6}u_{ttt}(\Delta t)^3+...\end{aligned} \tag{2.13}$$

$$\begin{aligned}\Delta_{-t}u(t,x) &= u(t,x)-u(t-\Delta t,x)\\ &= u_t\Delta t-\frac{1}{2}u_{tt}(\Delta t)^2+\frac{1}{6}u_t(\Delta t)^3-...\end{aligned} \tag{2.14}$$

$$\begin{aligned}\Delta_{+x}u(t,x) &= u(t,x+\Delta x)-u(t,x)\\ &= u_x\Delta x+\frac{1}{2}u_{xx}(\Delta x)^2+\frac{1}{6}u_{xxx}(\Delta x)^3+...\end{aligned} \tag{2.15}$$

$$\begin{aligned}\Delta_{-x}u(t,x) &= u(t,x)-u(t,x-\Delta x)\\ &= u_x\Delta x-\frac{1}{2}u_{xx}(\Delta x)^2+\frac{1}{6}u_{xxx}(\Delta x)^3-...\end{aligned} \tag{2.16}$$

Moreover

$$\Delta_{0x}u(t,x) = u_x\Delta x+\frac{1}{6}u_{xxx}(\Delta x)^3+... \tag{2.17}$$

and similarly

$$\begin{aligned}\delta_x^2u(t,x) &= u(t,x+\Delta x)-2u(t,x)+u(t,x-\Delta x)\\ &= u_{xx}(\Delta x)^2+\frac{1}{12}u_{xxxx}(\Delta x)^4+...\end{aligned} \tag{2.18}$$

We deduce that[3]

$$\frac{\Delta_{+t}u(t,x)}{\Delta t} = u_t+\mathcal{O}\left(\Delta t\right) \tag{2.19}$$

$$\frac{\Delta_{-t}u(t,x)}{\Delta t} = u_t+\mathcal{O}\left(\Delta t\right) \tag{2.20}$$

$$\frac{\Delta_{+x}u(t,x)}{\Delta x} = u_x+\mathcal{O}\left(\Delta x\right) \tag{2.21}$$

$$\frac{\Delta_{-x}u(t,x)}{\Delta x} = u_x+\mathcal{O}\left(\Delta x\right) \tag{2.22}$$

$$\frac{\Delta_{0x}u(t,x)}{\Delta x} = u_x+\mathcal{O}\left((\Delta x)^2\right) \tag{2.23}$$

$$\frac{\delta_x^2u(t,x)}{(\Delta x)^2} = u_{xx}+\mathcal{O}\left((\Delta x)^2\right) \tag{2.24}$$

[3]Recall that $f(x)$ is $\mathcal{O}(g)$ if there exists a positive constant C such that

$$\sup_{x\in\mathbb{R}}\frac{|f(x)|}{|g(x)|}\leq C.$$

The finite difference approximations can now be obtained by truncating the higher order terms.

Denote the approximate solution to problem (2.4) by $U_{i,j}^n$, in the sense that $U_{i,j}^n \approx u(t_n, x_i, y_j)$. A finite difference scheme is obtained by equating the difference approximations in time and space

$$\frac{\Delta_{\pm t} U_{i,j}^n}{\Delta t} = L U_{i,j}^n, \quad 1 \le i \le I-1,\ 1 \le j \le J-1, \tag{2.25}$$

Here, L is a generic difference operator. (2.25) can equivalently be stated in succinct matrix notation as

$$\mathbf{L}\mathbf{U}^{n+1} = \mathbf{B}\mathbf{U}^n, \quad n = 0, ..., N-1, \tag{2.26}$$

where $\mathbf{L}$ and $\mathbf{B}$ are $(I-1)(J-1) \times (I-1)(J-1)$ matrices, and $\mathbf{U}^s$ is the $(I-1)(J-1)$ vector

$$\left(U_{1,1}^s, ..., U_{1,J-1}^s, ..., U_{I,1}^s, ..., U_{I-1,J-1}^s\right)^T, \quad s = n, n+1.$$

2.1.2 Stability, Consistency and Convergence

In order to evaluate the adequacy of the numerical schemes, we need to introduce some pertinent notions.

Definition 2.27 (Truncation Error)**.** *The truncation error of the difference scheme (2.25) is defined as*

$$T(t,x,y) \triangleq \frac{\Delta_{\pm t} u(t,x,y)}{\Delta t} - Lu(t,x,y), \tag{2.28}$$

i.e. the residual from replacing the grid function U by u in the difference equation.

Definition 2.29 (Consistence)**.** *If*

$$T(t,x,y) \to 0 \quad as \quad \Delta t,\ \Delta x,\ \Delta y \to 0 \tag{2.30}$$

for any $(t,x,y) \in (0,T] \times (X_{min}, X_{max}) \times (Y_{min}, Y_{max})$, then we say that the scheme is consistent with the PDE (?).

Definition 2.31 (Convergence)**.** *If for any point $(t,x,y) \in (0,T] \times (X_{min}, X_{max}) \times (Y_{min}, Y_{max})$,*

$$t_n \to t,\ x_i \to x,\ y_j \to y \Rightarrow U_{i,j}^n \to u(t,x,y), \tag{2.32}$$

i.e. the numerical solution at node (t_n, x_i, y_j) approximates the exact solution as the grid gets denser, then we say that the scheme is convergent.

Definition 2.33 (Order of accuracy)**.** *If for a sufficiently smooth solution u,*

$$T(t,x,y) \leq C\left((\Delta t)^p + (\Delta x)^q + (\Delta y)^r\right), \quad \text{as} \quad \Delta t,\ \Delta x,\ \Delta y \to 0, \tag{2.34}$$

where p, q and r are the largest possible integers, then we say that the scheme has pth, qth and rth order of accuracy in Δt, Δx and Δy respectively.

Definition 2.35 (Stability)**.** *A difference scheme is stable with respect to the norm $\|\cdot\|$ if there exist positive constants Δx_0, Δy_0, Δt_0 and non-negative constants K and β such that*

$$\|\mathbf{U}^n\| \leq K e^{\beta t} \|\mathbf{U}^0\|, \tag{2.36}$$

for $0 < \Delta t \leq \Delta t_0$, $0 < \Delta x \leq \Delta x_0$, $0 < \Delta y \leq \Delta y_0$.

This definition of stability allows the solution to grow with time, although not with the number of time steps. There are various definitions of stability in the literature, where equation (2.36) with $\beta = 0$ is frequently encountered. This choice ensures that the solution remains bounded. However, we need to allow for exponential growth in schemes where $c(x,y)$ is non-zero. In practice, stability is often investigated using the Fourier technique due to Von-Neumann (consult the appendix for a brief outline).

Definition 2.37 (Von-Neumann Stability)**.** *Let λ be the amplification factor associated with a difference scheme. The scheme is stable in the Von Neumann sense if there exist positive constants Δx_0, Δy_0, Δt_0 and C such that*

$$|\lambda| \leq 1 + C\Delta t, \tag{2.38}$$

for $0 < \Delta t \leq \Delta t_0$, $0 < \Delta x \leq \Delta x_0$, $0 < \Delta y \leq \Delta y_0$.

Proving convergence can be very difficult in general. The so-called Lax Equivalence theorem connects consistence, convergence and stability, and asserts that for "nice" schemes it suffice to investigate stability.

Definition 2.39 (Well-posedness)**.** *A PDE is well-posed if the solution exists and depends continuously on the initial condition and boundary conditions.*

Theorem 2.40 (Lax Equivalence Theorem)**.** *A consistent difference scheme for a well-posed linear initial-value problem is convergent if and only if it is stable.*

2.2 Explicit Scheme

The most obvious choice of discretization of problem (2.4) is to employ the forward difference in time and central differences in space. With reference to the node (t_n, x_i, y_j) this amounts to

$$\frac{\Delta_{+t}U^n_{i,j}}{\Delta t} = b_{1,i,j}\frac{\Delta_{0x}U^n_{i,j}}{\Delta x} + b_{2,i,j}\frac{\Delta_{0y}U^n_{i,j}}{\Delta y} + a_{1,i,j}\frac{\delta^2_{0x}U^n_{i,j}}{(\Delta x)^2} + a_{2,i,j}\frac{\delta^2_{0y}U^n_{i,j}}{(\Delta y)^2} + c_{i,j}U^n_{i,j}. \quad (2.41)$$

The resulting scheme is one in which $U^{n+1}_{i,j}$ depends explicitly on the previous time step. Expanding equation (2.41) and collecting terms gives

$$\begin{aligned} U^{n+1}_{i,j} = {} & U^n_{i,j}(1 + \Delta t c_{i,j} - 2\mu_1 a_{1,i,j} - 2\mu_2 a_{2,i,j}) + U^n_{i-1,j}(\mu_1 a_{1,i,j} - \frac{\gamma_1}{2}b_{1,i,j}) + \\ & U^n_{i+1,j}(\mu_1 a_{1,i,j} + \frac{\gamma_1}{2}b_{1,i,j}) + U^n_{i,j-1}(\mu_2 a_{2,i,j} + \frac{\gamma_2}{2}b_{2,i,j}) + U^n_{i,j+1}(\mu_2 a_{2,i,j} + \frac{\gamma_2}{2}b_{2,i,j}), \end{aligned} \quad (2.42)$$

where $\gamma_1 = \frac{\Delta t}{\Delta x}$, $\gamma_2 = \frac{\Delta t}{\Delta y}$, $\mu_1 = \frac{\Delta t}{(\Delta x)^2}$ and $\mu_2 = \frac{\Delta t}{(\Delta y)^2}$. Although the explicit scheme is very tractable, it is rarely used in practice due to its poor stability properties. In the appendix we verify consistency, convergence and conditional stability[4]. Moreover, the scheme is shown to be first order accurate in time and second order in space.

2.3 Implicit Scheme

A backward difference in time and central differences in space yield

$$\frac{\Delta_{-t}U^{n+1}_{i,j}}{\Delta t} = b_{1,i,j}\frac{\Delta_{0x}U^{n+1}_{i,j}}{\Delta x} + b_{2,i,j}\frac{\Delta_{0y}U^{n+1}_{i,j}}{\Delta y} + a_{1,i,j}\frac{\delta^2_{x}U^{n+1}_{i,j}}{(\Delta x)^2} + a_{2,i,j}\frac{\delta^2_{y}U^{n+1}_{i,j}}{(\Delta y)^2} + c_{i,j}U^{n+1}_{i,j}, \quad (2.43)$$

and the approximation at $n+1$ is given implicitly in terms of the past time layer. Now we must solve a system comprised by equations of the form

$$\begin{aligned} & U^{n+1}_{i,j}(1 - \Delta t c_{i,j} + 2\mu_1 a_{1,i,j} + 2\mu_2 a_{2,i,j}) - U^{n+1}_{i-1,j}(\mu_1 a_{1,i,j} - \frac{\gamma_1}{2}b_{1,i,j}) - \\ & U^{n+1}_{i+1,j}(\mu_1 a_{1,i,j} + \frac{\gamma_1}{2}b_{1,i,j}) - U^{n+1}_{i,j-1}(\mu_2 a_{2,i,j} + \frac{\gamma_2}{2}b_{2,i,j)} - U^{n+1}_{i,j+1}(\mu_2 a_{2,i,j} + \frac{\gamma_2}{2}b_{2,i,j}) = U^n_{i,j}. \end{aligned} \quad (2.44)$$

This scheme will be unconditionally stable.

[4]Stability depending on the time-step size.

2.4 The θ-Method

If we take a convex combination of the explicit and implicit discretization we obtain

$$\begin{aligned}\frac{\Delta_{+t}U_{i,j}^n}{\Delta t} =&\theta\left[b_{1,i,j}\frac{\Delta_{0x}U_{i,j}^{n+1}}{\Delta x}+b_{2,i,j}\frac{\Delta_{0y}U_{i,j}^{n+1}}{\Delta y}+a_{1,i,j}\frac{\delta_x^2U_{i,j}^{n+1}}{(\Delta x)^2}+a_{2,i,j}\frac{\delta_y^2U_{i,j}^{n+1}}{(\Delta y)^2}+c_{i,j}U_{i,j}^{n+1}\right]\\ &(1-\theta)\left[b_{1,i,j}\frac{\Delta_{0x}U_{i,j}^{n}}{\Delta x}+b_{2,i,j}\frac{\Delta_{0y}U_{i,j}^{n}}{\Delta y}+a_{1,i,j}\frac{\delta_x^2U_{i,j}^{n}}{(\Delta x)^2}+a_{2,i,j}\frac{\delta_y^2U_{i,j}^{n}}{(\Delta y)^2}+c_{i,j}U_{i,j}^{n}\right],\end{aligned} \tag{2.45}$$

where $\theta \in [0,1]$.

- $\theta = 0 \Rightarrow$ the explicit scheme
- $\theta = \frac{1}{2} \Rightarrow$ the Crank-Nicolson scheme
- $\theta = 1 \Rightarrow$ the implicit scheme

Unconditional stability for the Crank-Nicolson and the implicit scheme for the one-dimensional case is verified in the appendix. Moreover, one may show that the Crank-Nicolson scheme is second-order accurate in time and space. For $\theta \neq \frac{1}{2}$ we have the usual first-order accuracy in time and second-order accuracy in space.

2.5 Alternating Direction Implicit (ADI)

Writing the θ-scheme in matrix form results in the system

$$(\mathbf{I}-\theta\Delta t\mathbf{L})\,\mathbf{U}^{n+1}=(\mathbf{I}+(1-\theta)\Delta t\mathbf{L})\,\mathbf{U}^n,\quad 0\le n\le N-1, \tag{2.46}$$

where $\mathbf{L}$ is a $(I-1)(J-1)\times(I-1)(J-1)$ matrix. We have seen that the explicit scheme is only conditionally stable, placing severe restrictions on the grid spacing and time-step size. Whereas implicit schemes such as Crank-Nicolson are unconditionally stable, they require solving the system of equations (2.46), which in general is very labourious in two or more dimensions. Also, forming the coefficient matrix $\mathbf{L}$ is not a trivial task.

ADI is a time splitting method developed to reduce multi-dimensional problems involving large systems of equations to smaller sub-problems treating each spatial direction separately. The various ADI schemes are easy to implement and are computationally efficient due to the tridiagonal structure produced in each time step. Next, we discuss two basic ADI schemes for solving problem (4).

In the remainder of this section the following notation will be useful,

$$\begin{aligned} A_1 &= b_1(x,y)\frac{\Delta_{0x}}{\Delta x} + a_1(x,y)\frac{\delta_x^2}{(\Delta x)^2} + \frac{1}{2}c(x,y) \\ A_2 &= b_2(x,y)\frac{\Delta_{0y}}{\Delta y} + a_2(x,y)\frac{\delta_y^2}{(\Delta y)^2} + \frac{1}{2}c(x,y). \end{aligned} \tag{2.47}$$

Note that $c(x,y)$ has been evenly distributed in the x and y direction. Denote by

$$R = \{(x_i, y_j) : \quad i = 1, ..., I-1,\ j = 1, ..., J-1\},$$

the interior of the spatial grid with boundary $\partial R = \partial R_x \cup \partial R_y \cup \partial R_{xy}$,

$$\begin{aligned} \partial R_x &= \{(x_i, y_j) : \quad i = 0, I,\ j = 1, ..., J-1\} \\ \partial R_y &= \{(x_i, y_j) : \quad i = 1, ..., I-1,\ j = 0, J\} \\ \partial R_{xy} &= \{(x_i, y_j) : \quad i = 0, I,\ j = 0, J\}. \end{aligned}$$

In terms of A_1 and A_2 and with reference to the node (t_n, x_i, y_j), we can write the θ-scheme as

$$(1 - \theta\Delta t A_1 - \theta\Delta t A_2)\, U_{i,j}^{n+1} = (1 + (1-\theta)\Delta t A_1 + (1-\theta)\Delta t A_2)\, U_{i,j}^{n}.$$

For $\theta = \frac{1}{2}$ we recover the Crank-Nicolson scheme which is second-order in time and space, and we may add any $\mathcal{O}((\Delta t)^2 + (\Delta x)^2 + (\Delta y)^2)$-term without altering the order of accuracy. Hence, the factorization

$$\left(1 - \frac{1}{2}\Delta t A_1\right)\left(1 - \frac{1}{2}\Delta t A_2\right) U_{i,j}^{n+1} = \left(1 + \frac{1}{2}\Delta t A_1\right)\left(1 + \frac{1}{2}\Delta t A_2\right) U_{i,j}^{n}, \tag{2.48}$$

remains second-order in time and space[5] This is called an *approximate factorization scheme*. The idea is to employ a time splitting to enhance efficiency while retaining stability and consistency.

The Peaceman-Rachford Scheme

The first ADI scheme for solving two dimensional parabolic problems was proposed by Peaceman and Rachford [36] in 1955:

$$\begin{aligned} \frac{U_{i,j}^{n+\frac{1}{2}} - U_{i,j}^{n}}{\Delta t} &= \frac{1}{2}\left(A_1 U_{i,j}^{n+\frac{1}{2}} + A_2 U_{i,j}^{n}\right) \\ \frac{U_{i,j}^{n+1} - U_{i,j}^{n+\frac{1}{2}}}{\Delta t} &= \frac{1}{2}\left(A_1 U_{i,j}^{n+\frac{1}{2}} + A_2 U_{i,j}^{n+1}\right) \end{aligned} \tag{2.49}$$

[5]We are effectively adding the term $\frac{1}{4}(\Delta t)^2 A_1 A_2 (U_{i,j}^{n+1} - U_{i,j}^{n})$ which is $\mathcal{O}((\Delta t)^3)$ since

$$U_{i,j}^{n+1} - U_{i,j}^{n} = \mathcal{O}(\Delta t).$$

The scheme is implicit in x and explicit in y in the first step, then implicit in y and explicit in x in the second step. We introduce the intermediate half-step value $U_{i,j}^{n+\frac{1}{2}}$, which is not necessarily an approximation to the solution, but rather a computational artifact. The scheme (2.49) can be rewritten in the following convenient form

$$\begin{cases} \left(1 - \frac{1}{2}\Delta t A_1\right) U_{i,j}^{n+\frac{1}{2}} &= \left(1 + \frac{1}{2}\Delta t A_2\right) U_{i,j}^{n} \\ \left(1 - \frac{1}{2}\Delta t A_2\right) U_{i,j}^{n+1} &= \left(1 + \frac{1}{2}\Delta t A_1\right) U_{i,j}^{n+\frac{1}{2}}. \end{cases} \tag{2.50}$$

Boundary conditions for $U_{i,j}^{n+\frac{1}{2}}$ are obtained by subtracting the second equation from the first in (2.49), which yields

$$U_{i,j}^{n+\frac{1}{2}} = \frac{1}{2}\left(1 + \Delta t A_2\right) U_{i,j}^{n} + \frac{1}{2}\left(1 - \Delta t A_2\right) U_{i,j}^{n+1}, \ i,j \in \partial R, \tag{2.51}$$

In the case of *time-homogeneous* boundary conditions $g_{i,j}^{n} = g_{i,j}, \ i,j \in \partial R$, we have that $U_{i,j}^{n+\frac{1}{2}} = g_{i,j}, \ i,j \in \partial R$.

Assuming that the operators $\left(1 - \frac{1}{2}\Delta t A_1\right)$ and $\left(1 + \frac{1}{2}\Delta t A_1\right)$ commute,

$$\begin{aligned} \left(1 - \frac{1}{2}\Delta t A_1\right)\left(1 - \frac{1}{2}\Delta t A_2\right) U_{i,j}^{n+1} &= \left(1 - \frac{1}{2}\Delta t A_1\right)\left(1 + \frac{1}{2}\Delta t A_1\right) U_{i,j}^{n+\frac{1}{2}} \\ &= \left(1 + \frac{1}{2}\Delta t A_1\right)\left(1 - \frac{1}{2}\Delta t A_1\right) U_{i,j}^{n+\frac{1}{2}} \\ &= \left(1 + \frac{1}{2}\Delta t A_1\right)\left(1 + \frac{1}{2}\Delta t A_2\right) U_{i,j}^{n+\frac{1}{2}} \end{aligned}$$

We see that (2.48) and (2.50) are in fact equivalent.

The Peaceman-Rachford scheme is essentially a predictor-corrector method. The error due to the explicit term in the first step is offset by the decrease in error in the second step. It can be verified that each sub-step is conditionally stable, whereas the scheme as a whole is unconditionally stable. Unfortunately, the extension to three dimensions is only conditionally stable and the scheme is not recommended for equations with mixed-derivatives.

The Douglas Scheme

Douglas and Rachford [] proposed another ADI scheme:

$$\begin{aligned} \frac{U_{i,j}^{*} - U_{i,j}^{n}}{\Delta t} &= \theta A_1 U_{i,j}^{*} + (1-\theta) A_1 U_{i,j}^{n} + A_2 U_{i,j}^{n} \\ \frac{U_{i,j}^{n+1} - U_{i,j}^{*}}{\Delta t} &= \theta A_2 \left(U_{i,j}^{n+1} - U_{i,j}^{n}\right) \end{aligned} \tag{2.52}$$

This particular form is taken from [], where the unconditional stability is proved for general parabolic two dimensional convection-diffusion equations. See also [] and [] for applications to the Heston stochastic volatility model. We can rewrite the above in computational form

$$\begin{cases} (1-\theta\Delta t A_1)\, U^*_{i,j} & = (1+(1-\theta)\Delta t A_1 + \Delta t A_2)\, U^n_{i,j} \\ (1-\theta\Delta t A_2)\, U^{n+1}_{i,j} & = U^*_{i,j} - \theta\Delta t A_2 U^n_{i,j} \end{cases} \tag{2.53}$$

Boundary conditions for $U^*_{i,j}$ are obtained from the second equation in (2.52) as

$$U^*_{i,j} = (1-\theta\Delta t A_2)U^{n+1}_{i,j} + \theta\Delta t A_2 U^n_{i,j},\ i,j \in \partial R. \tag{2.54}$$

Time-homogeneous boundary conditions are tackled as in the Peaceman-Rachford scheme.
The Douglas ADI scheme is second order accurate in time and space for $\theta = \frac{1}{2}$ and unconditionally stable for $\theta \geq \frac{1}{2}$. It is straightforward (in principle, at least) to extend the scheme to three dimensions, and it can be applied to problems with mixed derivatives.

ADI Implementation

We will now illustrate how to implement the Douglas ADI scheme[6]. We can write (2.53) as the system

$$\begin{aligned} \mathbf{A}_{1,j}\mathbf{U}^*_j &= \mathbf{r}_j, \quad j = 1, ..., J-1, \\ \mathbf{A}_{2,i}\mathbf{U}^{n+1}_i &= \mathbf{r}_i, \quad i = 1, ..., I-1, \end{aligned} \tag{2.55}$$

where

$$\mathbf{A}_{1,j} = \begin{pmatrix} \beta_{1,j} & \eta_{1,j} & & & & 0 \\ \alpha_{2,j} & \beta_{2,j} & \eta_{2,j} & & & \\ & \ddots & \ddots & \ddots & & \\ & & \ddots & \ddots & \ddots & \\ & & & \alpha_{I-2,j} & \beta_{I-2,j} & \eta_{I-2,j} \\ 0 & & & & \alpha_{I-1,j} & \beta_{I-1,j} \end{pmatrix}, \quad \mathbf{U}^*_j = \begin{pmatrix} U^*_{1,j} \\ U^*_{2,j} \\ \vdots \\ \\ \vdots \\ U^*_{I-2,j} \\ U^*_{I-1,j} \end{pmatrix},$$

$$\mathbf{r}_j = \begin{pmatrix} (1+(1-\theta)\Delta t A_1 + \Delta t A_2)\, U^n_{1,j} - \alpha_{1,j} U^*_{0,j} \\ (1+(1-\theta)\Delta t A_1 + \Delta t A_2)\, U^n_{2,j} \\ \vdots \\ \\ \vdots \\ (1+(1-\theta)\Delta t A_1 + \Delta t A_2)\, U^n_{I-2,j} \\ (1+(1-\theta)\Delta t A_1 + \Delta t A_2)\, U^n_{I-1,j} - \eta_{I,j} U^*_{I,j} \end{pmatrix},$$

[6]Implementation of the Douglas-Rachford scheme is identical.

and

$$\alpha_{i,j} = -\theta\left(\mu_1 a_{1,i,j} - \frac{\gamma_1}{2} b_{1,i,j}\right)$$
$$\beta_{i,j} = 1 - \theta\left(-2\mu_1 a_{1,i,j} + \Delta t \frac{c_{i,j}}{2}\right)$$
$$\eta_{i,j} = -\theta\left(\mu_1 a_{1,i,j} + \frac{\gamma_1}{2} b_{1,i,j}\right).$$

Similarly,

$$\mathbf{A}_{2,i} = \begin{pmatrix} \beta_{1,i} & \eta_{1,i} & & & & 0 \\ \alpha_{2,i} & \beta_{2,i} & \eta_{2,i} & & & \\ & \ddots & \ddots & \ddots & & \\ & & \ddots & \ddots & \ddots & \\ & & & \alpha_{J-2,i} & \beta_{J-2,i} & \eta_{J-1,j} \\ 0 & & & & \alpha_{J-1,i} & \beta_{J-1,i} \end{pmatrix}, \quad \mathbf{U}_i^{n+1} = \begin{pmatrix} U_{i,1}^{n+1} \\ U_{i,2}^{n+1} \\ \vdots \\ \vdots \\ U_{i,J-2}^{n+1} \\ U_{i,J-1}^{n+1} \end{pmatrix},$$

$$\mathbf{r}_i = \begin{pmatrix} U_{i,1}^* - \theta\Delta t A_2 U_{i,1}^n - \alpha_{1,i} U_{i,0}^{n+1} \\ U_{i,2}^* - \theta\Delta t A_2 U_{i,2}^n \\ \vdots \\ \vdots \\ U_{i,J-2}^* - \theta\Delta t A_2 U_{i,J-2}^n \\ U_{i,J-1}^* - \theta\Delta t A_2 U_{i,J-1}^n - \eta_{J,i} U_{i,J}^{n+1} \end{pmatrix},$$

and here there is a new set of α, β and η,

$$\alpha_{j,i} = -\theta\left(\mu_2 a_{2,i,j} - \frac{\gamma_2}{2} b_{2,i,j}\right)$$
$$\beta_{j,i} = 1 - \theta\left(-2\mu_2 a_{2,i,j} + \Delta t \frac{c_{i,j}}{2}\right)$$
$$\eta_{j,i} = -\theta\left(\mu_2 a_{2,i,j} + \frac{\gamma_2}{2} b_{2,i,j}\right).$$

We use the tridiagonal matrix algorithm (given in the appendix) to solve the systems of equations. In the case of constant coefficients these matrices can be LU-factorized to facilitate an even more efficient algorithm.

2.6 Example - The Heston Stochastic Volatility Model

Option pricing in models with multiple stochastic factors is of great interest in financial engineering. The ADI method is a prudent alternative to Monte Carlo techniques for modestly sized state spaces. We briefly illustrate an application of the Douglas ADI scheme to the two-dimensional Heston stochastic volatility model, comprised by the system of stochastic differential equations

$$\begin{cases} dS_t &= rS_t dt + \sqrt{V_t} S_t dW_t^1 \\ dV_t &= \kappa\left(\eta - V_t\right) dt + \sigma\sqrt{V_t} dW_t^2. \end{cases} \tag{2.56}$$

In brief, the asset price follows a geometric Brownian motion and the volatility is assumed to be a so-called Cox-Ingersoll-Ross process, known from interest rate modeling. The model is stated with respect to an equivalent martingale measure[7], under which $(W_t^1)_{0\leq t\leq T}$ and $(W_t^2)_{0\leq t\leq T}$ are Wiener processes with correlation factor $\rho \in [-1, 1]$. The parameter $\kappa > 0$ is the mean-reversion rate, $\eta > 0$ is the long-term mean and $\sigma > 0$ the so-called volatility-of-volatility. For $T > 0$, we would like to find the price of a European call option with maturity T and strik price K. Under the Feynman-kac representation the option price satisfies the backward PDE

$$\frac{\partial u}{\partial t} + \frac{1}{2}s^2 v\frac{\partial^2 u}{\partial s^2} + \frac{1}{2}\sigma^2 v\frac{\partial^2 u}{\partial v^2} + \rho\sigma sv\frac{\partial^2 u}{\partial s\partial v} + rs\frac{\partial u}{\partial s} + \kappa(\eta - v)\frac{\partial u}{\partial v} - ru = 0, \tag{2.57}$$

subject to the terminal condition $u(T, s, v) = (s - K)^+$. The spatial variables are localized to the bounded domain $(0, V_{\max}) \times (0, S_{\max})$ which is complemented by the following mixture of Dirichlet and Neumann boundary conditions:

$$u(t, s, v) = 0, \quad s = 0 \tag{2.58}$$

$$\frac{\partial u(t, s, v)}{\partial s} = 1, \quad s = S_{\max} \tag{2.59}$$

$$\frac{\partial u}{\partial t} + rs\frac{\partial u}{\partial s} + \kappa\eta\frac{\partial u}{\partial v} - ru = 0, \quad v = 0 \tag{2.60}$$

$$u(t, s, v) = s, \quad v = V_{\max} \tag{2.61}$$

We use the change of variable $\tau = T - t$ to transform the problem into an IBVP, whereupon we define $\bar{u}(\tau, x) = u(T - \tau, x)$ such that

$$\begin{aligned} \frac{\partial u(t, x)}{\partial t} &= \frac{\partial \tau}{\partial t}\frac{\partial u(T - \tau, x)}{\partial \tau} \\ &= -\frac{\partial \bar{u}(\tau, x)}{\partial \tau}. \end{aligned}$$

Denote by U the grid function approximating $\bar{u}$. In order to proceed, we must find a finite difference quotient for the mixed-derivative term. A Taylor expansion suggests the following second-order approximation

$$\frac{\delta_{sv}^2 U_{i,j}^n}{\Delta s \Delta v} = \frac{U_{i+1,j+1}^n + U_{i-1,j-1}^n - U_{i-1,j+1}^n - U_{i+1,j-1}^n}{4\Delta s \Delta v}. \tag{2.62}$$

[7] We assume there is no market price of risk associated with volatility.

To preserve the tridiagonal structure, the mixed-derivative will be treated explicitly. Consequently, we obtain the Douglas ADI scheme

$$\begin{cases} (1-\theta\Delta t A_1)\, U^*_{i,j} = (1 + A_0 + (1-\theta)\Delta t A_1 + \Delta t A_2)\, U^n_{i,j} \\ (1-\theta\Delta t A_2)\, U^{n+1}_{i,j} = U^*_{i,j} - \theta\Delta t A_2 U^n_{i,j}, \end{cases} \tag{2.63}$$

with

$$A_0 U^n_{i,j} = \rho\sigma v s \frac{\delta^2_{s,v}}{\Delta s \Delta v} \tag{2.64}$$

$$A_1 U^n_{i,j} = s_i v_j \frac{\Delta_{0s}}{\Delta s} U^n_{i,j} + \frac{1}{2} s_i^2 v_j \frac{\delta^2_s}{(\Delta s)^2} U^n_{i,j} - \frac{1}{2} r U^n_{i,j} \tag{2.65}$$

$$A_2 U^n_{i,j} = \kappa(\eta - v_j) \frac{\Delta_{0s}}{\Delta s} U^n_{i,j} + \frac{1}{2}\sigma^2 v_j \frac{\delta^2_s}{(\Delta s)^2} U^n_{i,j} - \frac{1}{2} r U^n_{i,j} \tag{2.66}$$

Neumann boundaries are implemented using second-order one-sided approximations of the derivatives.

r	σ	ρ	κ	η	T	K
0.03	0.3	0.8	2	0.2	1	100

Figure 2.1 shows the exact solution for the set of parameters given above. The corresponding finite difference approximation is displayed in figure 2.2. The *maximum absolute error*, defined as

$$\mathrm{MAE}(N) \triangleq \max_{0\le i\le I, 0\le j\le J} |\bar{u}(\tau_N, x_i, x_j) - U^N_{i,j}|, \tag{2.67}$$

has been plotted in figure 2.3 as a function of the number of time steps for two distinct sets of spatial bounds. Errors caused by the artificial conditions at $S_{\max}$ and $V_{\max}$ are lost if the region of interest is sufficiently far from the boundaries.

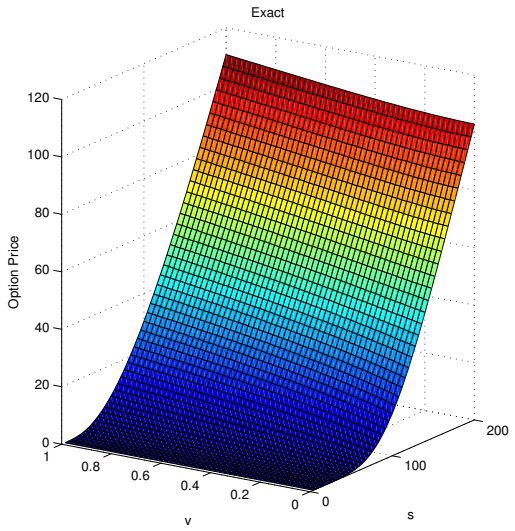

Figure 2.1: European call option price in the Heston model. Exact.

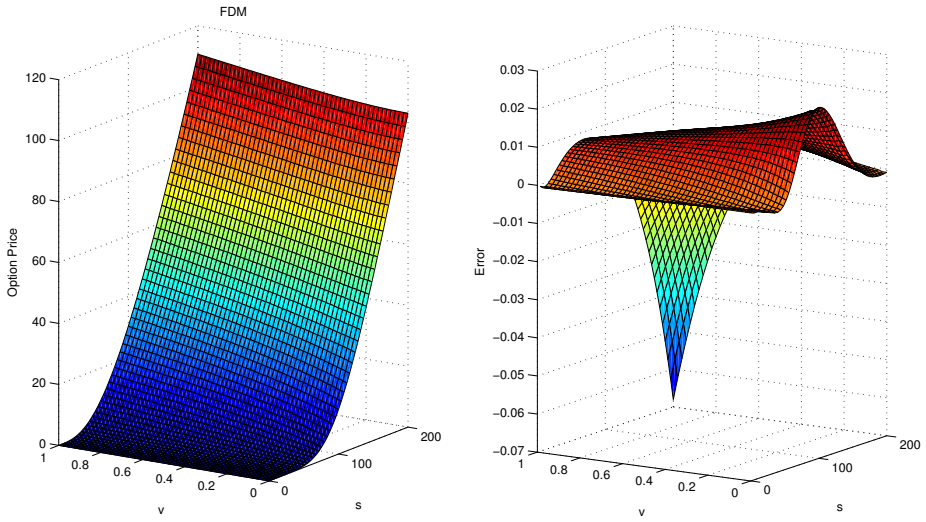

Figure 2.2: European call option price in the Heston model computed with Douglas ADI.

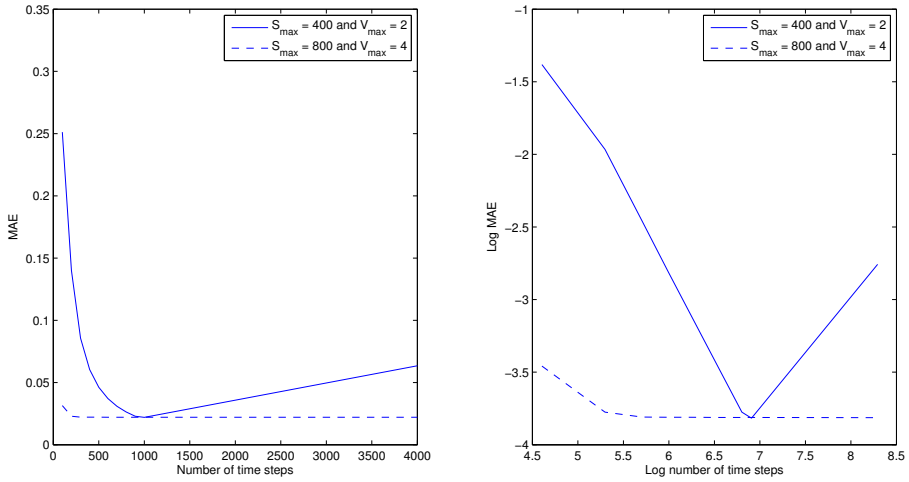

Figure 2.3: MAE for the European call option price in the Heston model.

Chapter 3

American Options

Whereas European options can be exercised only at a single expiration date, American style options allow for early exercise at any instant before maturity. The early exercise feature complicates the problem of pricing considerably, and the lack of closed-form solutions has resulted in a rich theory seeking to characterize the option price.

The results in the first part of this chapter are adapted from Myneni [35] and Elliott and Kopp [24].

3.1 General theory

We assume we are working in a complete[1] filtered probability space $(\Omega, \mathcal{F}, \{\mathcal{F}_t\}_{t\geq 0}, \mathbb{Q})$ satisfying the *usual conditions*, in the sense that

- $\mathcal{F}_0$ contains all the $\mathbb{Q}$-null sets of $\mathcal{F}$
- $\mathcal{F}_t = \cap_{u>t}\mathcal{F}_u$ for all $0 \leq t < \infty$, i.e. the filtration is right continuous

The usual conditions will be standing assumptions in all of what follows.

We consider a Black-Scholes market modeled by a bond (or savings account) evolving according to the differential equation

$$dR_t = rR_t dt, \quad R_0 = 1, \tag{3.1}$$

and a risky asset, which under an equivalent martingale measure $\mathbb{Q}$ is governed by the stochastic differential equation

$$\frac{dS_t}{S_t} = rdt + \sigma dW_t, \quad S_0 = x. \tag{3.2}$$

[1] That is, all subsets of measurable $\mathbb{Q}$-null sets are measurable.

Here, $(W_t)_{t\geq 0}$ is a Wiener process on $(\Omega, \mathcal{F}, \{\mathcal{F}_t\}_{t\geq 0}, \mathbb{Q})$. Let

$$\phi(t) = (\phi_2(t), \phi_2(t)),$$

be a trading strategy in the market, i.e. a set of progressively measurable processes with

$$\int_0^T |\phi_1(t)|dt + \int_0^T (\phi_2(t)S(t))^2 dt < \infty, \quad \text{a.s.} \tag{3.3}$$

where $\phi_1(t)$ and $\phi_2(t)$ denote the holdings at time t in the bond and the risky asset, respectively. We let $(C_t)_{t\geq 0}$ be a continuous and non-decreasing consumption process with $C_0 = 0$ a.s. Define the corresponding wealth process by

$$V_t(\phi) = \phi_1(t)R_t + \phi_2(t)S_t. \tag{3.4}$$

The triple (ϕ_1, ϕ_2, C) is said to be *admissible* if $V_t(\phi)$ is self-financing[2], i.e.

$$V_t(\phi) = \phi_1(0)R_0 + \phi_2(0)S_0 + \int_0^t \phi_1(u)dR(u) + \int_0^t \phi_2(u)dS(u) - C_t, \quad t \in [0, T], \tag{3.5}$$

and

$$\mathbb{E}_{\mathbb{Q}}\left[\int_0^T \phi_2^2(t)S_t^2\right] < \infty. \tag{3.6}$$

Assumption (3.6) acts as a credit constraint by limiting the amount held in the risky asset. Substituting for the dynamics of the risky asset yields

$$V_t(\phi) = V_0(\phi) + \int_0^t rV_u(\phi) + \int_0^t \sigma\phi_2(u)S_u dW_u - C_t. \tag{3.7}$$

Recall that a stopping time with respect to our probability space is a random variable $\tau(\omega)$ for $\omega \in \Omega$, such that the event $\{\tau(\omega) \leq t\}$ belongs to the sigma-algebra $\mathcal{F}_t$. Denote by $\mathcal{T}_{t,T}$ the set of all stopping times with values in $[t, T]$. In order to straddle the American put option price, we need the following lemma.

Lemma 3.8. *The process*

$$X_t \triangleq \operatorname*{ess\,sup}_{\tau\in\mathcal{T}_{t,T}} E_Q\left[e^{-r(\tau-t)}\left(K - S_\tau\right)^+ |\mathcal{F}_t\right], \quad t \in [0, T], \tag{3.9}$$

is a wealth process. That is, there exists an an admissible triple (ϕ_1, ϕ_2, C) corresponding to (3.9).

[2]The self-financing condition states that a change in the wealth process results enirely from net gains or losses.

Proof. The proof is taken from Myneni [35] and Elliott and Kopp [24].
Let

$$J_t = \operatorname*{ess\,sup}_{\tau \in \mathcal{T}_{t,T}} E_Q \left[e^{-r\tau} \left(K - S_\tau \right)^+ | \mathcal{F}_t \right]. \quad t \in [0, T],$$

J is the *Snell envelope*, i.e. the smallest supermartingale dominating the discounted payoff. Moreover, J is càdlàg, regular and of class D, thus has the Doob-Meyer decomposition

$$J_t = M_t - A_t,$$

as the difference of a right continuous martingale M, and a unique, predictable continuous and non-decreasing process A, with $A_0 = 0$. From the martingale representation property under $\mathbb{Q}$ (Karatzas and Shreve [30]) we know that there exists a progressively measurable process ψ such that

$$\begin{aligned} &\int_0^T \psi_u^2 du < \infty, \quad \text{a.s.} \\ &M_t = J_0 + \int_0^t \psi_u dW_u, \quad \forall t \in [0, T] \quad \text{a.s.} \end{aligned}$$

Clearly, $X_t = e^{rt} J_t$ with dynamics given by

$$dX_t = re^{rt} J_t dt + e^{rt} \psi_t dW_t - e^{rt} dA_t.$$

Hence, if we put $\phi_1 = J_t - \psi_t \sigma^{-1}$, $\phi_2(t) = e^{rt} \psi_t \sigma^{-1} S_t^{-1}$ and $C_t = \int_0^t e^{rt} dA_t$, we have that $X_t = V_t(\phi)$. □

Obivously, X_t hedges the American put option in the sense that

$$\begin{aligned} X_t &\geq (K - S_t)^+, \quad t \in [0, T) \quad \text{a.s.} \\ X_T &= (K - S_T)^+, \quad \text{a.s.} \end{aligned}$$

The optimal stopping time for the interval $[t, T]$ was charatcerized by El Karoui, and is known to be the first time J hits the discounted payoff. That is,

$$\rho_t = \inf \left\{ u \in [t, T] : J_u = e^{-ru} (K - S_u)^+ \right\}. \tag{3.10}$$

We are now ready to derive the arbitrage-free price of the option.

Theorem 3.11. *If V_0 is the initial value of the American put option, then*

$$V_0 = X_0 \tag{3.12}$$

is necessary and sufficient for there to be no arbitrage.

Proof. The proof is taken from Myneni [35] and Elliott and Kopp [24].
Suppose the option trades for the price $V_0 > X_0$ at time $t = 0$, and denote by (β_1, β_2, c) the trading strategy generating the wealth process X_t. Consider the strategy $(\phi_1, \phi_2, \phi_3, C)$ in the bond, stock and the option respectively, augmented by the early exercise policy $\tau \in \mathcal{T}_{0,T}$, given by

$$\begin{aligned}
\phi_1(t) &= \begin{cases} \beta_1(t), & t \in [0, \tau], \\ \beta_1(\tau) + \beta_2(\tau) R_\tau^{-1} S_\tau - R_\tau^{-1}(K - S_\tau)^+, & t \in (\tau, T], \end{cases} \\
\phi_2(t) &= \beta_2(t) \mathbf{1}_{[0,\tau]}(t), \\
\phi_3(t) &= -\mathbf{1}_{[0,\tau]}(t), \\
C_t &= c_{t \wedge \tau}.
\end{aligned}$$

Since X_t hedges the option,

$$\beta_1(\tau) R_\tau + \beta_2(\tau) S_\tau \geq (K - S_\tau)^+ \quad \text{a.s.},$$

from which it follows that $\phi_1(T) R_T \geq 0$ a.s. But since

$$\phi_1(0) + \phi_2(0) S_0 + \phi_3(0) V_0 = X_0 - V_0 < 0,$$

following $(\phi_1, \phi_2, \phi_3, C)$ leads to an arbitrage.
Now, suppose $V_0 < X_0$ at time $t = 0$. With the same trading strategy in X as above, and with exercise policy ρ_0 as defined in (3.10),

$$\begin{aligned}
\phi_1(t) &= \begin{cases} -\beta_1(t), & t \in [0, \rho_0], \\ -\beta_1(\rho_0) - \beta_2(\rho_0) R_{\rho_0}^{-1} S_{\rho_0} + R_{\rho_0}^{-1}(K - S_{\rho_0})^+, & t \in (\rho_0, T], \end{cases} \\
\phi_2(t) &= -\beta_2(t) \mathbf{1}_{[0,\rho_0]}(t), \\
\phi_3(t) &= \mathbf{1}_{[0,\rho_0]}(t), \\
C_t &= -c_{t \wedge \rho_0},
\end{aligned}$$

One can show that the stopped process $X_{t \wedge \rho_t}$ is a martingale (see [31] theorem 2.3.1). Therefore $c \equiv 0$ on $[0, \rho_0]$ and by definition of ρ_0

$$\beta_1(\rho_0) R_{\rho_0} + \beta_2(\rho_0) S_{\rho_0} = (K - S_{\rho_0})^+, \quad \text{a.s.}$$

Hence $\phi_1(T) R_T = 0$ a.s. and

$$\phi_1(0) + \phi_2(0) S_0 + \phi_3(0) V_0 = V_0 - X_0 < 0.$$

Again there is an arbitrage. □

Definition 3.13. *For $t \in [0, T]$ and $x \in \mathbb{R}^+$, define*

$$P(t, x) \triangleq \sup_{\tau \in \mathcal{T}_{t,T}} E_Q \left[e^{-r(\tau - t)} (K - S_\tau)^+ \, | S_t = x \right]. \tag{3.14}$$

Then $P(t, x)$ is the fair price of the American put option, i.e. the price that precludes arbitrage opportunities.

In as much as (3.10) and (3.14) jointly specify the solution to the option pricing problem, we cannot infer the American option prices explicitly. The characterization can nonetheless be fruitfully exploited for numerical purposes, which will be our next task.

The optimal stopping problem associated with the option price can be cast as a free-boundary problem, where the domain of the option price is partitioned in two regions according to a *free boundary*. The free boundary is a time dependent parametrization of the boundary separating option prices for which it is optimal to exercise immediately, and those for which it is optimal to wait. The free boundary is not known a priori, but rather a part of the solution. Notice that the early exercise feature ensures that $P(t, S_t) < (K - S_t)^+$ cannot prevail, otherwise there would be an arbitrage[3]. Obviously,

$$\begin{aligned} P(t, S_t) &\geq (K - S_t)^+, \quad \forall (t, S_t) \in [0, T) \times \mathbb{R}^+. \\ P(T, S_T) &= (K - S_T)^+. \end{aligned}$$

Thus, we can partition the domain of the option price into the *continuation region*

$$\mathcal{C} = \left\{ (t, x) \in [0, T) \times \mathbb{R}^+ \ : \ P(t, x) > (K - x)^+ \right\},$$

and the *stopping region*

$$\mathcal{S} = \left\{ (t, x) \in [0, T) \times \mathbb{R}^+ \ : \ P(t, x) = (K - x)^+ \right\},$$

We need the following properties of the option price (see Jaillet, Lamberton and Lapeyre [27]).

Proposition 3.15. *The American put option price P is continuous on $[0, T] \times \mathbb{R}^+$, $P(\cdot, t)$ is convex and non-increasing on $\mathbb{R}^+$ for every $t \in [0, T]$ and $P(x, \cdot)$ is non-increasing on $[0, T]$ for every $x \in \mathbb{R}^+$.*

The continuity and monotonicity suggest that P will touch the immediate payoff for some $0 < S_t^* < K,\ 0 \leq t < T$. The time-dependent contact point S_t^* for which

$$\begin{aligned} P(t, S_t) &> (K - S_t)^+,\ S_t > S_t^*, \\ P(t, S_t) &= (K - S_t)^+,\ S_t \leq S_t^*, \end{aligned} \tag{3.16}$$

is coined the *free boundary*, and convexity ensures that this point is indeed unique for each $t \geq 0$. We see that the optimal stopping time will be the first time instant the asset price hits the free boundary. The economical interpretation of the free boundary goes as follows: suppose $0 \leq t < T$. For $S_t > S_t^*$ immediate exercise yields the loss $(K - S_t)^+ - P(t, S_t) < 0$, which is certainly not optimal. If $S_t \leq S_t^*$,

[3] Purchasing the asset and the put and exercising the option immediately entails a sure gain.

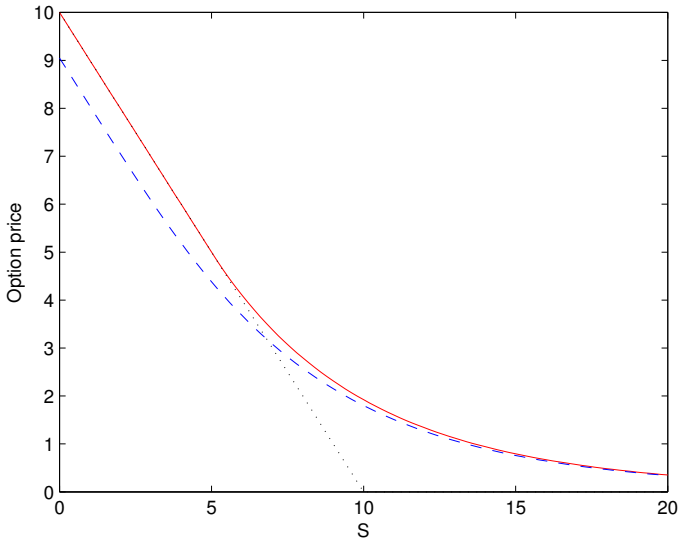

Figure 3.1: Price at $t = 0$ of an American put option computed by the Brennan-Schwartz algorithm, with $K = 10$, $r = 0.1$, $\sigma = 0.6$ and $T = 1$. Dashed line mark the corresponding European option. Dotted line mark the payoff function.

then $P(t, S_t) = K - S_t$ and a subsequent change in the underlying asset will cause a corresponding offset change in the option price. Waiting will only diminish the potential profit $Ke^{r(T-t)} - K$, so the option should be exercised as soon as S_t hits S_t^* and the proceeds K reinvested at the risk-free rate.

As S_t approaches the free-boundary, we must have that that

$$\lim_{x \to S_t^*} \frac{\partial P(t,x)}{\partial x} = -1 \quad \text{a.s.}$$

A proof can be found in Myneni [35]. A heuristic argument is that we cannot have $\frac{\partial P(t,x)}{\partial x} < -1$, in which case (3.16) would be violated, and $\frac{\partial P(t,x)}{\partial x} > -1$ implies an arbitrage. Moreover, P is continuously differentiable over the free boundary, which is known as the *principle of smooth fit* or *smooth pasting*.

Now, consider the Black-Scholes option pricing PDE

$$\frac{\partial P}{\partial t} + \frac{1}{2}\sigma^2 x^2 \frac{\partial^2 P}{\partial x^2} + rx\frac{\partial P}{\partial x} - rP = 0, \quad t \in [0, T). \tag{3.17}$$

For $S_t \leq S_t^*$, we can deduce that

$$P(t, S_t) = K - S_t, \ \frac{\partial P(t, S_t)}{\partial t} = 0, \ \frac{\partial P(t, S_t)}{\partial x} = -1, \ \frac{\partial^2 P(t, S_t)}{\partial x^2} = 0.$$

Inserted into the Black-Scholes equation this amounts to

$$\frac{\partial P}{\partial t} + \frac{1}{2}\sigma^2 x^2 \frac{\partial^2 P}{\partial x^2} + rx\frac{\partial P}{\partial x} - rP < 0, \quad t \in [0, T), \ x \leq S_t^*. \tag{3.18}$$

On the continuation region the American put price obeys the Black-scholes PDE (??), hence

$$\frac{\partial P}{\partial t} + \frac{1}{2}\sigma^2 x^2 \frac{\partial^2 P}{\partial x^2} + rx\frac{\partial P}{\partial x} - rP \leq 0, \quad t \in [0,T),\ x \in \mathbb{R}^+. \tag{3.19}$$

We are now ready to state a theorem which provides the basis for a numerical method due to Brennan and Schwarz [13]. See Jaillet, Lamberton and Lapeyre. [27] for a detailed proof of the theorem and a rigorous treatment in favor of the Brennan Schwartz algorithm.

Theorem 3.20. *Denote by* $(S_v^{t,x})_{t\leq v\leq T}$ *the unique solution to*

$$S_v = b(v, S_v)dv + \sigma(v, S_v)dW_v, \quad v \in [0,T], \tag{3.21}$$

starting from x *at time* t*, with corresponding infinitesimal generator*

$$\mathcal{L} = \frac{1}{2}\sigma(t,x)\frac{\partial^2}{\partial x^2} + b(t,x)\frac{\partial}{\partial x}. \tag{3.22}$$

Let f *denote the payoff function for the put option. Assume* u *is a regular solution of the following system of partial differential inequalities:*

$$\begin{cases} \frac{\partial u}{\partial t} + \mathcal{L}u - ru \leq 0, & t \in [0,T), u \geq f \\ \left(\frac{\partial u}{\partial t} + \mathcal{L}u - ru\right)(f-u) = 0, & t \in [0,T) \\ u(T,x) = f(x), & x \in \mathbb{R}^+. \end{cases} \tag{3.23}$$

Then

$$u(t,x) = P(t,x) = \sup_{\tau \in \mathcal{T}_{t,T}} E_Q\left[e^{-r(\tau-t)} f(S_\tau^{t,x})\right]. \tag{3.24}$$

Proof. This proof is adapted from Lamberton and Lapeyre [32]. The Itô formula applied to $\hat{u}(v,x) = e^{-rv}u(v,x)$ and $S_v^{t,x}$ yields

$$\hat{u}(v, S_v^{t,x}) = \hat{u}(t,x) + \int_t^v e^{-rs}\left(\frac{\partial u}{\partial v} + \mathcal{L}u - ru\right)(s, S_s^{t,x})ds + \int_t^v e^{-rs}\frac{\partial u(s, S_s^{t,x})}{\partial x}\sigma(s, S_s^{t,x})dW_s.$$

So

$$M_v = \hat{u}(v, S_v^{t,x}) - \int_t^v e^{-rs}\left(\frac{\partial u}{\partial v} + \mathcal{L}u - ru\right)(s, S_s^{t,x}))ds$$

is a $\mathbb{Q}$-martingale. The Optional sampling theorem applied to this martingale with the stopping times t and τ gives $E_{\mathbb{Q}}[M_\tau] = E_{\mathbb{Q}}[M_t]$. As $\frac{\partial u}{\partial v} + \mathcal{L}u - ru \leq 0$, we have that

$$u(t,x) \geq E_{\mathbb{Q}}\left[e^{-r(\tau-t)}u(\tau, S_\tau^{t,x})\right].$$

Furthermore, using that $u \geq f$,

$$u(t,x) \geq E_{\mathbb{Q}}\left[e^{-r(\tau-t)} f(S_\tau^{t,x})\right].$$

Hence

$$u(t,x) \geq \sup_{\tau \in \mathcal{T}_{t,T}} E_{\mathbb{Q}}\left[e^{-r(\tau-t)} f(S_\tau^{t,x})\right] = P(t,x).$$

Let $\tau^* = \inf\{t \leq s \leq T : u(s, S_s^{t,x}) = f(S_s^{t,x})\}$, and observe that τ^* is a $\{\mathcal{F}_t\}_{t\geq 0}$ stopping time. We know that for $s \in [t, \tau^*)$

$$\left(\frac{\partial u}{\partial v} + \mathcal{L}u - ru\right)(s, S_s^{t,x}) = 0.$$

In this case, the Optional sampling theorem yields

$$\begin{aligned} u(t,x) &= E_{\mathbb{Q}}\left[e^{-r(\tau^*-t)} u(\tau^*, S_{\tau^*}^{t,x})\right] \\ &= E_{\mathbb{Q}}\left[e^{-r(\tau^*-t)} f(S_{\tau^*}^{t,x})\right]. \end{aligned}$$

Moreover, $u(t,x) \leq P(t,x)$, so $u(t,x) = P(t,x)$ and τ^* is the optimal stopping time. □

3.2 The Brennan-Schwartz Algorithm

Brennan and Schwartz [13] proposed a simple and efficient algorithm to solve the system of inequalities (3.23) by finite differences. They applied an implicit scheme and proceeded as in the European case, but with a modification in the tridiagonal matrix algorithm accounting for early exercise. To ease notation, we assume time-independent coefficients, i.e

$$b(t,x) \equiv b(x) \quad \text{and} \quad \sigma(t,x) \equiv \sigma(x).$$

Assume the spatial domain has been localized to $(0, S_{\max})$ with homogeneous Dirichlet boundary conditions. The computational grid is given by

$$\{(t_n, s_i) : \quad n = 0, ..., N,\ i = 0, ..., I\}.$$

The discretized system of inequalities can be written as

$$\begin{cases} \mathbf{L}\mathbf{U}^{n+1} \leq \mathbf{b} \\ \mathbf{U}^n \geq \mathbf{f} \\ \left(\mathbf{L}\mathbf{U}^{n+1} - \mathbf{b}\right)^T \left(\mathbf{U}^n - \mathbf{f}\right) = 0 \end{cases} \tag{3.25}$$

where $\mathbf{L} = \mathbf{I} + \theta \Delta t \mathbf{A}$ is a $(I-1) \times (I-1)$ matrix,

$$\mathbf{U}^n = \left(U_1^n, ..., U_{I-1}^n\right)^T \in \mathbb{R}^{I-1} \tag{3.26}$$

$$\mathbf{f} = \left(f(s_1), ..., f(s_{I-1})\right)^T \in \mathbb{R}^{I-1} \tag{3.27}$$

$$\mathbf{b} = \left(\mathbf{I} - (1-\theta)\Delta t \mathbf{A}\right) \mathbf{U}^n \in \mathbb{R}^{I-1} \tag{3.28}$$

and

$$\mathbf{A} = \begin{pmatrix} \beta_1 & \gamma_1 & & & 0 \\ \alpha_2 & \beta_2 & \gamma_2 & & \\ & \ddots & \ddots & \ddots & \\ & & \alpha_{I-2} & \beta_{I-2} & \gamma_{I-2} \\ 0 & & & \alpha_{I-1} & \beta_{I-1} \end{pmatrix}, \quad \begin{cases} \alpha_i = \frac{1}{2}\left(\frac{\sigma_i^2}{\Delta x^2} - \frac{b_i}{\Delta x}\right) \\ \beta_i = \frac{1}{2}\left(\frac{\sigma_i^2}{\Delta x^2} - r\right) \\ \gamma_i = \frac{1}{2}\left(\frac{\sigma_i^2}{\Delta x^2} + \frac{b_i}{\Delta x}\right) \end{cases}.$$

We solve the system (3.25) by the modified tridiagonal matrix algorithm:

$$\gamma_i' = \begin{cases} \frac{\gamma_i}{\beta_i}, & i = 1 \\ \frac{\gamma_i}{\beta_i - \gamma_{i-1}'\alpha_i}, & i = 2, ..., I-2 \end{cases}$$

$$b_i' = \begin{cases} \frac{b_i}{\beta_i}, & i = 1 \\ \frac{b_i - b_{i-1}'\alpha_i}{\beta_i - \gamma_{i-1}'\alpha_i}, & i = 2, ..., I-1 \end{cases}$$

$$\begin{cases} U_{I-1}^{n+1} & = \max\left\{b_{I-1}', f(s_{I-1})\right\} \\ U_i^{n+1} & = \max\left\{b_i' - \gamma_i' U_{i+1}', f(s_i)\right\}, \quad i = I-2, ..., 1 \end{cases}$$

Time-homogeneous boundary conditions can be chosen according to

- Dirichlet type: $u(t_n, x_0) = g_0$, $u(t_n, x_I) = g_I$
- Neumann type: $\frac{\partial u(t_n, x_0)}{\partial x} = g_0$, $\frac{\partial u(t_n, x_I)}{\partial x} = g_I$

for $n = 0, ..., N-1$. Non-homogeneous Dirichlet boundaries are realized in the the vector $\mathbf{b}$ as

$$\mathbf{b} = \left(\mathbf{I} - (1-\theta)\Delta t \mathbf{A}\right)\mathbf{U}^n + \begin{pmatrix} -\alpha_1 g_0 \\ 0 \\ \vdots \\ -\gamma_{I-1} g_I \end{pmatrix},$$

whereas non-homogeneous Neumann boundaries[4] alter the matrix $\mathbf{A}$ to

$$\mathbf{A} = \begin{pmatrix} \beta_1 + \alpha_1 & \gamma_1 & & & 0 \\ \alpha_2 & \beta_2 & \gamma_2 & & \\ & \ddots & \ddots & \ddots & \\ & & \alpha_{I-2} & \beta_{I-2} & \gamma_{I-2} \\ 0 & & & \alpha_{I-1} & \beta_{I-1} + \gamma_{I-1} \end{pmatrix}.$$

[4]Using a first-order (one-sided) approximation to the derivative.

In chapter 5 we apply an extension of this algorithm in conjunction with the Douglas ADI scheme. The idea is taken from Villeneuve and Zanette [43] and Villeneuve and Zanette [44] where the Douglas-Rachford ADI scheme is applied to American two-factor options. The method is referred to as LCP-ADI (linear complementarity problem ADI), and essentially involves an application of the Brennan-Schwartz algorithm in each direction of the ADI scheme.

3.3 The Longstaff-Schwartz Algorithm

We have formulated the American option price in terms of an optimal stopping problem and a set of partial differential inequalities. The system of inequalities can be solved by finite difference methods such as the Brennan-Schwartz algorithm. However, multiple dimensions are notoriously difficult to handle with finite differences.

The algorithm due to Longstaff and Schwartz [33] confines the stopping problem to a discrete optimization problem which can be tackled by Monte Carlo and dynamic programming. By replacing the continuum of exercise dates by a finite subset, we can essentially approximate the American option by a so-called *Bermudan* option. The algorithm involves simulating asset paths and replacing conditional expectations by projections onto a finite set of basis functions. Since we are restricting the set of stopping times to a smaller subset, the approximation is expected to produce a sub-optimal early exercise strategy, effectively yielding a low-biased estimate for the option value. Analogously, if the exercise strategy is based on information anticipating the future, we obtain a high-biased estimator. In combination, simulation of low- and high-biased estimators can be used to construct a confidence interval for the option. A detailed account on American options and simulation techniques is given in Glasserman [25]. Here we discuss the algorithm as presented in the original paper by Longstaff and Schwartz.

Let T denote the maturity of the option. We divide the time to maturity into N equidistant intervals of length Δt, such that $0 = t_0 < t_1 < ... < t_N = T$, and generate independent sample paths $\left\{S_i^{(j)}\right\}_{i=1}^{N}$, $j = 1, ...M$, where M is the number of Monte Carlo simulations. Let $I_i^{(j)}$ denote the intrinsic value of the option at time t_i for the jth asset path, i.e. the payoff from immediate exercise. Similarly, let $C_i^{(j)}$ denote the continuation value from not exercising the option at time t_i. Dynamic programming yields the following backward recursion for the American put option:

$$\begin{cases} V_N^{(j)} = I_N^{(j)} = \left(K - S_N^{(j)}\right)^+ \\ V_i^{(j)} = \max\left\{I_i^{(j)}, C_i^{(j)}\right\}, \quad i = N-1, ..., 0, \end{cases} \tag{3.29}$$

where

$$C_i^{(j)} = \mathbb{E}_{\mathbb{Q}}\left[e^{-r\Delta t} V_{i+1}^{(j)} \mid S_i^{(j)}\right]. \tag{3.30}$$

In order to keep track of the early exercise strategies we introduce some additional notation. Let $\mathcal{T}_{i,N}$ denote the possible stopping times at time t_i taking values in the finite set $\{i, ..., N\}$. The stopping times are defined as

$$\tau_i^{(j)} \triangleq \min\left\{k \geq i \mid V_k^{(j)} = I_k^{(j)}\right\}, \tag{3.31}$$

which can be used to reformulate the continuation value. Let

$$C_i^{(j)} = \mathbb{E}_{\mathbb{Q}}\left[e^{-r\Delta t(\tau_{i+1}^{(j)} - i)} I_{\tau_{i+1}}^{(j)} \mid S_i^{(j)}\right]. \tag{3.32}$$

This expression will be the key quantity in the regression.

To reduce computational efforts, Longstaff and Schwartz proposed to use only in-the-money sample paths. Accommodating for "moneyness", dynamic programming in terms of stopping times amounts to

$$\begin{cases} \tau_N^{(j)} & = N \\ \tau_i^{(j)} & = i\mathbf{1}_{\left\{I_i^{(j)} \geq C_i^{(j)}\right\} \cap \left\{I_i^{(j)} > 0\right\}} \\ & \quad + \tau_{i+1}\mathbf{1}_{\left\{I_i^{(j)} < C_i^{(j)}\right\} \cup \left\{I_i^{(j)} = 0\right\}}, \quad i = N-1, ..., 0. \end{cases} \tag{3.33}$$

Note that the exercise strategy cannot be deduced along individual paths separately, as this would exploit knowledge of the future and imply clairvoyance. Instead, in each time step we use the simulated asset paths to obtain an estimate of the continuation value. The conditional expectation in (3.32) is an element in L^2, and we can readily justify representing $C_i^{(j)}$ as a linear combination of basis functions from a countable $\mathcal{F}_{t_i}$-measurable set. Thus, in each time step i prior to maturity we must solve the regression problem

$$e^{-r\Delta t(\tau_{i+1}^{(j)} - i)} I_{\tau_{i+1}}^{(j)} = \sum_{k=1}^{K} \beta_{k,i} \psi_k(S_i^{(j)}) + \epsilon_j, \quad j = 1, ..., M, \tag{3.34}$$

for a suitable choice of basis functions $\psi_i^{(j)} = \left(\psi_1(S_i^{(j)}), ..., \psi_K(S_i^{(j)})\right)^T$. A simple least-squares procedure yields

$$\hat{\beta}_i = \arg \min_{\beta_i \in \mathbb{R}^K} \mathbf{1}_{\left\{I_{\tau_{i+1}}^{(j)} > 0\right\}} \sum_{j=1}^{M} \left(e^{-r\Delta t(\tau_{i+1}^{(j)} - i)} I_{\tau_{i+1}}^{(j)} - \beta_i \cdot \psi_i^{(j)}\right)^2. \tag{3.35}$$

Put $\hat{C}_i^{(j)} = \hat{\beta}_i \cdot \psi_i^{(j)}$. The algorithm proceeds by replacing the continuation value by its least-squares estimate, and deducing the exercise decision from the recursion (3.33). We obtain an exercise strategy $\hat{\tau}^{(j)},\ j = 1, ..., M$, for each sample path. The Least-Square Monte Carlo (LSM) option price will be given by

$$\hat{V}_0 = \max\left\{I_0, \frac{1}{M} \sum_{j=1}^{M} e^{-r\Delta t \hat{\tau}^{(j)}} I_{\hat{\tau}^{(j)}}^{(j)}\right\}, \tag{3.36}$$

where $I_0 = (K - S_0)^+$ is the immediate payoff at time $t = 0$ and S_0 is the (deterministic) initial asset price.

According to Longstaff and Schwartz [33] the algorithm is fairly robust to the choice of basis functions. They also indicate, through numerical testing, that a modest number of basis functions provide satisfactory results. Even the simple set of monomials $\psi_1(x) = 1,\ \psi_2(x) = x,\ \psi_3(x) = x^2$ is performing well[5]. Orthogonal polynomials, including the Hermite, Laguerre and Legendre are also common. A numerical convergence study for the Black-Scholes model is provided in 3.2. We employ the simple monomials and use Matlab's built-in binomial tree algorithm as our reference. Convergence is measured in the *maximum absolute difference* (MAD), and one may verify the (infamous) square-root convergence of Monte Carlo. Solutions in both algorithms are given in figure 3.3 (lines overlap).

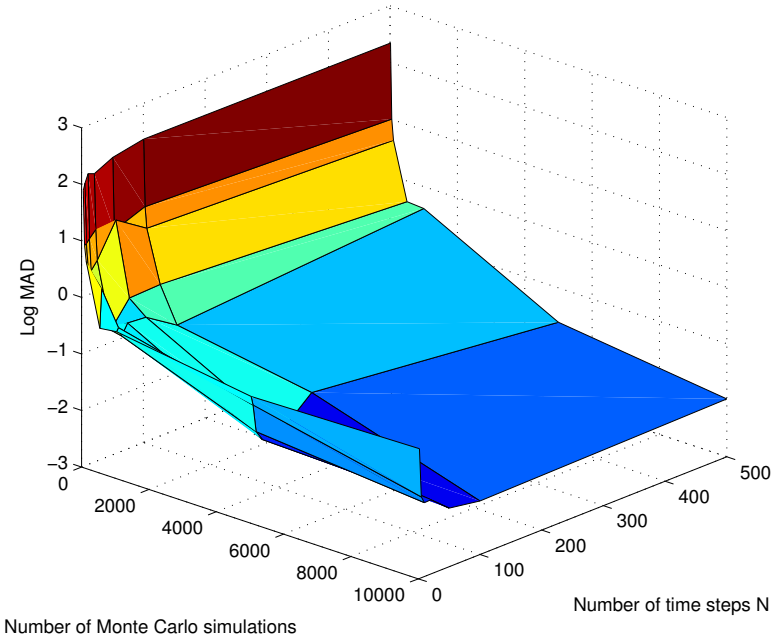

Figure 3.2: Convergence of the Longstaff-Schwartz algorithm for the Black-Scholes model.

[5]For multi-factor models cross-products should be included.

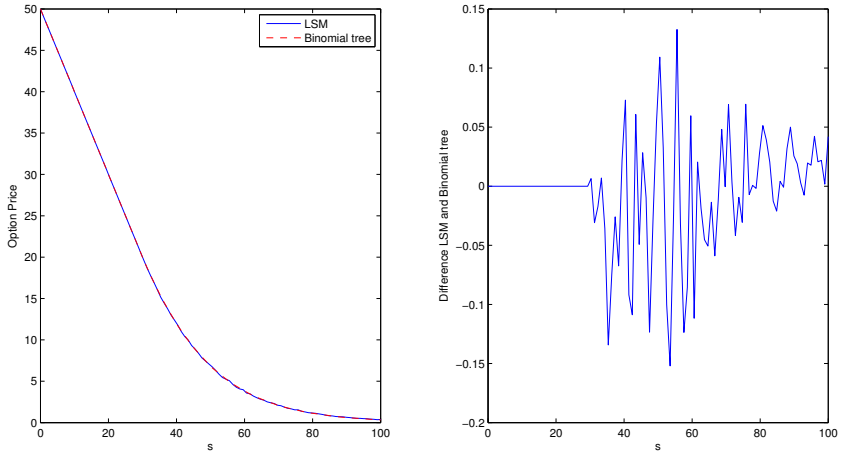

Figure 3.3: Price of an American put option computed by the Longstaff-Schwartz algorithm and Matlab's binomial tree algorithm.

Chapter 4

Carma Processes

The parametric class of *continuous-time autoregressive moving average* processes is the natural extension of the discrete ARMA models from time series analysis. CARMA provides a convenient modeling framework accounting for memory effects and mean-reversion, with the the decisive benefit of stochastic calculus over discrete-time models. Early works on CARMA processes go all the way back to the 1950s. A renewed interest in these models stems from the prevailing interest in financial econometrics, and in particular in Ornstein-Uhlenbeck processes (OU) such as the acclaimed stochastic volatility model proposed by Barndorff-Nielsen and Shepard [3]. CARMA can be seen as a higher-order generalization of the stationary OU process, and can easily reproduce a variety of temporal dependence structures. They effectively provide a flexible alternative to modeling by linear combinations of independent OU processes. CARMA models have also been successfully applied to irregularly-sampled data, as is frequently encountered in finance or in the case of data with missing observations. An introduction to CARMA processes is given in Brockwell [15] and Brockwell [14]. Recent applications of CARMA models include interest rate modeling, electricity markets, weather markets and stochastic volatility.

We review Lévy-driven CARMA processes and indicate how they extend the familiar OU process. OU is a special case of the *continuous time autoregressive* (CAR) processes, and will also be referred to as CAR(1).

4.1 Lévy-driven CARMA processes

Definition 4.1. *A Lévy-driven CARMA(p,q) process* $(Y_t)_{t\geq 0}$ *(with* $0 \leq q < p$*) is defined as the solution of the state-space equations*

$$Y_t = \mathbf{b}^T \mathbf{X}_t \tag{4.2}$$

$$d\mathbf{X}_t = \mathbf{A}\mathbf{X}_t dt + \mathbf{e}_p dL_t \tag{4.3}$$

with

$$\mathbf{A} = \begin{pmatrix} 0 & 1 & 0 & \cdots & 0 \\ 0 & 0 & 1 & \cdots & 0 \\ \vdots & \vdots & \ddots & \vdots & \\ 0 & 0 & 0 & \cdots & 1 \\ -\alpha_p & -\alpha_{p-1} & -\alpha_{p-2} & \cdots & -\alpha_1 \end{pmatrix}, \quad \mathbf{e}_p = \begin{pmatrix} 0 \\ 0 \\ \vdots \\ 0 \\ 1 \end{pmatrix},$$

$$\mathbf{b} = \begin{pmatrix} 1 \\ b_1 \\ \vdots \\ b_{p-2} \\ b_{p-1} \end{pmatrix}, \quad \mathbf{X}_t = \begin{pmatrix} X_t \\ X_t^{(1)} \\ \vdots \\ X_t^{(p-2)} \\ X_t^{(p-1)} \end{pmatrix}.$$

where $(L_t)_{t\geq 0}$ is a Lévy process and $\alpha_1, ..., \alpha_p > 0$ and $b_1, ..., b_{p-1}$ are complex-valued coefficients such that $b_j = 0$ for $q < j \leq p$. For $p = 1$, the matrix $\mathbf{A}$ is to be understood as $\mathbf{A} = -\alpha_1$.

In the case $b_j = 0,\ j \geq 1$, the Y becomes a CAR(p) process.

The CARMA process can be represented as the suitably interpreted[1] strictly stationary solution to the pth order linear SDE

$$a(D)Y_t = b(D)DL_t, \quad t \geq 0, \tag{4.4}$$

in which D denotes differentiation with respect to time, and

$$\begin{aligned} a(z) &\triangleq z^p + \alpha_1 z^{p-1} + ... + \alpha_p \\ b(z) &\triangleq 1 + b_1 z + ... + b_{p-1} z^{p-1} \end{aligned} \tag{4.5}$$

are the characteristic polynomials of Y. Here, stationarity is assumed in the sense that all finite dimensional distributions are shift-invariant. To this end, we make the following standing assumptions to ensure strict stationarity:

- The characteristic polynomials have no common zeros.
- $E\left[\ln |L_1|^+\right] < \infty$.
- All eigenvalues $\lambda_1, ..., \lambda_p$ of $\mathbf{A}$ are distinct and have strictly negative real parts, i.e. $\mathcal{R}e(\lambda_j) < 0, \quad j = 1, ..., p$.

A proof can be found in Brockwell and Lindner [17]. These assumptions also make sure that $\mathbf{X}$ is a causal process, making Y causal as well. It is easy to check that the eigenvalues of the matrix $\mathbf{A}$ correspond to the zeros of the autoregressive polynomial

[1] DL_t does not exist in the usual sense.

$a(z)$.

The following lemma can be proved by an application of the multi-dimensional Itô formula for semimartingales (Protter [38]).

Lemma 4.6. *The solution of (4.3) starting at time $s \geq 0$ is given by the stochastic process*

$$\mathbf{X}_t = e^{\mathbf{A}(t-s)}\mathbf{X}_s + \int_s^t e^{\mathbf{A}(t-u)}\mathbf{e}_p dL_u, \quad t \geq s, \tag{4.7}$$

where, for any square matrix $\mathbf{A}$, the matrix exponential is defined as

$$e^{\mathbf{A}} \triangleq \mathbf{I} + \sum_{k\geq 1} \frac{1}{k!}\mathbf{A}^k. \tag{4.8}$$

Note that the integral is interpreted as integration with respect to a semimartingale. Given $\mathbf{X}_s$, we can now express Y as

$$Y_t = \mathbf{b}^T e^{\mathbf{A}(t-s)}\mathbf{X}_s + \int_s^t \mathbf{b}^T e^{\mathbf{A}(t-u)}\mathbf{e}_p dL_u, \quad t \geq s. \tag{4.9}$$

By the independent increment property of Lévy processes, $\mathbf{X}$ and Y are readily seen to be Markov processes. The Markov property is the key to the derivation of the pricing PDEs in chapter 5.

The CARMA process is often given in terms of its *kernel*,[2] $g(t) = \mathbf{b}^T e^{\mathbf{A}t}\mathbf{e}_p \mathbf{1}_{[0,\infty)}(t)$, and we may write

$$Y_t = \int_{-\infty}^t g(t-u)dL_u.$$

The kernel determines the memory of the CARMA process, and gives the weights with which the past observations enter the integral (??). Since $\mathbf{A}$ is a *companion* matrix with distinct eigenvalues, it is diagonalizable as

$$\mathbf{A} = \mathbf{V}\mathbf{\Lambda}\mathbf{V}^{-1}, \tag{4.10}$$

where $\mathbf{\Lambda} = \text{diag}\{\lambda_1, ..., \lambda_p\}$ and $\mathbf{V}$ is the *Vandermonde* matrix corresponding to the λ's. It follows that the right eigenvectors corresponding to the matrix $\mathbf{A}$ are

$$\left[1, \lambda_j, \lambda_j^2, ..., \lambda_j^{p-1}\right], \quad j = 1, ..., p.$$

[2]This formulation requires an extension of L to a process defined on the index set $(-\infty, \infty)$. This is done by introducing an independent copy, $\left(\tilde{L}_t\right)_{t\geq 0}$, and defining

$$L_t^* = L_t \mathbf{1}_{[0,\infty)}(t) - \tilde{L}_{-t-}\mathbf{1}_{(-\infty,0]}(t), \quad \infty < t < \infty.$$

Then relabel L^* as L.

Brockwell and Lindner [17] assert that

$$\mathbf{b}^T e^{\mathbf{A}t}\mathbf{e}_p = \frac{1}{2\pi i}\int_\gamma \frac{b(z)}{a(z)}e^{tz}dz, \tag{4.11}$$

where γ is a simple closed curve enclosing all eigenvalues of $\mathbf{A}$. We may deduce that (see the appendix)

$$g(t) = \sum_{j=1}^{p} e^{\lambda_j t}\frac{b(\lambda_j)}{a^{(1)}(\lambda_j)}, \quad t \geq 0, \tag{4.12}$$

where $a^{(1)}$ denotes differentiation of $a(\cdot)$. This representation of the kernel provides a decomposition of Y into a sum of dependent and possibly complex-valued CAR(1) processes,

$$Y_t = \sum_{i=1}^{p} Y_t^{(i)}, \quad t \geq 0, \tag{4.13}$$

where

$$Y_t^{(i)} = \kappa_i \int_{-\infty}^{t} e^{\lambda_i(t-u)}dL_u \quad \text{and} \quad \kappa_i = \frac{b(\lambda_i)}{a^{(1)}(\lambda_i)}, \ i = 1, ..., p.$$

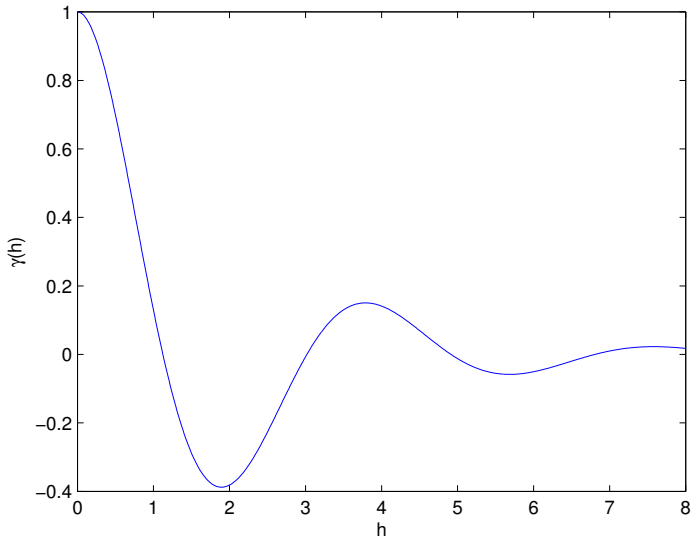

Figure 4.1: ACF for a CAR(2) with $\alpha_1 = 1$, $\alpha_2 = 3$, $\sigma = 1$ and $t = 0$. The autoregressive coefficients yield complex eigenvalues.

Furthermore, if $\mathbb{E}[L_1^2] < \infty$, the autocovariance function is given by

$$\gamma(h) = \text{Cov}[Y_{t+h}, Y_t] = \sigma^2 \sum_{j=1}^{p} \frac{b(\lambda_j)b(-\lambda_j)}{a^{(1)}(\lambda_j)a(-\lambda_j)}e^{\lambda_j|h|}, \tag{4.14}$$

where $\sigma^2 = \text{Var}[L_1]$. For a CAR(1) process, $b(z) = 1$ and $a(z) = z + \alpha$, which amounts to

$$\gamma(h) = \frac{\sigma^2}{2\alpha} e^{-\alpha|h|}.$$

Under the assumptions of stationarity and square-integrability the autocorrelation function (ACF) is given by

$$\rho(h) = \text{Corr}[Y_{t+h}, Y_t] = \frac{\gamma(h)}{\gamma(0)}. \tag{4.15}$$

We see that the ACF of a CAR(1) process is constrained by monotonicity, whereas CARMA allows for a more complex ACF without introducing additional factors. Figure 4.1 shows the ACF of a CARMA process with damped oscillatory autocorrelation. Observe that the CARMA process is driven by a single source of randomness, although the state vector is p-dimensional. From the eigen-decomposition (4.10) we have that $e^{\mathbf{A}t} = \mathbf{V} e^{\Lambda t} \mathbf{V}^{-1}$, so the components of the vector $e^{\mathbf{A}t}\mathbf{X}_s$ are linear combinations of the eigenvalues, and each component will exhibit different speed of mean-reversion[3]. Moreover, with $q \geq 1$ we are able to mimic the effect of multiple CAR(1) factors while retaining the advantage of working with a single distribution. In this respect, CARMA(2,1) is a parsimonious, yet flexible model for a variety of applications.

4.2 Gaussian CARMA processes

We end this chapter by considering the class of Gaussian CARMA models suitable for wind-speed and temperature modeling. The observation and state equations take the form

$$Y_t = \mathbf{b}^T X_t, \tag{4.16}$$

$$d\mathbf{X_t} = \mathbf{A} X_t dt + \mathbf{e}_p \sigma(t) dW_t, \quad t \geq 0, \tag{4.17}$$

where $(W_t)_{t \geq 0}$ is a Wiener process and $\sigma(t)$ is a continuous, real valued function bounded away from zero. In weather modeling $\sigma(t)$ is observed to be a periodic function. Benth [5] shows that Y remains stationary when volatility is bounded. A straightforward application of the multi-dimensional Itô formula verifies that the solution of (4.17), starting at time s, is the multi-dimensional Gaussian OU process

$$\mathbf{X}_t = e^{\mathbf{A}(t-s)} \mathbf{X}_s + \int_s^t e^{\mathbf{A}(t-u)} \mathbf{e}_p \sigma(u) dW_u, \quad t \geq s. \tag{4.18}$$

By well-known properties of the Itô integral,

$$\mathbb{E}[Y_t \mid X_s] = \mathbf{b}^T e^{\mathbf{A}(t-s)} X_s, \tag{4.19}$$

$$\text{Var}[Y_t \mid X_s] = \int_s^t \left(\mathbf{b}^T e^{\mathbf{A}(t-u)} \mathbf{e}_p \right)^2 \sigma^2(u) du. \tag{4.20}$$

[3] Recall, we are assuming distinct eigenvalues with negative real parts.

It can be verified that the limiting distribution of Y exists under the above assumptions and is Gaussian with mean zero and variance

$$\lim_{t\to\infty} \int_0^t \left(\mathbf{b}^T e^{\mathbf{A}(t-u)}\mathbf{e}_p\right)^2 \sigma^2(u)du.$$

Chapter 5

Modeling and Pricing in Electricity and Weather Markets

In this chapter we present spot electricity and temperature models and discuss the implications of non-storability on pricing. We derive pricing PIDEs and PDEs which we attempt to solve with numerical methods discussed in the preceding chapters.

5.1 Electricity Derivatives

Over the last decades there has been a vast deregulation of electricity markets, starting in the late 1980s when the UK initiated a privatization and restructuring of the electricity sector. By now, the European market is fully liberalized, and both physical and purely financial contracts are available for producers, retailers, consumers and speculators. The rich interplay between regulation, production and distribution renders electricity markets highly complex, and a variety of contracts are traded in order to control risk and secure efficient operation of the physical network.

Forward prices can be modeled by a direct specification of the forward dynamics or be derived in terms of the spot. The lack of storability makes the spot-forward connection questionable, and the Heath-Jarrow-Morton framework from fixed-income markets is often adopted for a direct approach. Spot price modeling is nonetheless interesting per se, and we consider a two-factor jump-diffusion model in which we eventually derive forward prices numerically and in closed-form. The general setup is taken from Benth et al. [6], and the CAR(1) process will be our main modeling tool.

Let $(S_t)_{t\geq 0}$ be a stochastic process modeling the spot electricity price defined on the complete filtered probability space $\left(\Omega, \mathcal{F}, \{\mathcal{F}\}_{t\geq 0}, \mathbb{P}\right)$ satisfying the usual conditions. Our first step is to decide on either of the following basic classes of models:

Arithmetic Model

$$\begin{aligned} S_t &= \Lambda(t) + \sum_{i=1}^{m} X_t^i + \sum_{j=1}^{n} Y_t^j, \\ X_0^i + Y_0^j &= S_0 - \Lambda(0), \quad i = 1, ..., m,\ j = 1, ..., n \end{aligned} \tag{5.1}$$

Geometric Model

$$\begin{aligned} \ln S_t &= \ln \Lambda(t) + \sum_{i=1}^{m} X_t^i + \sum_{j=1}^{n} Y_t^j, \\ X_0^i + Y_0^j &= \ln S_0 - \ln \Lambda(0), \quad i = 1, ..., m,\ j = 1, ..., n \end{aligned} \tag{5.2}$$

Here, Λ is a deterministic seasonality function,

$$dX_t^i = (\mu_i(t) - \alpha_i(t) X_t^i)dt + \sum_{k=1}^{p} \sigma_{ik}(t) dW_t^k, \quad i = 1, ..., m, \tag{5.3}$$

and

$$dY_t^j = (\delta_j(t) - \beta_j(t) Y_t^j)dt + \eta_j(t) dL_t^j, \quad j = 1, ...n. \tag{5.4}$$

$\left(W_t^k\right)_{t \geq 0}$ are independent Wiener processes and $(L_t)_{t \geq 0}$ is a Lévy process independent of W_t^k for all $t \geq 0$ and $k = 1, ..., p$. This setup subsumes many spot price models advocated in the literature, and can be employed to account for the stylized features observed in the market, such as

- Seasonality (yearly, monthly, weekly and daily)
- Mean reversion
- Price spikes
- Time dependent volatility

Note that since Lévy processes have independent and stationary increments, this framework does not capture the time dependency in jump size and jump intensity observed in the market[1]. The class of *independent increment* (II) processes treated in Benth et al. [6] provide the necessary degree of generality.

The most common models for commodity and equity prices are of geometric type, i.e. having an exponential structure. Geometric models ensure non-negativity of prices[2], making them a natural choice for modeling purposes. However, in energy markets such as electricity and gas, our main interest is pricing contracts delivering the spot over some prescribed period of time, so-called *swap* contracts, and contracts

[1] In the Nordic markets large price spikes are more frequent during winter.

[2] Negative prices are occasionally observed in electricity and gas markets. In electricity markets this is due to an excess of power in the grid, in which case paying someone to consume the electricity is cheaper that shutting down generators.

derived from the swaps. Geometric models often yield complicated expressions for the these contracts, whereas the additive structure of arithmetic models allows considerably more tractability. Moreover, negative prices can be circumvented by using a subordinator (or more generally, an increasing II process) in the driving noise, so there is no reason to confine the spot models to those of geometric type.

A Jump-Diffusion Spot Model

We give a brief excursion to Lévy processes intended to introduce notation and terminology. Let $L = (L_t)_{t\geq 0}$ be a stochastic process defined on our probability space.

Definition 5.5. *An adapted process L with $L_0 = 0$ a.s. is a* Lévy process *if*

- *L has* independent increments, *i.e. $L_t - L_s$ is independent of $\mathcal{F}_s$ for $0 \leq s < t < \infty$*
- *L has* stationary increments, *i.e. $L_t - L_s$ has the same distribution as L_{t-s} for $0 \leq s < t < \infty$*
- *L is* continuous in probability, *i.e. for all $s \geq 0$*

$$\lim_{t\to s} P\left(|L_t - L_s| \geq \epsilon\right) = 0, \quad \forall \epsilon > 0$$

Every Lévy process has a unique càdlàg[3] modification, and we therefore assume that L is indeed already càdlàg. Define the *jump* of L at time $t \geq 0$ as

$$\Delta L_t \stackrel{\Delta}{=} L_t - L_{t-}, \quad \text{where} \quad L_{t-} = \lim_{s\uparrow t} L_s. \tag{5.6}$$

Associated with L is a *Poisson random measure* $N = (N(t, A), t \geq 0, A \in \mathbb{R}_0)$ defined as

$$N(t, A) \stackrel{\Delta}{=} \sum_{s\leq t} \mathbf{1}_{\Delta L_s \in A}, \tag{5.7}$$

where A is a Borel subset in $\mathbb{R}_0 = \mathbb{R}\backslash\{0\}$. N counts the number of jumps falling in the set A occuring before or at time t, and since L is càdlàg there can only be a finite number of jumps bounded from below (i.e. $N(t, A) < \infty$ if $0 \notin A$). The corresponding *Lévy measure* is defined as

$$\nu(A) \stackrel{\Delta}{=} \mathbb{E}\left[N(1, A)\right], \quad A \in \mathcal{B}(\mathbb{R}_0), \tag{5.8}$$

which is a σ-finite measure on $\mathcal{B}(\mathbb{R}_0)$, satisfying

$$\int_{\mathbb{R}_0} (|z|^2 \wedge 1)\nu(dz) < \infty. \tag{5.9}$$

[3] A right continuous process with left limits.

Theorem 5.10 (The Lévy-Itô Decomposition)**.** *If L is a Lévy process, then there exists $a \in \mathbb{R}$, $\sigma \in \mathbb{R}_+ \cup \{0\}$, a Wiener process W and a Poisson random measure N such that*

$$L_t = at + \sigma W_t + \int_0^t \int_{|z|<1} z\tilde{N}(dt, dz) + \int_0^t \int_{|z|\geq 1} zN(dt, dz). \tag{5.11}$$

Proof. See Applebaum [2]. □

The triple (a, σ, ν) is called the characteristic triple of the Lévy process L. From the Lévy-Itô decomposition one may derive the celebrated *Lévy-Khintchine formula*.

Theorem 5.12 (The Lévy-Khintchine Formula)**.** *If L is a Lévy process then for each $u \in \mathbb{R}$ and $t \geq 0$,*

$$\mathbb{E}\left[e^{iuL_t}\right] = \exp\left(t\psi_L(u)\right), \tag{5.13}$$

where ψ_L is the cumulant *function*[4] *of L_1 given by*

$$\psi_L(u) = iau - \frac{1}{2}\sigma^2 u^2 + \int_{\mathbb{R}_0} \left(e^{iuz} - 1 - iuz\mathbf{1}_{|z|<1}(z)\right)\nu(dz). \tag{5.14}$$

Proof. See Applebaum [2]. □

We now turn to a special case in the class of geometric models proposed above. For simplicity, we consider a forward contract delivering the spot at the single instant τ, i.e $f(t,\tau) = \mathbb{E}_{\mathbb{Q}}\left[S_\tau | \mathcal{F}_t\right]$. Suppose the log spot price has dynamics

$$d\ln S_t = d\ln\Lambda(t) + dX_t + dY_t, \tag{5.15}$$

where

$$dX_t = -\alpha X_t + \sigma dW_t, \tag{5.16}$$
$$dY_t = -\alpha Y_t + dL_t, \tag{5.17}$$

and $(L_t)_{t\geq 0}$ is a compound Poisson process with intensity λ and normally distributed jump size. That is, L is a pure jump Lévy process with characteristic triple $(\int_{|z|<1} z\nu(dz), 0, \nu)$. The Lévy measure is given by $\nu(dz) = \lambda f\left(z; a, b^2\right) dz$, where $f(z; a, b^2)$ is the density function of a Gaussian variable with mean a and variance b^2. Observing that

$$X_t + Y_t = \ln S_t - \ln\Lambda(t),$$

we may write

$$d\ln S_t = d\ln\Lambda(t) - \alpha(\ln S_t - \ln\Lambda(t))dt + \sigma dW_t + \int_{\mathbb{R}_0} zN(dt, dz). \tag{5.18}$$

[4]The log-characteristic function, also known as the Lévy exponent.

This is essentially the model proposed by Cartea and Figueroa [18], and can be seen as a mean-reverting analogue of the familiar Merton model for equity prices. The dynamics of the spot price is readily obtained from the Itô formula for semi-martingales. We obtain

$$dS_t = S_{t-} d \ln S_t + \frac{1}{2} S_{t-} d \left[\ln S, \ln S\right]_t^c + \left[e^{\ln S_{t-} + \Delta \ln S_t} - e^{\ln S_{t-}} - S_{t-} \Delta \ln S_t\right],$$

which amounts to

$$\frac{dS_t}{S_{t-}} = \alpha(\mu(t) - \ln S_t)dt + \sigma dW_t + \int_{\mathbb{R}_0} (e^z - 1) N(dt, dz), \tag{5.19}$$

where

$$\mu(t) = \frac{1}{\alpha}\left(\frac{d \ln \Lambda(t)}{dt} + \frac{1}{2}\sigma^2\right) + \ln \Lambda(t). \tag{5.20}$$

The seasonal component is usually modeled as a combination of a periodic signal (season) and a linear trend (inflation). Benth et al. [8] propose to model the seasonal component by a mixture of a deterministic function and a non-stationary stochastic process, gauging the uncertainty in the level to which the spot price mean-reverts. In this setup one is able to separate the low frequent variation in the trend from the short term stationary variations. Observe that the base and spike signal in our model share the same constant speed of mean-reversion α, which is somewhat restrictive. However, this specification yields closed-form forward prices which we use to benchmark a numerical procedure for solving the forward price PIDE.

5.1.1 Forward Pricing by PIDEs

The fundamental theorems of asset pricing assert the equivalence of market completeness and no-arbitrage, and the equivalence of no-arbitrage and the existence of a unique equivalent martingale measure (EMM)[5]. In markets with jumps completeness is in general lost. The EMM is no longer unique and there will be a continuum of pricing measures. In electricity and weather markets the underlying quantities are intangible assets which cannot be stored. In these situations buy-and-hold hedging arguments break down, rendering all equivalent measures applicable for pricing. To define a suitable pricing measure, we can employ the *Esscher transformation* to obtain a parametric family of measures that can be calibrated to observed market prices.

Esscher transform

Let $(\hat{\theta}, \tilde{\theta})$ denote the (constant) market price of risk for the jump and diffusion components. The Esscher transform is defined via the Radon-Nikodym density

[5] An equivalent martingale measure is a probability measure equivalent to the physical mesaure under which all tradeable assets are martingales after discounting.

process

$$\left.\frac{d\mathbb{Q}}{d\mathbb{P}}\right|_{\mathcal{F}_t} = \hat{Z}_t^\theta \times \tilde{Z}_t^\theta, \quad t \in [0,T], \tag{5.21}$$

where

$$\hat{Z}_t^\theta = e^{\hat{\theta}W_t - t\psi_W(-i\hat{\theta})}, \tag{5.22}$$

$$\tilde{Z}_t^\theta = e^{\hat{\theta}L_t - t\psi_L(-i\tilde{\theta})}. \tag{5.23}$$

Here, ψ_W and ψ_L are the cumulant functions of W and L. It follows from Girsanov's theorem that $W_t^\theta = W_t - \hat{\theta}t$ is a $\mathbb{Q}$-Wiener process. The characteristics of L under $\mathbb{Q}$ can be deduced from its characteristic function, and from Bayes' rule we obtain

$$\begin{aligned}
\mathbb{E}_{\mathbb{Q}}\left[e^{iuL_t}\right] &= \frac{\mathbb{E}\left[e^{iuL_t}\tilde{Z}_t^\theta\right]}{\mathbb{E}\left[\tilde{Z}_t^\theta\right]} \\
&= \mathbb{E}\left[e^{(iu+\tilde{\theta})L_t - t\psi_L(-i\tilde{\theta})}\right] \\
&= \exp\left(t\psi_L(u-i\tilde{\theta}) + \tilde{\theta}L_t - t\psi_L(-i\tilde{\theta})\right) \\
&= \exp\left(t\left\{\int_{\mathbb{R}_0}\left(e^{i(u-i\tilde{\theta})z}-1\right)\nu(dz) - \int_{\mathbb{R}_0}\left(e^{i(-i\tilde{\theta})z}-1\right)\nu(dz)\right\}\right) \\
&= \exp\left(t\int_{\mathbb{R}_0}\left(e^{iuz}-1\right)e^{\tilde{\theta}z}\nu(dz)\right).
\end{aligned}$$

The Lévy measure is exponentially tilted under $\mathbb{Q}$, changing the intensity and size of the jumps. Still, $N^\theta(t,A) = N(t,A)$, and we see that the paths have been re-weighted, but the set of possible paths is unaltered.

We follow Cartea and Figueroa [18] and assume that there is no market price on jump risk. We are effectively assuming that the jump risk is non-systematic, and thus can be diversified. This corresponds to the assumption of the original Merton model, where correlated diffusions represented systematic risk, whereas jump components were assumed independent.

With market price of risk given by $(\hat{\theta}, 0)$, the spot model has $\mathbb{Q}$-dynamics

$$\frac{dS_t}{S_{t-}} = \alpha(\hat{\mu}(t) - \ln S_t)dt + \sigma dW_t^\theta + \int_{\mathbb{R}_0}(e^z - 1)N(dt,dz), \tag{5.24}$$

with

$$\hat{\mu}(t) = \mu + \frac{\sigma}{\alpha}\hat{\theta}. \tag{5.25}$$

We can now state the price of a forward contract written on the spot dynamics (5.24).

Lemma 5.26 (Forward Price)**.** *The forward price at time $t \geq 0$ for a contract with settlement at time $T \geq t$ is given by*

$$f(t,T) = \Lambda(T)\left(\frac{S_t}{\Lambda(t)}\right)^{e^{-\alpha(T-t)}} \exp\left(\hat{\theta}\int_t^T \sigma(s)e^{-\alpha(T-s)}ds\right) \times$$
$$\exp\left(\frac{1}{2}\int_t^T \sigma^2(s)e^{-2\alpha(T-s)}ds + \int_t^T \exp\left(ae^{-\alpha(T-s)} + \frac{b^2}{2}e^{-2\alpha(T-s)}\right)\lambda ds - \lambda(T-t)\right) \tag{5.27}$$

Proof. Under $\mathbb{Q}$ the log spot has dynamics

$$d\ln S_t = \alpha(\tilde{\mu} - \ln S_t)dt + \sigma dW_t^\theta + \int_{\mathbb{R}_0} zN(dt,dz),$$

where

$$\tilde{\mu}(t) = \frac{1}{\alpha}\left(\frac{d\ln\Lambda(t)}{dt} + \sigma\hat{\theta}\right) + \ln\Lambda(t).$$

Itô's formula applied to to the function $g(t,x) = e^{\alpha t}x$ and $\ln S_t$ yields

$$d\left(e^{\alpha t}\ln S_t\right) = \alpha e^{\alpha t}\ln S_t dt + e^{\alpha t}d\ln S_t + \left[e^{\alpha t}(\ln S_{t-} + \Delta\ln S_t) - e^{\alpha t}\Delta\ln S_t\right],$$

whereupon we integrate over $(t,T]$,

$$\begin{aligned}\ln S_T =& e^{-\alpha(T-t)}\ln S_t + \alpha\int_t^T e^{-\alpha(T-s)}\tilde{\mu}(s)ds + \int_t^T \sigma(s)e^{-\alpha(T-s)}dW_s^\theta + \\ &\int_t^T\int_{\mathbb{R}_0} e^{-\alpha(T-s)}zN(ds,dz).\end{aligned}$$

Straightforward integration-by-parts shows that

$$\int_t^T e^{-\alpha(T-s)}\frac{d\ln\Lambda(s)}{ds}ds = \ln\Lambda(T) - e^{-\alpha(T-t)}\ln\Lambda(t) - \int_t^T \alpha e^{-\alpha(T-s)}d\ln\Lambda(s)ds,$$

and the log spot is given by

$$\begin{aligned}\ln S_T =& \ln\Lambda(T) + e^{-\alpha(T-t)}(\ln S_t - \ln\Lambda(t)) + \hat{\theta}\int_t^T \sigma(s)e^{-\alpha(T-s)}ds + \\ &\int_t^T \sigma(s)e^{-\alpha(T-s)}dW_s^\theta + \int_t^T\int_{\mathbb{R}_0} e^{-\alpha(T-s)}zN(ds,dz).\end{aligned}$$

The forward price is obtained as

$$\begin{aligned}f(t,T) &= \mathbb{E}_{\mathbb{Q}}\left[S_T|\mathcal{F}_t\right] \\ &= \mathbb{E}_{\mathbb{Q}}\left[e^{\ln S_T}|\mathcal{F}_t\right] \\ &= \Lambda(T)\left(\frac{S_t}{\Lambda(t)}\right)^{e^{-\alpha(T-t)}}\exp\left(\hat{\theta}\int_t^T \sigma(s)e^{-\alpha(T-s)}ds\right)\times \\ &\quad \mathbb{E}_{\mathbb{Q}}\left[\exp\left(\int_t^T \sigma(s)e^{-\alpha(T-s)}dW_s^\theta\right)\right]\mathbb{E}_{\mathbb{Q}}\left[\exp\left(\int_t^T\int_{\mathbb{R}_0} e^{-\alpha(T-s)}N(ds,dz)\right)\right],\end{aligned}$$

where we have used the independence and independent increment property of W and N. Since the Itô integral is Gaussian with zero mean and variance given by the Itô isometry, the first expectation is readily given as the moment generating function of a Gaussian variable,

$$\mathbb{E}_{\mathbb{Q}}\left[\exp\left(\int_t^T \sigma(s)e^{-\alpha(T-s)}dW^{\theta}(s)\right)\right] = \exp\left(\frac{1}{2}\int_t^T \sigma^2(s)e^{-2\alpha(T-s)}ds\right).$$

The last expectation needs special attention, and the details are spelled out in the appendix. We find that

$$\mathbb{E}_{\mathbb{Q}}\left[\exp\left(\int_t^T \int_{\mathbb{R}_0} e^{-\alpha(T-s)}zN(ds,dz)\right)\right] =$$
$$\exp\left(\int_t^\tau \exp\left(ae^{-\alpha(T-s)} + \frac{b^2}{2}e^{-2\alpha(T-s)}\right)\lambda ds - \lambda(T-t)\right).$$

□

Forward price PIDE

In general there will not be an explicit formula for the forward price, and we would like to address a numerical solution to the forward pricing problem in the jump-diffusion model. We derive the corresponding pricing PIDE, and our main purpose in this section is to illustrate how to deal with the integral term arising from the jump dynamics. Note that the compound Poisson process is a finite activity Lévy process, meaning that the Lévy measure is non-singular at zero. A discussion of the infinite activity case can be found in Cont and Voltchkova [21] and Cont and Tankov [20].

Lemma 5.28 (Forward price PIDE)**.** *The forward price at time $t \geq 0$ for a contract with settlement at time $T \geq t$ satisfies the following backward PIDE*

$$\begin{cases} \frac{\partial u}{\partial t} + \mathcal{L}u + \mathcal{I}u = 0, \quad \forall (t,x) \in [0,T) \times \mathbb{R}, \\ u(T,x) = x, \quad x \in \mathbb{R}. \end{cases} \tag{5.29}$$

Here

$$(\mathcal{L}u)(t,x) = \alpha\left(\hat{\mu} - \ln(x)\right)x\frac{\partial u}{\partial x} + \frac{1}{2}x^2\sigma(t)^2\frac{\partial^2 u}{\partial x^2}, \tag{5.30}$$

$$(\mathcal{I}u)(t,x) = \int_{\mathbb{R}_0}\left[u(t,xe^z) - u(t,x)\right]\nu(dz). \tag{5.31}$$

Proof. Since S is a Markov process, we may write the forward price as $u(t,S_t)$, where

$$u(t,x) = E_Q\left[S_T^{t,x}\right].$$

A straightforward application of Itô's formula yields

$$\begin{aligned}
du(t,S_t) =& \frac{\partial u}{\partial t}dt + \frac{\partial u}{\partial x}dS_t + \frac{1}{2}\frac{\partial^2 u}{\partial x^2}d[S,S]_t^c + \left[u(t,S_{t-}+\Delta S_t) - u(t,S_{t-}) - \frac{\partial u}{\partial x}\Delta S_t\right]. \\
=& \left[\frac{\partial u}{\partial t} + \alpha(\hat{\mu}(t) - \ln S_t)S_t\frac{\partial u}{\partial x} + \frac{1}{2}\sigma^2(t)S_t^2\frac{\partial^2 u}{\partial x^2}\right]dt + \\
& \frac{\partial u}{\partial x}\sigma(t)S_t dW_t^\theta + \int_{\mathbb{R}_0}\frac{\partial u}{\partial x}S_{t-}\left(e^z-1\right)N(dt,dz) + \\
& \int_{\mathbb{R}_0}\left(u(t,S_{t-}+S_{t-}(e^z-1)) - u(t,S_{t-}) - \frac{\partial u}{\partial x}S_{t-}(e^z-1)\right)N(dt,dz) \\
=& A_t dt + dM_t,
\end{aligned}$$

where

$$A_t = \frac{\partial u}{\partial t} + \alpha(\hat{\mu}(t) - \ln S_t)S_t\frac{\partial u}{\partial x} + \frac{1}{2}\sigma^2(t)S_t^2\frac{\partial^2 u}{\partial x^2} + \int_{\mathbb{R}_0}\left[u(t,S_{t-}e^z) - u(t,S_{t-})\right]\nu(dz)$$

and

$$dM_t = \frac{\partial u}{\partial x}\sigma(t)S_t dW_t^\theta + \int_{\mathbb{R}_0}\left[u(t,S_{t-}e^z) - u(t,S_{t-})\right]\tilde{N}(dt,dz).$$

The forward price is a $\mathbb{Q}$-martingale by construction, thus $A(t) = 0$. □

5.1.2 Localization and Discretization

We adopt a splitting scheme to solve problem (5.29) where we treat the differential and integral part separately. Due to the non-local nature of the integral[6], we incur a truncation error when disregarding jumps reaching outside the computational grid. However, by the exponential tapering of the Lévy measure this error decays exponentially with the size of the localized domain. The localization is in effect equivalent to a truncation of the Lévy measure itself.

Recall that

$$\nu(dz) = \lambda f\left(z; a, b^2\right)dz,$$

where $f(z; a, b^2)$ is the density function of a Gaussian variable with mean a and variance b^2 . It is convenient to employ the exponential transformation $y = e^z$ and work with the log-normally distributed jumps. Denote by $\tilde{\nu}$ the corresponding Lévy measure,

$$\tilde{\nu}(dy) = \frac{\lambda}{y}f\left(\ln y; a, b^2\right)dy. \tag{5.32}$$

[6]The log-spot Lévy measure is supported on the whole real line.

We use the change of variable $\tau = T - t$ and define $\bar{u}(\tau, x) = u(T - \tau, x)$ to transform the option pricing problem into an IBVP as we did in chapter 2. The pricing PIDE takes the form

$$\frac{\partial \bar{u}}{\partial \tau} = L\bar{u} + I\bar{u}, \tag{5.33}$$

with initial condition $\bar{u}(0, x) = x$. We introduce a computational grid

$$\{(\tau_n, s_i), \quad n = 0, ..., N, \ i = 0, ..., I\},$$

for the localized domain $(0, T] \times (0, S_{\max})$, where $\tau_n = T - n\Delta t$, $s_i = i\Delta s$, $\Delta t = \frac{T}{N}$ and $\Delta s = \frac{s_I}{I}$. The discretized jumps are defined as $y_{i,j} = \frac{s_j}{s_i}$, and we interpret s_i and s_j as the spot values immediately before and after the jump has taken place. For $i = 1, ..., I$ the jumps will be bounded by zero from below and by $y_i^{\max} = \frac{s_I}{s_i}$ from above, and we put $y_{0,j} = 0$ for all $j = 0, .., I$. In the node (τ_n, s_i) the truncated integral takes the form

$$\int_0^\infty (\bar{u}(\tau_n, s_i y) - \bar{u}(\tau_n, s_i)) \, \mathbf{1}_{[0, y_i^{\max}]}(y) \tilde{\nu}(dy). \tag{5.34}$$

To approximate the integral we use the trapezoidal rule and obtain

$$\begin{aligned}\int_0^\infty [\bar{u}(\tau_n, s_i y) - \bar{u}(\tau_n, s_i)] \, \mathbf{1}_{[0, y_i^{\max}]}(y) \tilde{\nu}(dy) &= \sum_{j=0}^{I-1} \int_{y_{i,j}}^{y_{i,j+1}} [\bar{u}(\tau_n, s_i y) - \bar{u}(\tau_n, s_i)] \, \tilde{\nu}(dy) \\ &\approx \sum_{j=0}^{I} [\bar{u}(\tau_n, s_j) - \bar{u}(\tau_n, s_i)] \, \tilde{\nu}_{i,j},\end{aligned}$$

where $s_j = s_i y_{i,j}$ and

$$\begin{aligned}\tilde{\nu}_{i,0} &= \frac{y_{i,1} - y_{i,0}}{2} \tilde{\nu}(y_{i,0}), \\ \tilde{\nu}_{i,j} &= \frac{y_{i,j+1} - y_{i,j-1}}{2} \tilde{\nu}(y_{i,j}), \quad j = 1, ..., I - 1, \\ \tilde{\nu}_{i,I} &= \frac{y_{i,I} - y_{i,I-1}}{2} \tilde{\nu}(y_{i,I}).\end{aligned}$$

We use an implicit-explicit operator splitting, and treat the integral operator explicitly due to the dense matrix structure produced in the discretization. If we denote by U the grid function approximating $\bar{u}$ and $\tau_n = T - n\Delta t$, we have the following finite difference scheme for $\theta \in [0, 1]$:

$$\begin{aligned}\frac{\Delta_\tau U_i^n}{\Delta t} &= \theta L U_i^{n+1} + (1 - \theta) L U_i^n + I U_i^n, \quad n = 0, ..., N - 1, \ i = 0, ..., I, \\ U_i^0 &= s_i, \quad i = 0, ..., I,\end{aligned} \tag{5.35}$$

where

$$LU_i^n = \alpha \left(\hat{\mu}(\tau_n) - \ln(s_i)\right) s_i \frac{\Delta_{0s} U_i^n}{\Delta s} + \frac{1}{2} \sigma^2(\tau_n) (s_i)^2 \frac{\delta_s^2 U_i^n}{(\Delta s)^2}, \ s = n, n + 1, \tag{5.36}$$

$$IU_i^n = \sum_{j=0}^{I} \left[U_j^n - U_i^n\right] \tilde{\nu}_{i,j}. \tag{5.37}$$

5.1.3 Numerical Results

We employ parameters similar to those in Benth et al. [4], where the jump-diffusion model is calibrated to German spot price data. Parameters are given in the table below. We use the composite Simpson's rule with 10 subintervals to evaluate all integrals, and assume $\Lambda(t) \equiv 1$ for numerical ease.

α	σ	λ	b	a
0.28	2.5	5	0.5	$-\frac{b^2}{2}$

Observe that the choice of a ensures that $\mathbb{E}\left[\int_0^t \int_{\mathbb{R}_0} (e^z - 1)\, N(ds, dz)\right] = 0$, such that the jumps do not give a systematic contribution to the spot price. In order to validate convergence, we define the *maximum relative error*

$$\text{MRE} \triangleq \max_{0 \le i \le M, 0 \le n \le M} \frac{|\bar{u}(\tau_n, s_i) - U_i^n|}{\bar{u}(\tau_n, s_i)}. \tag{5.38}$$

The exact solution is shown in figure 5.1. Prices are obtained for time to delivery ranging from 0 to 3 years and initial spot prices ranging from 0 to 200 (e.g. denominated in NOK/MWh).

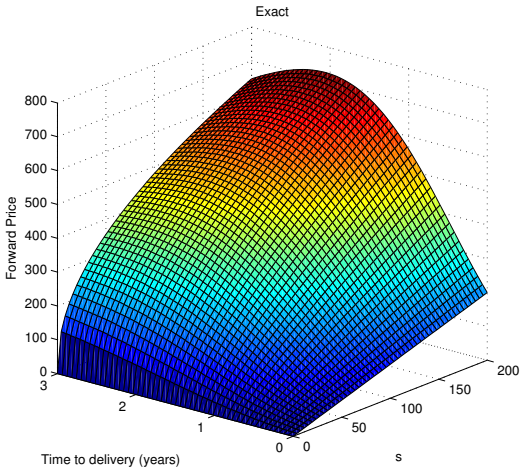

Figure 5.1: Forward price computed by the closed-form formula.

Figure 5.2 displays the numerical approximation when the exact solution is assigned as Dirichlet boundary conditions. Note that the error plotted on the right is the difference between the exact and the approximated solution. MRE is roughly 7%.

The numerical solution is seemingly correct, but there appears to be problems with convergence. The maximum relative error is plotted in figure 5.3 as a function of the number of grid points in each direction for different speeds of mean-reversion. The plot indicates that the error does not tend to zero as the grid is refined.

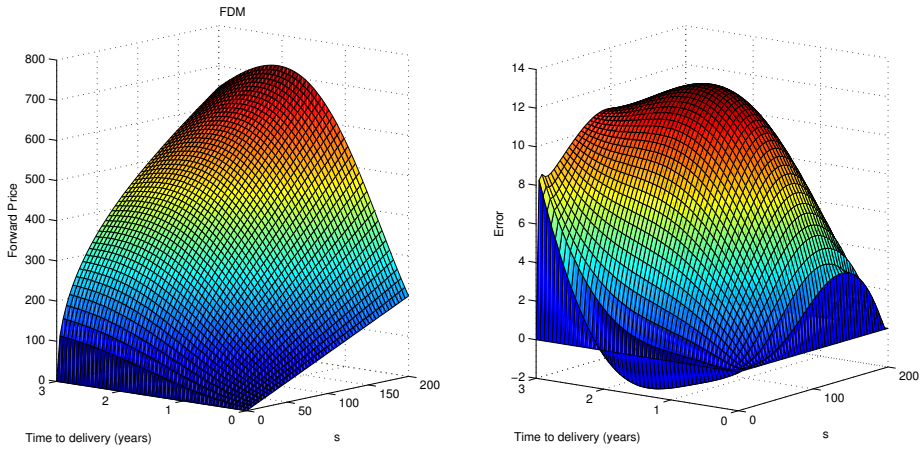

Figure 5.2: Forward price computed by the finite difference scheme (5.35), with $N = 50$ and $I = 50$.

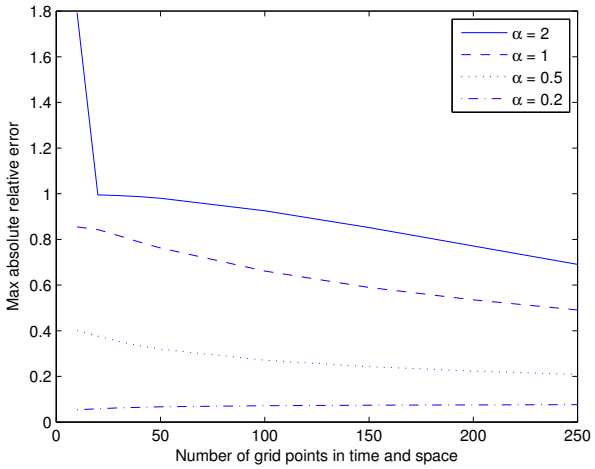

Figure 5.3: MRE for the finite difference scheme for various speeds of mean-reversion.

5.2 Temperature Derivatives

The first known weather derivative deal took place in 1996 as a bilateral electricity contract with an embedded weather rebate clause. In 1997 a market for trading OTC weather derivatives emerged, whereupon the Chicago Mercantile Exchange (CME) introduced the first exchange-traded weather futures and corresponding options in 1999. A multi-billion dollar industry developed within a few years of its inception, with a notional value of $12 billion in 2011. The CME offers futures and options on temperature indices for cities in the US, Canada, Europe, Japan and Australia. Similarly, there are futures settled against precipitation indices and the CME Hurricane Index (CHI), and also futures settled against a frost index based on the temperature in Amsterdam[7]. The options are usually of European style, but also American style binary options for precipitation and hurricane futures are avail-

[7]The frost index gauge the danger of frost on the runway at the Schipol airport in Amsterdam.

able for trading. In this section we discuss temperature derivatives and attempt to price European and American options on a CARMA spot temperature model. Most of the results and theory in this section are taken from Benth [5].

The contracts traded at CME are linked to temperature indices that facilitate trading weather as a commodity. The indices track the so-called *heating-degree days* and *cooling-degree days* in addition to the *cumulative average temperature*. Let T_t denote the mean temperature on day t, defined as the average of the maximum and minimum temperature measured that day. That is,

$$T_t = \frac{T_t^{\max} + T_t^{\min}}{2}. \tag{5.39}$$

The index based on aggregated heating-degree days quantify monthly or seasonal deviation from a threshold of 18 degrees Celsius during the winter season (lasting from October to April). A heating-degree day (HDD) is mathematically defined as $\mathrm{HDD}(t) = (c - T_t)^+$, where $c = 18$. The index geared to the aggregated HDD is effectively measuring the demand for heating. Analogously, the index based on aggregated cooling-degree days applies during the summer season, where a cooling-degree day (CDD) is defined as $\mathrm{CDD}(t) = (T_t - c)^+$. In European and Canadian locations the aggregated CDD is replaced by the cumulative average temperature (CAT) index, which is defined as $\mathrm{CAT}(\tau_1, \tau_2) = \sum_{t=\tau_1}^{\tau_2} T_t$, for the measurement period $[\tau_1, \tau_2]$. The futures are settled against the indices times a cash amount pertaining to the regional currency. For the contractual measurement period $[\tau_1, \tau_2]$, $\tau_1 \leq \tau_2$, the futures deliver

$$\mathrm{HDD}(\tau_1, \tau_2) = a \sum_{t=\tau_1}^{\tau_2} (c - T_t)^+, \tag{5.40}$$

$$\mathrm{CDD}(\tau_1, \tau_2) = a \sum_{t=\tau_1}^{\tau_2} (T_t - c)^+, \tag{5.41}$$

$$\mathrm{CAT}(\tau_1, \tau_2) = a \sum_{t=\tau_1}^{\tau_2} T_t, \tag{5.42}$$

where a is the constant cash amount (e.g. \$20). Notice that the HDD and CDD indices comprise strips of put and call options on the spot temperature. In the sequel we let $a = 1$ and replace summation by integration for analytical ease. Thus, we redefine (5.40)-(5.42) and consider futures contracts written on the indices

$$\mathrm{HDD}(\tau_1, \tau_2) \triangleq \int_{\tau_1}^{\tau_2} (c - T_\tau)^+ \, d\tau, \tag{5.43}$$

$$\mathrm{CDD}(\tau_1, \tau_2) \triangleq \int_{\tau_1}^{\tau_2} (T_\tau - c)^+ \, d\tau, \tag{5.44}$$

$$\mathrm{CAT}(\tau_1, \tau_2) \triangleq \int_{\tau_1}^{\tau_2} T_\tau d\tau. \tag{5.45}$$

Settlement is at the end of the measurement period.

In order to obtain futures and corresponding option prices, we must provide an adequate description of the temperature evolution. In Benth [5] and Benth et al. [6] empirical evidence supports the application of CARMA models to describe *deseasonalized* temperature. Moreover, they propose to model the temperature dynamics as

$$T_t = \Lambda(t) + Y_t, \quad t \geq 0, \tag{5.46}$$

where $\Lambda(t)$ is a continuous and bounded deterministic seasonality function, and Y is the Gaussian CARMA(p,q) process defined in chapter 4. We saw that the limiting distribution of Y is Gaussian with mean zero, so the temperature dynamics will be mean-reverting towards $\Lambda(t)$, being its long-term level. In particular, they find that deseasonalized temperature follows a CAR(3) process.

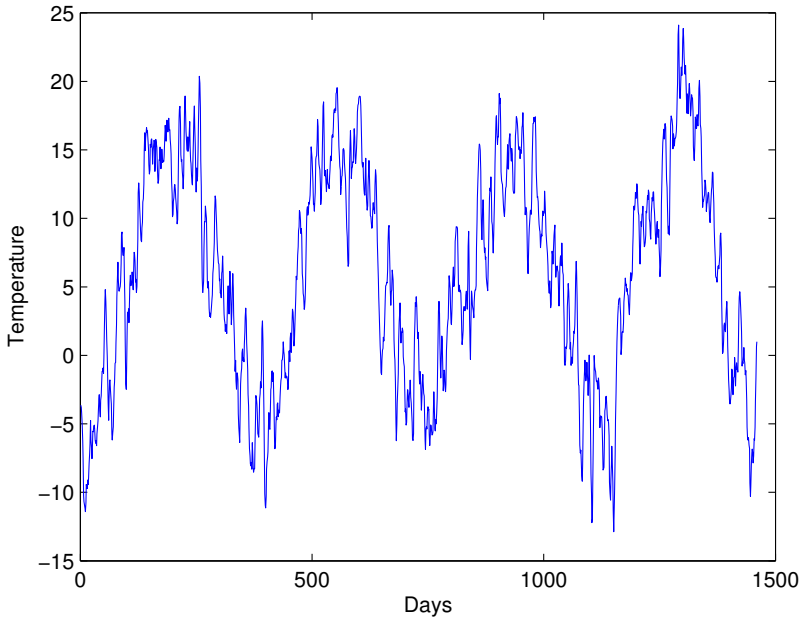

Figure 5.4: Temperature simulation. Y follows a CAR(3) process with parameters taken from Benth [5] p. 126.

5.2.1 Temperature Futures

Adopting the notation in Benth[5], we would like to determine the price at time $t \leq \tau_1$ of a futures contract written on the generic index $\text{Ind} \in \{\text{HDD}, \text{CDD}, \text{CAT}\}$ given by

$$F_{\text{Ind}}(t, \tau_1, \tau_2) = \mathbb{E}_{\mathbb{Q}}\left[\text{Ind}(\tau_1, \tau_2) \mid \mathcal{F}_t\right]. \tag{5.47}$$

$\mathbb{Q}$ is a suitable equivalent probability measure[8] which is parameterized by the bounded, measurable and real-valued function $\theta_0(t)$ and the vector $\theta = (\theta_p, ..., \theta_1)^T$, $\theta_i <$

[8]Recall that buy-and-hold strategies do not exist, thus $\mathbb{Q}$ need not be an equivalent martingale measure.

$\alpha_i,\ i = 1, ..., p$. Benth[5] shows that a Girsanov transformation is viable with density process given by

$$\left.\frac{d\mathbb{Q}}{d\mathbb{P}}\right|_{\mathcal{F}_t} = \exp\left(\int_0^t \frac{\theta_0(s) + \theta^T \mathbf{X}_s}{\sigma(s)} dW_s - \frac{1}{2}\int_0^t \frac{\left(\theta_0(s) + \theta^T \mathbf{X}_s\right)^2}{\sigma^2(s)} ds\right), \tag{5.48}$$

for $t \in [0, \tau]$, $\tau < \infty$. If we let

$$d\widetilde{W}_t = \sigma^{-1}(t)\left(\theta_0(t) + \theta^T \mathbf{X}_t\right) dt + dW_t, \tag{5.49}$$

then $\left(\widetilde{W}_t\right)_{0 \le t \le \tau}$ will be a $\mathbb{Q}$-Wiener process. This is a structure preserving class of measure changes, in the sense that Y is still a CARMA process with respect to $\mathbb{Q}$, but with a new level and speed of mean-reversion. Moreover, the dynamics of $\mathbf{X}_t$ after the change of measure is

$$d\mathbf{X}_t = \left(\mathbf{e}_p \theta_0(t) + \mathbf{A}_\theta \mathbf{X}_t\right) dt + \mathbf{e}_p \sigma(t) d\widetilde{W}_t, \tag{5.50}$$

where

$$A_\theta = \begin{bmatrix} 0 & 1 & 0 & \cdots & 0 \\ 0 & 0 & 1 & \cdots & 0 \\ \vdots & \vdots & \vdots & \ddots & \\ 0 & 0 & 0 & \cdots & 1 \\ -(\alpha_p - \theta_p) & -(\alpha_{p-1} - \theta_{p-1}) & -(\alpha_{p-2} - \theta_{p-2}) & \cdots & -(\alpha_1 - \theta_1)) \end{bmatrix}.$$

The market price of risk parameters θ and $\theta_0(t)$ must be calibrated from observed futures prices. In our applications we assume that there is no market price of risk, effectively choosing the physical measure as the pricing measure (i.e. $\mathbb{Q} = \mathbb{P}$).

The following arbitrage relation is easily shown to exist

Lemma 5.51. *It holds that*

$$F_{CDD}(t, \tau_1, \tau_2) - F_{HDD}(t, \tau_1, \tau_2) = F_{CAT}(t, \tau_1, \tau_2) - c(\tau_2 - \tau_1). \tag{5.52}$$

Proof. See Benth[5] □

In light of lemma 5.51, we restrict our discussion to CAT and CDD futures. Given the CARMA initial state $\mathbf{X}_s$, The temperature dynamics (5.46) for $t \ge s$ can be written as

$$T_t = m(s, t, \mathbf{X}_s) + \Sigma(s, t) Z, \tag{5.53}$$

with

$$m(s,t,\mathbf{X}_s) = \Lambda(t) + \mathbf{b}^T e^{\mathbf{A}(t-s)}\mathbf{X}_s, \tag{5.54}$$

$$\Sigma_0^2(s,t) = \int_s^t \left(\mathbf{b}^T e^{\mathbf{A}(t-u)}\mathbf{e}_p\right)^2 \sigma^2(u)du, \tag{5.55}$$

and $Z \sim \mathcal{N}(0,1)$. For $0 \leq v \ \leq u$, we introduce

$$C(u,v) = \mathbf{A}^{-1}\left(e^{\mathbf{A}u} - e^{\mathbf{A}v}\right). \tag{5.56}$$

Note that $\det(\mathbf{A}) = -\alpha_p$, so $\mathbf{A}$ is indeed invertible. We proceed by stating the CAT and CDD futures prices and corresponding dynamics in a series of propositions. Proofs can be found in Benth [5], chapter 5.

Proposition 5.57. *For $t \leq \tau_1 < \tau_2$, it holds that*

$$F_{CAT}(t,\tau_1,\tau_2) = \int_{\tau_1}^{\tau_2} \Lambda(s)ds + \mathbf{b}^T C(\tau_2 - t, \tau_1 - t)X_t. \tag{5.58}$$

Proposition 5.59. *The $\mathbb{Q}$-dynamics of $F_{CAT}(t,\tau_1,\tau_2)$ for $t \leq \tau_1 < \tau_2$ is*

$$dF_{CAT}(t,\tau_1,\tau_2) = \mathbf{b}^T C(\tau_2 - t, \tau_1 - t)\mathbf{e}_p\sigma(t)dW_t. \tag{5.60}$$

Define

$$\Psi(x) \triangleq x\Phi(x) + \phi(x), \tag{5.61}$$

where $\Phi(x)$ is the standard normal distribution function and $\phi(x) = \Phi'(x)$.

Proposition 5.62. *For $t \leq \tau_1 < \tau_2$, it holds that*

$$F_{CDD}(t,\tau_1,\tau_2) = \int_{\tau_1}^{\tau_2} \Sigma_0(t,s)\Psi\left(\frac{m(t,s,\mathbf{X}_t) - c}{\Sigma_0(t,s)}\right)ds \tag{5.63}$$

Proposition 5.64. *The $\mathbb{Q}$-dynamics of $F_{CDD}(t,\tau_1,\tau_2)$ for $t \leq \tau_1 < \tau_2$ is*

$$dF_{CDD}(t,\tau_1,\tau_2) = \sigma(t)\int_{\tau_1}^{\tau_2} \mathbf{b}^T e^{\mathbf{A}(s-t)}\mathbf{e}_p\Phi\left(\frac{m(t,u,\mathbf{X}_t) - c}{\Sigma_0(t,s)}\right)dsdW_t. \tag{5.65}$$

5.2.2 Option Pricing by PDEs

For the Gaussian CARMA(p,q) temperature model, option prices can be derived in (semi) closed-form. We first state and prove the option price on spot temperature,

then give the results on European call options on CAT and CDD futures taken from Benth [5]. Put option prices can be obtained by the put-call parity.

Let $f(x) = (x - K)^+$ for some constant K.

Proposition 5.66. *The price of a call option at time $t \geq 0$ with exercise time $T \geq t$ and strike price K written on the spot temperature (??), is given by*

$$C_t = e^{-r(T-t)}\Sigma_0(t,T)\Psi\left(d(t,T,\mathbf{X}_t)\right), \tag{5.67}$$

where

$$d(t,T,\mathbf{x}) = \frac{m(t,T,\mathbf{x}) - K}{\Sigma_0(t,T)}, \tag{5.68}$$

and Ψ as above.

Proof. Since Y_t is a Markov process,

$$\begin{aligned}
C_t &= \mathbb{E}_{\mathbb{Q}}\left[e^{-r(T-t)}f(Y_T) \mid \mathcal{F}_t\right] \\
&= \mathbb{E}_{\mathbb{Q}}\left[e^{-r(T-t)}f(\Lambda(T) + \mathbf{b}^T\mathbf{X}_T^{t,\mathbf{x}})\right]_{\mathbf{x}=\mathbf{X}_t} \\
&= e^{-r(T-t)}\int_{\mathbb{R}}\left[m(t,T,\mathbf{x}) + \Sigma_0(t,T)z - K\right]\mathbf{1}_{\{m(t,T,\mathbf{x})+\Sigma_0(t,T)z>K\}}\phi(z)dz\Big|_{\mathbf{x}=\mathbf{X}_t} \\
&= e^{-r(T-t)}\Sigma_0(t,T)\left(\int_{-\infty}^{d(t,T,\mathbf{x})} d(t,T,\mathbf{x})\phi(y)dy + \int_{-\infty}^{d(t,T,\mathbf{x})}(-y)\phi(y)dy\right)\Big|_{\mathbf{x}=\mathbf{X}_t} \\
&= e^{-r(T-t)}\Sigma_0(t,T)\Psi(d(t,T,\mathbf{X}_t)),
\end{aligned}$$

where we have used the change of variables $z = -y$. □

Proposition 5.69. *The price of a call option at time $t \geq 0$ with exercise time $\tau \geq t$ and strike price K written on a CAT futures with measurement period $[\tau_1, \tau_2]$ is*

$$\begin{aligned}
C_{CAT}(t,\tau,K,\tau_1,\tau_2) = e^{-r(\tau-t)}\big[&(F_{CAT}(t,\tau_1,\tau_2) - K)\,\Phi(d(t,\tau,\tau_1,\tau_2,K)) \\
&+ \Sigma_{CAT}(t,\tau,\tau_1,\tau_2)\phi(d(t,\tau,\tau_1,\tau_2,K))\big],
\end{aligned} \tag{5.70}$$

where

$$\Sigma^2_{CAT}(t,\tau,\tau_1,\tau_2) = \int_t^\tau \mathbf{b}^T C(\tau_2 - s, \tau_1 - s)\mathbf{e}_p\mathbf{e}_p^T C(\tau_2 - s, \tau_1 - s)^T\mathbf{b}^T\sigma^2(s)ds, \tag{5.71}$$

and

$$d(t,\tau,\tau_1,\tau_2,K) = \frac{F_{CAT}(t,\tau_1,\tau_2) - K}{\Sigma_{CAT}(t,\tau,\tau_1,\tau_2)}. \tag{5.72}$$

The call option price on CDD futures is not explicitly given in terms of the index dynamics. However, the following semi closed-form formula can be tackled by means of Monte Carlo and numerical integration.

Proposition 5.73. *The price of a call option at time $t \geq 0$ with exercise time $\tau \geq t$ and strike price K written on a CDD futures with measurement period $[\tau_1, \tau_2]$, $\tau \leq \tau_1$, is*

$$C_{CDD}(t, \tau, \tau_1, \tau_2) = e^{-r(\tau - t)} \mathbb{E}_{\mathbb{Q}} \left[\left(\int_{\tau_1}^{\tau_2} \Sigma_0(\tau, s) \Psi \left(\frac{m(t, s, \mathbf{x}) - c + Z\Sigma(t, \tau, s)}{\Sigma_0(\tau, s)} \right) ds - K \right)^+ \right]_{\mathbf{x} = \mathbf{X}_t} \tag{5.74}$$

where

$$\Sigma^2(t, \tau, s) = \int_t^{\tau} \mathbf{b}^T e^{\mathbf{A}(s-u)} \mathbf{e}_p \mathbf{e}_p^T e^{\mathbf{A}^T(s-u)} \mathbf{b} \sigma^2(u) du. \tag{5.75}$$

Option Price PDEs

Lemma 5.76. *Let $u \in C^{1,2}((0, \tau) \times \mathbb{R}^p)$. The value at time $t \geq 0$ of a European call option with maturity $\tau \geq t$ and strike price K on the temperature spot model (5.46) verifies the backward PDE*

$$\begin{cases} \frac{\partial u}{\partial t} + \mathcal{L}u - ru = 0, \quad \forall (t, \mathbf{x}) \in [0, \tau) \times \mathbb{R}^p, \\ u(\tau, \mathbf{x}) = f(\Lambda(\tau) + \mathbf{b}^T \mathbf{x}), \quad \mathbf{x} \in \mathbb{R}^p. \end{cases} \tag{5.77}$$

Here

$$(\mathcal{L}u)(t, \mathbf{x}) = \sum_{j=1}^{p} b_j(t, \mathbf{x}) \frac{\partial u}{\partial x_j} + \frac{1}{2} \sum_{i,j=1}^{p} a_{i,j}(t, \mathbf{x}) \frac{\partial^2 u}{\partial x_i \partial x_j}, \tag{5.78}$$

where

$$\begin{cases} b_j(t, \mathbf{x}) = x_j, \quad j = 1, ..., p-1 \\ b_p(t, \mathbf{x}) = -\sum_{i=1}^{p} \alpha_{p+1-i} x_i \end{cases} \tag{5.79}$$

and

$$\begin{cases} a_{i,j}(t, \mathbf{x}) = 0, \quad i, j = 1, ..., p-1 \\ a_{p,p}(t, \mathbf{x}) = \sigma^2(t). \end{cases} \tag{5.80}$$

Proof. We may write the call option price at time t as $u(t, \mathbf{X}_t)$, where

$$u(t, \mathbf{x}) = \mathbb{E}_{\mathbb{Q}} \left[f(\Lambda(\tau) + \mathbf{b}^T \mathbf{x}) \right].$$

The multi-dimensional Itô formula applied to $\hat{u}(t,\mathbf{x}) = e^{-rt}u(t,\mathbf{x})$ and $\mathbf{X}_t$ yields

$$d\hat{u}(t,\mathbf{X}_t) = A_t dt + dM_t,$$

where

$$A_t = e^{-rt}\left(\frac{\partial u}{\partial t} + \mathcal{L}u - ru\right)(t,\mathbf{X}_t)$$
$$dM_t = e^{-rt}\frac{\partial u(t,\mathbf{X}_t)}{\partial x_p}\sigma(t)dW_t.$$

Since

$$\hat{u}(t,\mathbf{X}_t) - M_t = \int_0^t A_s ds,$$

is a $\mathbb{Q}$-martingale and $\int_0^t A_s ds$ is a continuous process of finite variation, we must have that $A_t = 0$ $\mathbb{Q}$-a.s. □

Lemma 5.81. *Let $u \in C^{1,2}((0,\tau)\times\mathbb{R}^p)$. The value at time $t \geq 0$ of a European call option with maturity $\tau \geq t$ and strike price K on a CAT futures verifies the backward PDE*

$$\begin{cases} \frac{\partial u}{\partial t} + \mathcal{L}u - ru = 0, \quad \forall (t,x) \in [0,\tau)\times\mathbb{R}, \\ u(\tau,x) = f(x), \quad x \in \mathbb{R}. \end{cases} \tag{5.82}$$

Here

$$(\mathcal{L}u)(t,x) = \frac{1}{2}\left(\mathbf{b}^T C(\tau_2 - t, \tau_1 - t)\mathbf{e}_p\sigma(t)\right)^2 \frac{\partial^2 u(t,x)}{\partial x^2}. \tag{5.83}$$

Proof. It follows from (5.58) that $F_{\mathrm{CAT}}(t,\tau_1,\tau_2)$ is a Markov process, and we may write the call option price at time t as $u(t, F_{\mathrm{CAT}}(t,\tau_1,\tau_2))$, where

$$u(t,x) = \mathbb{E}_{\mathbb{Q}}\left[f(F^{t,x}_{\mathrm{CAT}}(\tau,\tau_1,\tau_2))\right].$$

An application of Itô's formula to $\hat{u}(t,x) = e^{-rt}u(t,x)$ and $F_{\mathrm{CAT}}(t,\tau_1,\tau_2)$ yields

$$d\hat{u}(t,\mathbf{X}_t) = A_t dt + dM_t,$$

where

$$A_t = e^{-rt}\left(\frac{\partial u}{\partial t} + \mathcal{L}u - ru\right)(t, F_{\mathrm{CAT}}(t,\tau_1,\tau_2))$$
$$dM_t = e^{-rt}\mathbf{b}^T C(\tau_2 - t, \tau_1 - t)\mathbf{e}_p\sigma(t)\frac{\partial u(t, F_{\mathrm{CAT}}(t,\tau_1,\tau_2))}{\partial x}dW_t.$$

Since

$$\hat{u}(t, F_{\mathrm{CAT}}(t,\tau_1,\tau_2)) - M_t = \int_0^t A_s ds,$$

is a $\mathbb{Q}$-martingale and $\int_0^t A_s ds$ is a continuous process of finite variation, we must have that $A_t = 0$ $\mathbb{Q}$-a.s. □

Options on CDD futures are different. The Markov property allows us to write the option price as[9]

$$u(t,\mathbf{x}) = \mathbb{E}_{\mathbb{Q}}\left[f(F_{\text{CDD}}(\tau,\tau_1,\tau_2,\mathbf{X}_\tau^{t,\mathbf{x}}))\right]_{\mathbf{x}=\mathbf{X}_t}, \tag{5.84}$$

given the CARMA state $\mathbf{X}_t$, if we define

$$F_{\text{CDD}}(t,\tau_1,\tau_2,\mathbf{x}) = \int_{\tau_1}^{\tau_2} \Sigma_0(t,s)\Psi\left(\frac{m(t,s,\mathbf{x})-c}{\Sigma_0(t,s)}\right) ds. \tag{5.85}$$

We can then cast the price as the solution to a PDE in terms of the CARMA states, in which case the payoff function would be $f \circ F_{\text{CDD}}(\mathbf{x})$. However, this approach rests on a slightly awkward and complicated connection between the option price and the CARMA states, and we were unable to produce any sensible numerical results.

In the case of American put options, the pricing PDEs are replaced by their respective partial differential inequalities, with the obvious modifications due to the payoff function. These are solved with the methods described in chapter 3.

5.2.3 Localization and Discretization

We solve one-dimensional problems with the θ-method and two-dimensional problems with ADI. In this section we illustrate localization and discretization of problem (5.77) where deseasonalized temperature is assumed to follow a CARMA(2,1) process.

We model temperature as

$$T_t = \Lambda(t) + Y_t, \quad t \geq 0,$$

where Y is the CARMA(2,1) process

$$\begin{aligned} Y_t &= \mathbf{b}^T\mathbf{X}_t, \\ d\mathbf{X}_t &= \mathbf{A}X_t dt + \sigma(t)\mathbf{e}_p dW_t, \end{aligned}$$

and

$$\mathbf{A} = \begin{pmatrix} 0 & 1 \\ -\alpha_2 & -\alpha_1 \end{pmatrix}, \quad \mathbf{e}_p = \begin{pmatrix} 0 \\ 1 \end{pmatrix}, \mathbf{b} \quad = \begin{pmatrix} 1 \\ b_1 \end{pmatrix}, \quad \mathbf{X}_t = \begin{pmatrix} X_t \\ X_t^{(1)} \end{pmatrix}.$$

We have that $Y_t = X_t + b_1 X_t^{(1)}$ with state dynamics

$$\begin{cases} dX_t &= X_t^{(1)} dt, \\ dX_t^{(1)} &= -(\alpha_2 X_t + \alpha_1 X_t^{(1)})dt + \sigma(t)dW_t. \end{cases} \tag{5.86}$$

[9] f and F_{CDD} are continuous and thus measurable, hence $f \circ F_{\text{CDD}}$ is also measurable.

We transform the problem into an IBVP by the change of variable $\bar{\tau} = \tau - t$, and consider the corresponding pricing equation in $\bar{u}(\bar{\tau}) = u(\tau - t)$,

$$\frac{\partial \bar{u}}{\partial \bar{\tau}} = x_1 \frac{\partial \bar{u}}{\partial x_1} - (\alpha_2 x_1 + \alpha_1 x_2) \frac{\partial \bar{u}}{\partial x_2} + \frac{1}{2}\sigma^2(\tau - \bar{\tau}) \frac{\partial^2 \bar{u}}{\partial x_2^2} - r\bar{u}, \tag{5.87}$$

with the initial condition $\bar{u}(0, \mathbf{x}) = f(\Lambda(\tau) + \mathbf{b}^T \mathbf{x})$. The states are confined to the finite domain

$$\Omega = \left(X_1^{min}, X_1^{max}\right) \times \left(X_2^{min}, X_2^{max}\right),$$

with the exact solution assigned as Dirichlet boundary conditions. In other words, there will be no error on the boundaries. Discretization in time and space yields the computational grid

$$\{(\bar{\tau}_n, x_{1,i}, x_{2,j}), \quad n = 0, ..., N,\ i = 0, ..., I,\ j = 0, ..., J\},$$

where

$$\begin{aligned} \bar{\tau}_n &= \tau - n\Delta t, & \Delta t &= \frac{\tau}{N}, \\ x_{1,i} &= x_{1,0} + i\Delta x_1, & \Delta x_1 &= \frac{x_{1,I} - x_{1,0}}{I}, \\ x_{2,j} &= x_{2,0} + j\Delta x_2, & \Delta x_2 &= \frac{x_{2,J} - x_{2,0}}{J}. \end{aligned}$$

As usual, we let U be the grid function approximating $\bar{u}$ and obtain the following Douglas ADI scheme:

$$\begin{cases} (1 - \theta\Delta t A_1)\, U_{i,j}^* = (1 + (1-\theta)\Delta t A_1 + \Delta t A_2)\, U_{i,j}^n \\ (1 - \theta\Delta t A_2)\, U_{i,j}^{n+1} = U_{i,j}^* - \theta\Delta t A_2 U_{i,j}^n \end{cases} \tag{5.88}$$

with

$$A_1 U_{i,j}^n = x_{1,i} \frac{\Delta_{0x_1}}{\Delta x_1} U_{i,j}^n - \frac{1}{2} r U_{i,j}^n \tag{5.89}$$

$$A_2 U_{i,j}^n = -(\alpha_2 x_{1,i} + \alpha_1 x_{2,j}) \frac{\Delta_{0x_2}}{\Delta x_2} U_{i,j}^n + \frac{1}{2}\sigma^2(\bar{\tau}_n) \frac{\delta_{x_2}^2}{(\Delta x_2)^2} U_{i,j}^n - \frac{1}{2} r U_{i,j}^n. \tag{5.90}$$

5.2.4 Numerical Results

We now illustrate the performance of the numerical option pricing schemes. First, we give results on European call and American put options in two CARMA spot temperature models, then briefly discuss a European call on the CAT futures. Observe that we denote time in days, as the CARMA models are naturally set on a daily time-scale. We refer to the error as the difference between the exact and the approximated solution, and to investigate convergence we employ the *maximum absolute error* which we define as

$$\text{MAE}(N) \stackrel{\Delta}{=} \max_{0 \le i \le I, 0 \le j \le J} |\bar{u}(\tau_N, x_{1,i}, x_{2,j}) - U_{i,j}^N|. \tag{5.91}$$

The seasonal component will be taken from Benth et al. [6], where a CAR(3) model is fitted to temperature data observed in Stockholm. They find that

$$\Lambda(t) = 6.3750 + 0.0001t + 10.4411 \cos\left(\frac{2\pi(t + 165.7591)}{365}\right).$$

Carma parameters are chosen according to the table below and we assume constant volatility for convenience. The set of autoregressive coefficients in the CARMA(2,1) model are deliberately chosen to match a set of non-complex eigenvalues ($\lambda_1 = -0.2$ and $\lambda_2 = -1$) to reduce the risk of numerical instabilities. We choose $\theta = \frac{1}{2}$ in the Douglas ADI scheme, and use the composite Simpson's rule with 10 subintervals to perform numerical integration.

Model	α_1	α_2	b_1	σ (daily)	r (annually)	τ (days)
CAR(1)	0.1	-	-	3.5	0.05	0-30
CARMA(2,1)	1.2	0.2	1	3.5	0.05	1, 5

European Options on Temperature Spot

Figure 5.5 and figure 5.6 show option prices on spot temperature in the CAR(1) model computed by the exact formula (5.67) and by finite differences. We observe minor oscillations due to the non-smooth initial condition that die out as we step away from maturity. This was not the case with the forward price, where the initial condition is smooth. We see that the price is insensitive to the CARMA state for longer maturities.

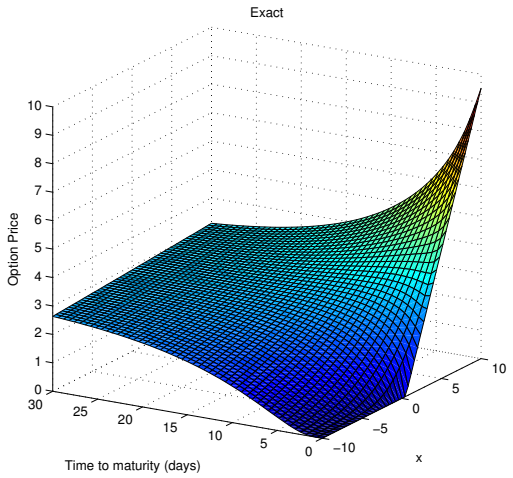

Figure 5.5: European call option in CAR(1) model. Exact solution.

Option prices in the CARMA(2,1) model computed with the Douglas ADI scheme are shown in figure 5.9 and figure 5.10, corresponding to 1 and 5 days to maturity, respectively. The exact solution is given in figure 5.8. The ADI approximation is somewhat inflated, which can be seen from the error plotted on the right and in the curvature in the surface. This inconsistency disappears when time to maturity

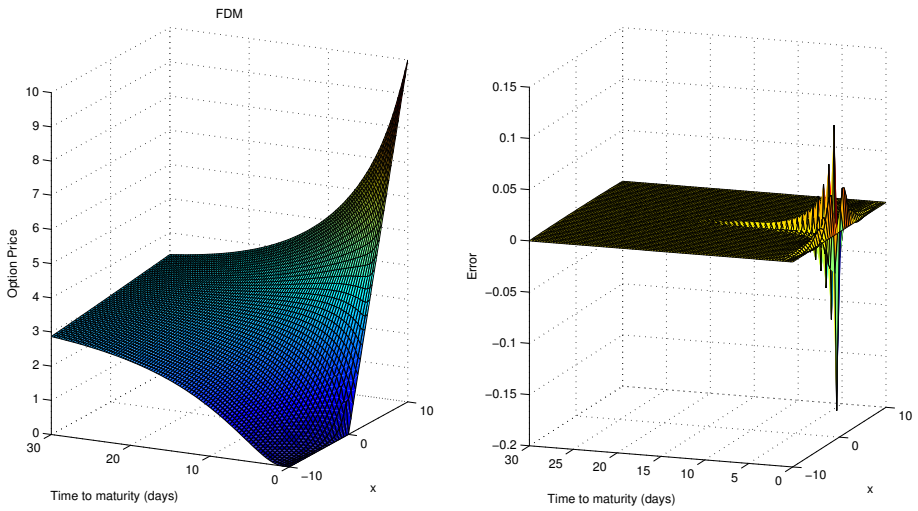

Figure 5.6: European call option in CAR(1) model computed with the θ-method. $I = N = 50$.

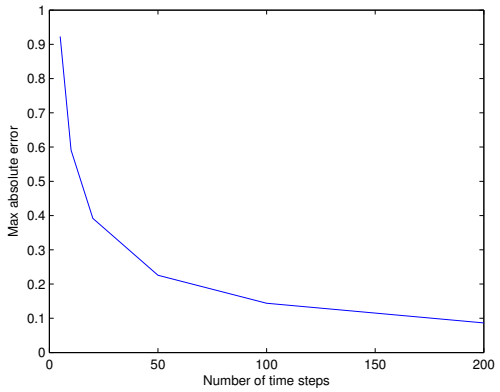

Figure 5.7: MAE for the European call option in CAR(1) model.

increases. Numerical testing reveals that the approximation quickly deteriorates as we expand the range of x_2, but is seemingly unaffected by the range of x_1. More testing shows that the quality of the approximation is parameter sensitive, in particular with respect to the diffusion coefficient; larger diffusion improves the approximation, whereas smaller diffusion leads to a deterioration. Moreover, the convergence of the scheme is questionable; smaller time-steps yield a marginally smaller error, but for a sufficiently refined spatial mesh the error is seen to increase. We have plotted the MAE in figure 5.11, and we note that the coarser grid yields lower MAE.

American Options

We use Longstaff-Schwartz (LSM) to benchmark the results on American options. As in chapter 3, we use $\psi_1(x) = 1,\ \psi_2(x) = x,\ \psi_3(x) = x^2$ as basis functions. Con-

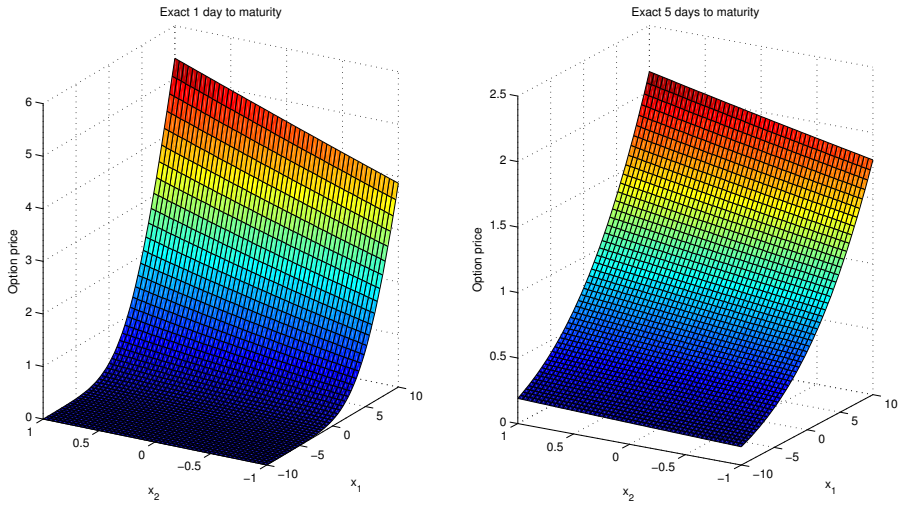

Figure 5.8: European call option in CARMA(2,1) model. Exact solution.

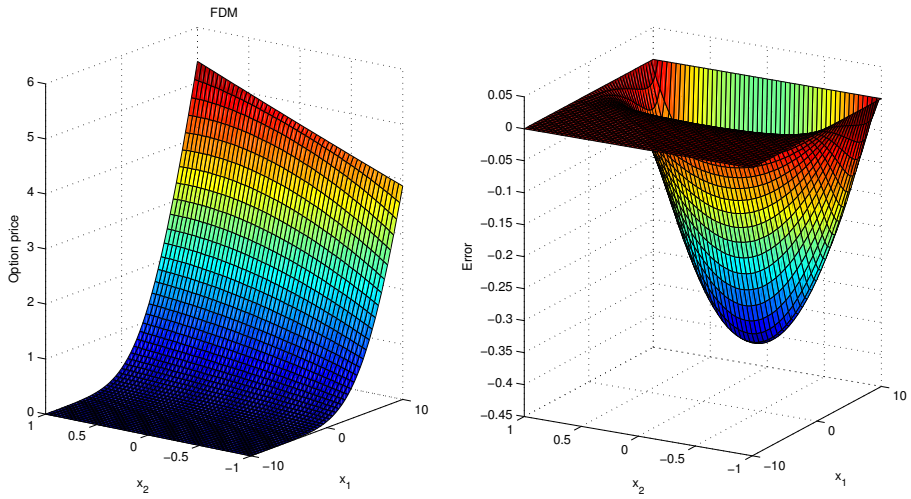

Figure 5.9: European call option in CARMA(2,1) model computed with Douglas ADI. 1 day to maturity. $I = J = 50$ and $N = 100$.

structing the price surface in the CARMA(2,1) model requires $(I+1) \times (J+1)$ runs of the algorithm, which is potentially very time-consuming. To find a compromise between accuracy and computational time we go back to figure 3.2 in chapter 3. A visual inspection suggests that we should (at least) employ roughly 1000 Monte Carlo samples and 50 time steps.

Figure 5.12 shows the price of an American put option in the CAR(1) model obtained by LSM; figure 5.13 shows the result from the Brennan-Schwartz algorithm with the free-boundary superimposed. The LSM estimates are assigned as Dirichlet boundaries. The outermost boundary layers are not included in the plot due to irregularities stemming from the simulations. The approximations seem to agree. Figure 5.12 shows the price of an American put with expiration in 5 days computed by LSM, and figure 5.15 shows the corresponding price computed by the so-called

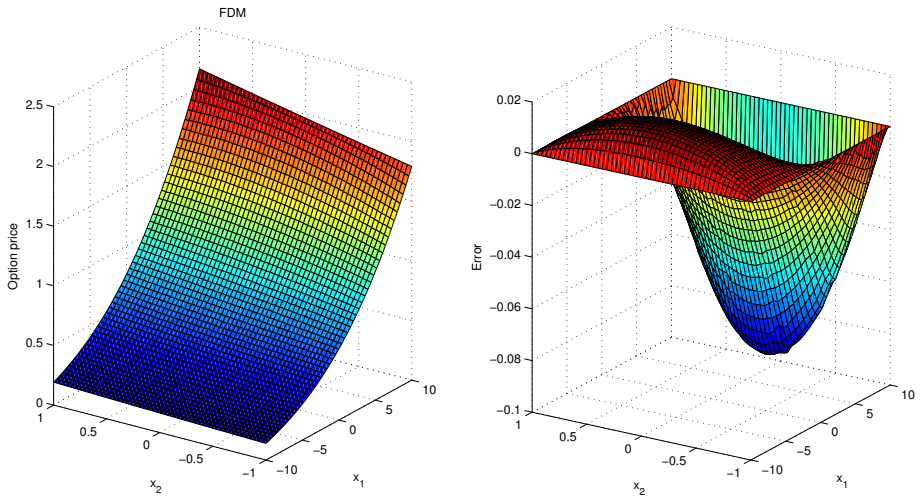

Figure 5.10: European call option in CARMA(2,1) model computed with the Douglas ADI method. 5 days to maturity. $I = J = 50$ and $N = 100$.

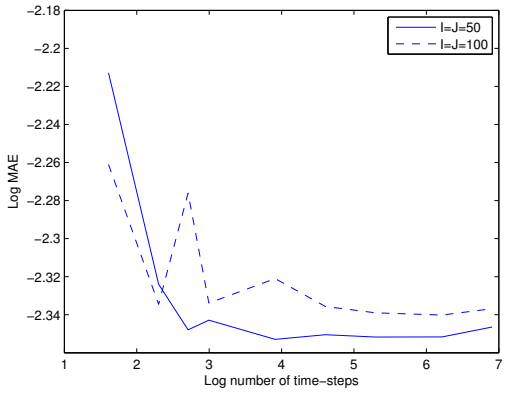

Figure 5.11: MAE for the European call option in CARMA(2,1) model.

LCP-ADI proposed in Villeneuve and Zanette [43] and Villeneuve and Zanette [44] with LSM boundaries. Recomputing the boundary conditions in each time step is infeasible, and we use the LSM estimate for $t = 0$ in all iterations. It appears that the irregularities from the boundary are affecting the interior. In figure 5.16 we have recomputed the LCP-ADI price with smoothed LSM boundaries, using a 5-point moving-average available in Matlab. The irregularities have disappeared.

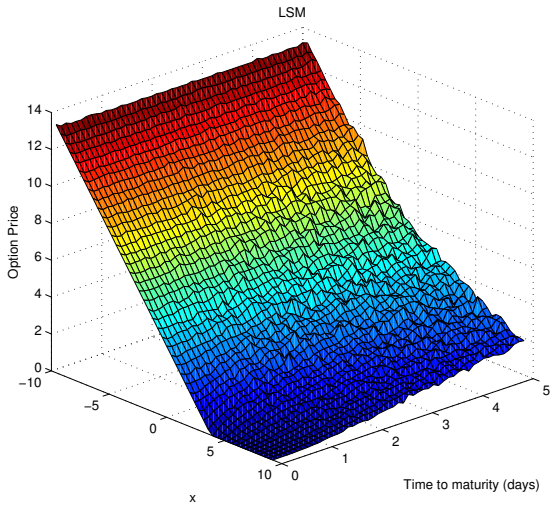

Figure 5.12: American put option in CARMA(1,0) model computed with LSM.

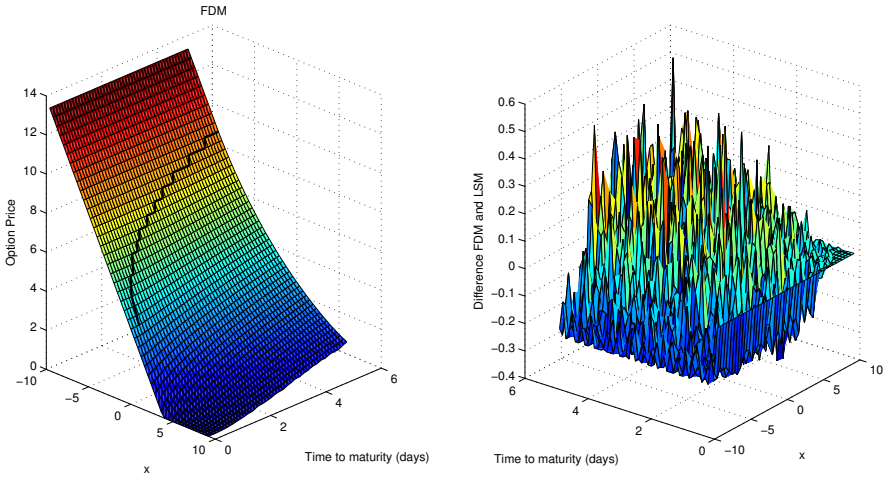

Figure 5.13: American put option in CAR(1) model computed with the Brennan-Schwartz algorithm. The line imposed on the price surface is the free-boundary implied by the algorithm.

European Call Option on CAT and CDD Futures

The pricing PDE for the CAT futures option is related to the CARMA model only through the diffusion coefficient. It is thus much simpler than for the spot temperature contracts. We consider a CAT futures with maturity $\tau = 50$ and delivery period $[51, 81]$, and price a call option with strike $K = 0$ when temperature is driven by CARMA(2,1). We have plotted the exact solution in figure 5.17, with the corresponding finite difference approximation in figure 5.18. We observe the familiar oscillations close to maturity.

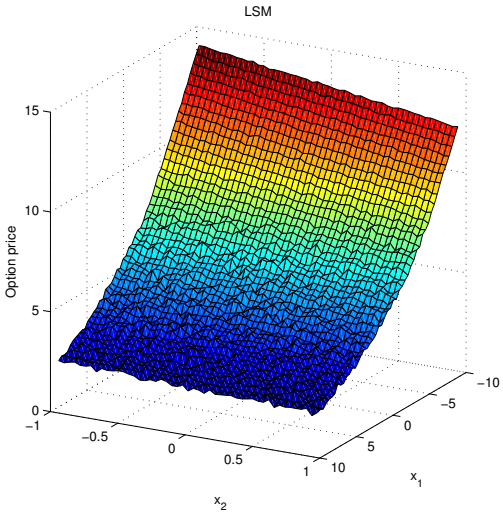

Figure 5.14: American put option in CARMA(2,1) model computed with LSM. 5 days to maturity.

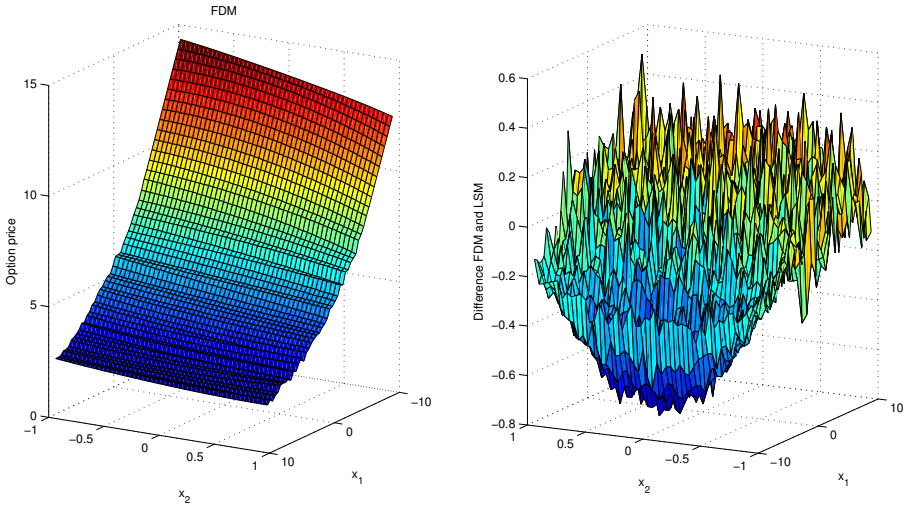

Figure 5.15: American put option in CARMA(2,1) model computed with the LCP-ADI. 5 days to maturity. $I = J = 50$

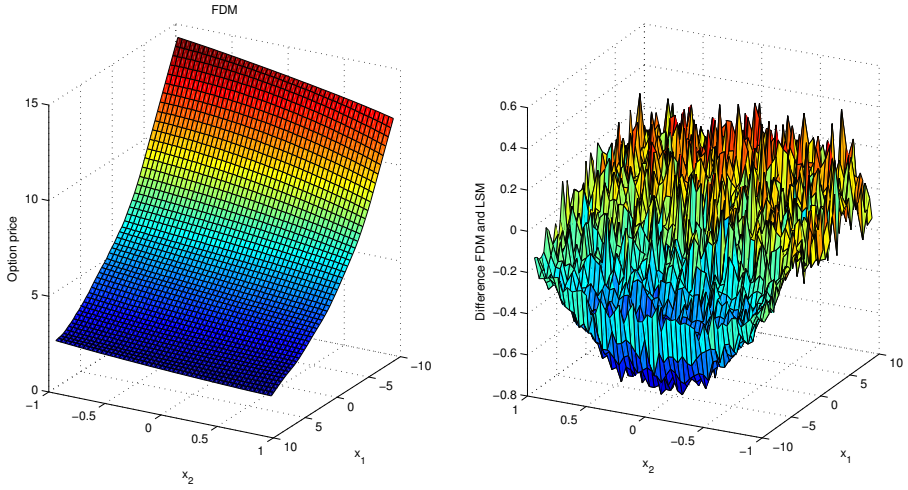

Figure 5.16: American put option in CARMA(2,1) model computed with the LCP-ADI and smoothed boundaries.

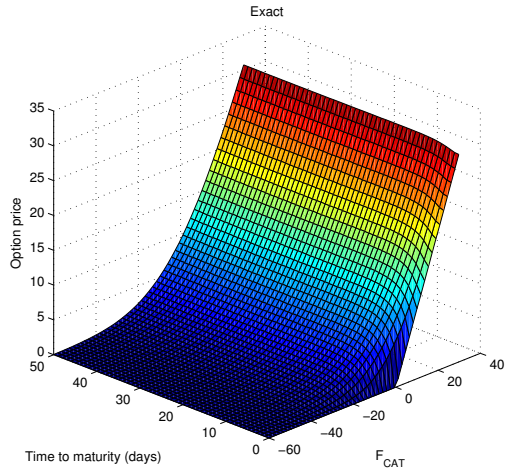

Figure 5.17: European call option in CAR(1) model. Exact.

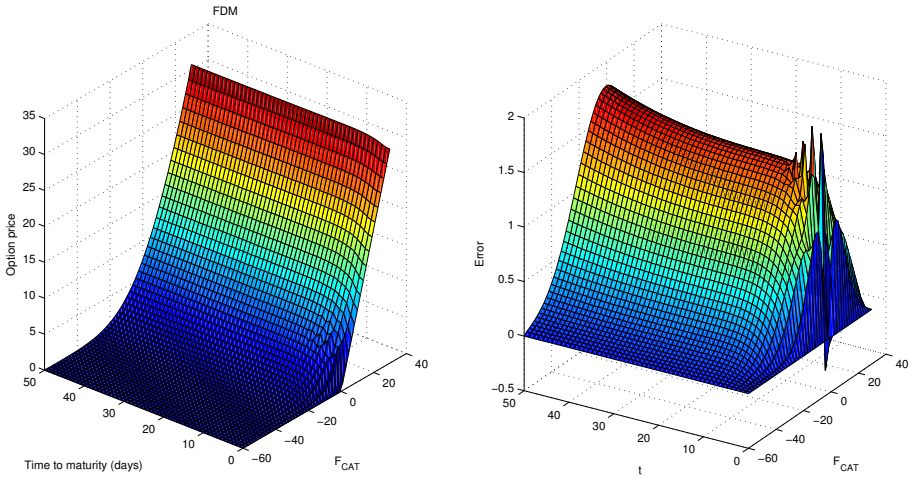

Figure 5.18: European call option on CAT futures in CARMA(2,1) model computed with the θ-method. $I = N = 50$.

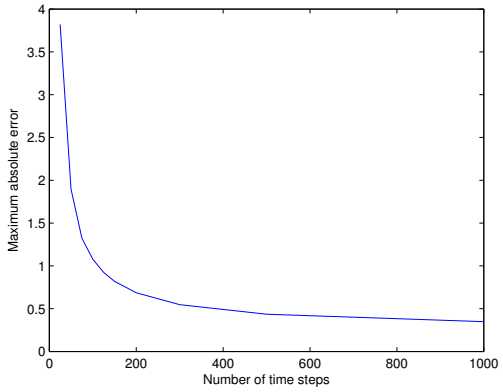

Figure 5.19: MAE for European call option on CAT futures in CARMA(2,1) model.

Chapter 6

Discussion and Concluding Remarks

We have studied finite difference schemes for numerical option and forward pricing in CARMA models. The CARMA state dynamics is generally multi-dimensional, and we proposed an ADI method to facilitate efficient computation. The numerical schemes were applied to contracts in the electricity and temperature markets, and we illustrated how to adapt the finite difference schemes to solve a PIDE for an electricity spot forward contract.

Our findings are somewhat dubious. From theory we expect to see a decrease in error as the computational grid is refined, but the numerical results indicate that the error quickly stabilizes, or increase beyond a certain grid resolution. The CARMA state has a degenerate diffusive term with a stochastic driver in only one direction which is likely to cause trouble. An idea would be to add a small artificial diffusion to the degenerate state(s), or equivalently let the CARMA dynamics be driven by a multi-dimensional Wiener process. Numerical testing, however, did not indicate a significant improvement. A related potential source of error is the relative size of convection and diffusion, and we briefly indicate how this is often tackled.

Convection-dominated problems are widely known to cause spurious oscillations and numerical errors. Consider the model problem

$$\frac{\partial u}{\partial t} = b(x)\frac{\partial u}{\partial x} + a(x)\frac{\partial^2 u}{\partial x^2}, \quad u(0,x) = u_0. \tag{6.1}$$

The degree of convection-domination is associated with the *mesh Péclet number* $\frac{|b(x)|}{a(x)}\Delta x$, for which large values indicate potential numerical issues. An *upwind scheme* can be used to introduce artificial numerical diffusion which smears the approximation. The simplest upwind scheme employs a one-sided approximation to

the spatial derivative according to the direction of propagation, that is

$$\begin{aligned} \frac{\partial u}{\partial x} &\approx \frac{\Delta_{-x} u}{\Delta x}, \quad b(x) < 0, \\ \frac{\partial u}{\partial x} &\approx \frac{\Delta_{+x} u}{\Delta x}, \quad b(x) > 0. \end{aligned} \tag{6.2}$$

In an explicit difference scheme, upwinding leads to

$$U_i^{n+1} = U_i^n + b(x_i) \left[\mathbf{1}_{\{b(x_i)>0\}} \frac{\Delta_{+x} U_i^n}{\Delta x} + \mathbf{1}_{\{b(x_i)<0\}} \frac{\Delta_{-x} U_i^n}{\Delta x} \right] + a(x_i) \frac{\delta_x^2 U_i^n}{(\Delta x)^2}. \tag{6.3}$$

Rewriting (6.3) in terms of central differences yields

$$U_i^{n+1} = U_i^n + b(x_i) \frac{\Delta_{0x} U_i^n}{\Delta x} + \left[a(x_i) + \epsilon(x_i) \right] \frac{\delta_x^2 U_i^n}{(\Delta x)^2}, \tag{6.4}$$

and we see that the diffusion coefficient is compounded by

$$\epsilon(x_i) = b(x_i) \left(\mathbf{1}_{\{b(x_i)>0\}} \frac{\Delta x}{2} - \mathbf{1}_{\{b(x_i)<0\}} \frac{\Delta x}{2} \right). \tag{6.5}$$

Numerical testing did however not show any consistent improvement from upwinding in our schemes.

We have been measuring the error in a maximum norm, which is (arguably) the most relevant error metric in a financial context. We believe that the error observed in the numerical results is acceptable for many applications, and probably negligible compared to other sources of error. In conclusion: we have partly achieved our objective to adopt an efficient numerical procedure for CARMA models. The results indicate that the complexity of the CARMA dynamics does not permit a straightforward implementation of a finite difference scheme. Hopefully, our findings can serve as a caveat.

Bibliography

[1] Andersen, L., and Andreasen, J. Jump-diffusion models: Volatility smile fitting and numerical methods for pricing. *Rev Derivatives Research* , 4, pp. 231-262, 2000.

[2] Applebaum., D. *Lévy Processes and Stochastic Calculus*. Cambridge University Press, Cambridge, 2004.

[3] Barndorff-Nielsen, O.E., and Shepard, N. Modelling by Lévy processes for Financial Econometrics. *Lévy processes - Theory and Applications*, in Barndorff-Nielsen, O.E., Mikosch, T., and Resnick, S.I., editors, Birkhäuser: Boston, pp. 283-318, 2001.

[4] Benth, F.E., Kiesel, R. and Nazarova, A. A critical empirical study of three electricity spot price models. *Energy Economics* 34:5, pp. 1589-1616, 2012.

[5] Benth, F.E. and Saltyte Benth, J. *Modeling and Pricing in Financial Markets for Weather Derivatives*. World Scientific, 2013.

[6] Benth, F.E., Benth, J.S., and Koekebakker, S. *Stochastic Modelling of Electricity and Related Markets*. World Scientific, 2008.

[7] Benth, F.E., Kallsen, J., and Meyer-Brandis, T. A non-Gaussian Ornstein-Uhlenbeck process for electricity spot price modeling and derivatives pricing. Appl. Math. Finance, 14(2), pp. 153-169, 2007.

[8] Benth,F.E., Klüppelberg, C., Müller, G. and Vos, L. Forward Pricing in electricity markets based on stable CARMA spot models. 2011.

[9] Benth, F.E., Koekebakker, S. and Zakamouline, V. A continuous time model for interest rate with autoregressive and moving average components. *In AIP Conference Proceedings*. Volume 1281, pp. 531-534, 2010.

[10] Benth, F.E., Kallsen, J., and Meyer-Brandis, T. A non-Gaussian Ornstein-Uhlenbeck process for electricity spot price modeling and derivatives pricing, *Appl. Math. Finance*. 14(2), pp. 153-169, 2007.

[11] Benth, F.E. and Sgarra, C. The risk premium and the Esscher transform in power markets. *Stoch. Analysis Appl*, 2009.

[12] Bernhardt, C., Kluppelberg, C. and Meyer-Brandis, T. Estimating high quantiles for electricity prices by stable linear models. *J. Energy Markets*, 1(1), pp. 3-19, 2008.

[13] Brennan, M.J., and Schwartz, E.S. The valuation of American put options, *J. Finance*, 32, pp. 449-462, 1977.

[14] Brockwell, P.J. Lévy driven CARMA processes. *Ann. Inst. Math.*, 53, pp. 113-124, 2001.

[15] Brockwell, P.J. Continuous-time ARMA Processes. *Handbook of Statistics 19; Stochastic Processes: Theory and Methods*, Elsevier, Amsterdam, 2001.

[16] Brockwell, P.J., Davis, R. A. and Yang, Y. Estimation for non-negative Lévy-driven CARMA processes. *J. Business & Economic Stat.* 29(2), pp. 250-259, 2011.

[17] Brockwell, P.J. and Lindner, A. Existence and uniqueness of stationary Lévy-driven CARMA processes. *Stoch. Proc. Appl.*, 119(8), pp. 2660-2681, 2009.

[18] Cartea, A., and Figueroa, M.G. Pricing in electricity markets A mean reverting jump diffusion model with seasonality. *Applied Mathematical Finance* 12(4), pp. 313-335, 2005.

[19] Chan, T. Pricing contingent claims on stocks driven by Lévy processes. *The Annals of Applied Probability*, 9, 1999.

[20] Cont, R. and Tankov, P. *Financial modelling with jump processes*. Chapman & Hall / CRC Press, 2003.

[21] Cont, R., and Voltchkova, E. A Finite Difference Scheme for Option Pricing in Jump Diffusion and Exponential Lévy Models. *SIAM J. Numer. Anal.* 43(4), pp. 1596-1626, 2005.

[22] Douglas, J., and Rachford, H.H. On the numerical solution of heat conduction problems in two and three space variables. *Trans. Amer. Math. Soc.* 82, pp. 421-439, 1956.

[23] Eberlein, E. Applications of generalized hyperbolic Lévy motion to finance. *Lévy processes - Theory and Applications*, in Barndorff-Nielsen, O.E., Mikosch, T., and Resnick, S.I., editors, Birkhäuser: Boston, pp. 319-336, 2001.

[24] Elliott, R.J., and Kopp, P.E. *Mathematics of Financial Markets*. Springer-Verlag, 1999.

[25] Glasserman, P. Monte *Carlo Methods in Financial engineering*. Springer, 2004.

[26] in 't Hout, K. ADI scheme in the numerical solution of the Heston PDE. *Proceedings to Numerical Analysis and Applied Mathematics*, 2007.

[27] Jaillet, P., Lamberton, D., and Lapeyre, B. Variational inequalities and the pricing of American options. *Acta Appl. Math. 21*, pp. 263-289, 1990.

[28] Karatzas, I. On the pricing of American options. *Appl. Math. Optimization* 17, pp. 37-60, 1988.

[29] Karatzas, I., and Shreve, S.E. *Brownian Motion and Stochastic Calculus*. Springer, 1988.

[30] Karatzas, I., and Shreve, S.E. *Methods of Mathematical finance*. Springer, 1998.

[31] Lamberton, D. *Optimal stopping and American options*. Lecture notes, Ljubljana Summer School on Financial Mathematics, 2009.

[32] Lamberton, D., and Lapeyre, B. *Introduction to stochastic calculus applied to finance*. Chapman and Hall, 1996.

[33] Longstaff, F., Schwartz, E.S. Valuing American Options by Simulation: A Simple Least Squares Approach. *The Review of Financial Studies* 14, pp. 113-147, 2001.

[34] Mitchell, A.R., and Griffiths, D.F. *The Finite Difference Method in Partial Differential Equations*. Wiley, New York, 1980.

[35] Myneni, R. The pricing of the American option. *Ann. Appl. Probab.*, 2, pp. 1-23, 1992.

[36] Peaceman, D.W., and Rachford, H.H. The numerical solution of parabolic and elliptic differential equations, *J. Soc. Ind. Appl. Math.*, 3, pp. 28-41, 1955.

[37] Pham, H. Optimal stopping of controlled jump-diffusion processes: a viscosity solution approach. *Journal of Mathematical Systems Estimation and Control*, 8(1), pp. 1-27, 1998.

[38] Protter, P. *Stochastic integration and differential equations*. Springer, 2003.

[39] Raible, S. *Lévy processes in finance: Theory, numerics, and empirical facts*. PhD thesis, Albert- Ludwigs-Universität Frieburg, 2000.

[40] Lucia, J.J. and Schwartz, E.S. Electricity prices and power derivatives: evidence from the Nordic Power Exchange. *Rev. Derivatives Res.* 5(1), pp. 5-50, 2002.

[41] R. Seydel. *Tools for Computational Finance*. Springer Verlag, Berlin, 2003.

[42] Tavella, D. and Randall, C. *Pricing financial instruments: the finite difference method*. Wiley, 2000.

[43] Villeneuve, S. and Zanette, A. *Comparison of Finite Difference Methods for Pricing American options on two stocks*, 2009.

[44] Villeneuve, S. and Zanette, A. Parabolic ADI methods for pricing American options on two stocks. *Math. Oper. Res.*, 27, pp. 121-149, 2002.

Appendix A

Appendix

A.1 Fourier Analysis of the Heat Equation

Consider the initial-value problem

$$\frac{\partial u}{\partial t} = a\frac{\partial^2 u}{\partial x^2}, \quad u(0,x) = u_0(x), \tag{A.1}$$

with $a > 0$ and suppose $u \in L^2(\mathbb{R})$. Recall the Fourier transform and its inverse given by

$$\hat{u}(t,\xi) = \frac{1}{\sqrt{2\pi}} \int_{\mathbb{R}} u(t,x) e^{-i\xi x} dx, \tag{A.2}$$

$$u(t,x) = \frac{1}{\sqrt{2\pi}} \int_{\mathbb{R}} \hat{u}(t,\xi) e^{i\xi x} d\xi. \tag{A.3}$$

Assume that the grid function $\{U_i^n\}_{i\in\mathbb{Z}}$ with equidistant grid-spacing h is bounded in the discrete l^2-mesh norm, i.e.

$$\|U^n\|_2 \triangleq \left(\sum_{j\in\mathbb{Z}} h|U_j^n|^2 \right)^{\frac{1}{2}} < \infty. \tag{A.4}$$

The discrete analogue of the Fourier transform and its inverse are given by

$$\hat{U}^n(\xi) = \frac{1}{\sqrt{2\pi}} \sum_{j=-\infty}^{\infty} h e^{-ijh\xi} U_j^n, \tag{A.5}$$

$$U_j^n = \frac{1}{\sqrt{2\pi}} \int_{-\frac{\pi}{h}}^{\frac{\pi}{h}} e^{ijh\xi} \hat{U}^n(\xi) d\xi, \tag{A.6}$$

for $\xi \in [-\frac{\pi}{h}, \frac{\pi}{h}]$. A simple explicit scheme for solving (A.1) is

$$U_j^{n+1} = (1 - 2a\mu)U_j^n + a\mu(U_{j+1}^n + U_{j-1}^n), \tag{A.7}$$

where $\mu = \frac{\Delta t}{(\Delta x)^2}$. Employ the Fourier inverse transformation (A.6) and apply this to the right hand side of (A.7). We obtain

$$U_j^{n+1} = \frac{1}{\sqrt{2\pi}} \int_{-\frac{\pi}{h}}^{\frac{\pi}{h}} e^{ijh\xi} \left[1 - 2a\mu + a\mu(e^{ih\xi} + e^{-ih\xi})\right] \hat{U}^n(\xi) d\xi.$$

By uniqueness of the Fourier transform we conclude that

$$\hat{U}^{n+1}(\xi) = g(h\xi)\hat{U}^n(\xi), \tag{A.8}$$

where

$$g(h\xi) = e^{ijh\xi} \left[1 - 2a\mu + a\mu(e^{ih\xi} + e^{-ih\xi})\right]. \tag{A.9}$$

$g(h\xi)$ is the so-called *amplification factor*. When we advance the numerical solution from one time step to the next, the Fourier transform is scaled by this factor. An induction argument shows that $\hat{U}^n(\xi) = g(h\xi)^n \hat{U}^0(\xi)$, and by Parseval's theorem[1]

$$\begin{aligned} \|U^n\|_2^2 = \sum_{j\in\mathbb{Z}} h|U_j^n|^2 &= \int_{-\frac{\pi}{h}}^{\frac{\pi}{h}} |\hat{U}^n(\xi)|^2 d\xi \\ &= \int_{-\frac{\pi}{h}}^{\frac{\pi}{h}} |g(h\xi)|^{2n} |\hat{U}^0(\xi)|^2 d\xi. \end{aligned}$$

Thus, stability in the l^2-norm is achieved whenever $|g(h\xi)|^{2n}$ is properly bounded.

The amplification factor can be written as

$$g(h\xi) = 1 - 4a\mu \sin^2\left(\frac{h\xi}{2}\right), \quad \xi \in [-\frac{\pi}{h}, \frac{\pi}{h}]. \tag{A.10}$$

We see that $|g(h\xi)| \leq 1$ if $2a\mu \leq 1$, i.e. if the *Courant-Friedrichs-Lewy* (CFL) condition is satisfied. In this case

$$|g(h\xi)|^{2n} \leq 1 \Rightarrow \|U^n\|_2^2 \leq \|U^0\|_2^2. \tag{A.11}$$

If the CFL condition is not satisfied, there are high-frequency components of the solution corresponding to $|\xi|$ in a neighborhood of $\frac{\pi}{h}$, where $|g(h\xi)|^{2n}$ will grow without bound and the scheme will exhibit instability.

In practice, Von-Neumann stability is investigated by replacing U_j^n by $g^n e^{ijh\xi}$, and deducing the amplification factor for the Fourier mode $e^{ijh\xi}$.

A.2 Consistency, Convergence and Stability for the Explicit Scheme

We derive theoretical properties of the two-dimensional explicit scheme in chapter 2.

[1] The Fourier transform is unitary.

Consistency and Truncation Error

The truncation error is given by

$$\begin{aligned} T(t,x,y) \triangleq & \frac{\Delta_{+t}u(t,x,y)}{\Delta t} - b(x,y)\frac{\Delta_{0x}u(t,x,y)}{\Delta x} - b(x,y)\frac{\Delta_{0y}u(t,x,y)}{\Delta y} \\ & - a(x,y)\frac{\delta_{0x}^2 u(t,x,y)}{(\Delta x)^2} - a(x,y)\frac{\delta_{0y}^2 u(t,x,y)}{(\Delta y)^2} - c(x,y)u(t,x,y) \end{aligned}$$

Using the equations (??)

$$\begin{aligned} T(t,x,y) = & \frac{u_t\Delta t + \frac{1}{2}u_{tt}(\Delta t)^2 + \mathcal{O}((\Delta t)^3)}{\Delta t} - b_1(x,y)\frac{u_x\Delta x + \frac{1}{6}u_{xxx}(\Delta x)^3 + \mathcal{O}((\Delta x)^5)}{\Delta x} \\ & - b_2(x,y)\frac{u_y\Delta y + \frac{1}{6}u_{yyy}(\Delta y)^3 + \mathcal{O}((\Delta y)^5)}{\Delta y} \\ & - a_1(x,y)\frac{u_{xx}(\Delta x)^2 + \frac{1}{12}u_{xxxx}(\Delta x)^4 + \mathcal{O}((\Delta x)^6)}{(\Delta x)^2} \\ & - a_2(x,y)\frac{u_{yy}(\Delta y)^2 + \frac{1}{12}u_{yyyy}(\Delta y)^4 + \mathcal{O}((\Delta y)^6)}{(\Delta y)^2} - c(x,y)u(t,x,y) \\ & = \underbrace{u_t - [b_1(t,x,y)u_x + b_2(t,x,y)u_y + a_1(x,y)u_{xx} + a_2(x,y)u_{yy} + c(x,y)u]}_{=0} \\ & + \mathcal{O}((\Delta t) + (\Delta x)^2 + (\Delta y)^2). \end{aligned}$$

Hence, the truncation error is first-order in time and second-order in space. Moreover, since $T(t,x,y) \to 0$ as $\Delta t,\ \Delta x,\ \Delta y \to 0$ the scheme is also *consistent*.

Convergence

Define the error of the scheme at the node (t_n, x_i, y_j) as

$$e_{i,j}^n = U_{i,j}^n - u(t_n, x_i, y_j). \tag{A.12}$$

We know that the $U_{i,j}^n$ solves the difference equation and therefore has zero truncation error, whereas $u(t_n, x_i, y_j)$ leaves the term $T(t_n, x_i, y_j)$.

$$Te_{i,j}^n = \frac{e_{i,j}^{n+1}}{\Delta t} - Le_{i,j}^n = -T(t_n, x_i, y_j).$$

$$\begin{aligned} \Rightarrow e_{i,j}^{n+1} = & e_{i,j}^n - \Delta t T(t_n, x_i, y_j) + b_{1,i,j}\gamma_1\Delta_{0x}e_{i,j}^n + b_{2,i,j}\gamma_2\Delta_{0y}e_{i,j}^n + a_{1,i,j}\mu_1\delta_x^2 \\ & + a_{2,i,j}\mu_2\Delta_y^2 e_{i,j}^n + \Delta t c_{i,j}e_{i,j} \\ & = e_{i,j}^n(1 + \Delta t c_{i,j} - 2\mu_1 a_{1,i,j} - 2\mu_2 a_{2,i,j}) - \Delta t T(t_n, x_i, y_j) \\ & + e_{i-1,j}^n(\mu_1 a_{1,i,j} - \frac{1}{2}\gamma_1 b_{1,i,j}) + e_{i+1,j}^n(\mu_1 a_{1,i,j} + \frac{1}{2}\gamma_1 b_{1,i,j}) \\ & + e_{i,j-1}^n(\mu_2 a_{2,i,j} - \frac{1}{2}\gamma_2 b_{2,i,j}) + e_{i,j+1}^n(\mu_2 a_{2,i,j} + \frac{1}{2}\gamma_2 b_{2,i,j}) \end{aligned}$$

In order for the coefficients in front of the error terms to be non-negative, we need to impose the restrictions

$$\frac{\gamma_1|b_{1,i,j}|}{\mu_1 a_{1,i,j}} \leq 2, \quad \frac{\gamma_2|b_{2,i,j}|}{\mu_2 a_{2,i,j}} \leq 2, \quad \Delta t c_{i,j} + 2\mu_1\gamma_1 + 2\mu_2\gamma_2 \leq 1, \quad i = 0, ..., I,\ j = 0, ..., J.$$

Now, observe that

$$|e_{i,j}^{n+1}| \leq (1 + c_{i,j})\max\left\{|e_{i-1,j}^n|, |e_{i+1,j}^n|, |e_{i,j-1}^n|, |e_{i,j+1}^n|, |e_{i,j}^n|\right\} + \Delta t M(\Delta t + (\Delta x)^2 + (\Delta y)^2),$$

and define

$$E^n = \max_{0\leq i\leq I,\ 0\leq j\leq J} |e_{i,j}^n|,$$
$$c = \max_{0\leq i\leq I,\ 0\leq j\leq J} |c_{i,j}|,$$

such that

$$E^{n+1} \leq E^n(1 + \Delta t c) + M(\Delta t + (\Delta x)^2 + (\Delta y)^2).$$

By induction we obtain

$$\begin{aligned} E^n &\leq E^0(1 + \Delta t c)^n + \Delta t M(\Delta t + (\Delta x)^2 + (\Delta y)^2)\sum_{k=0}^{n-1}(1 + \Delta t c)^k \\ &= \Delta t M(\Delta t + (\Delta x)^2 + (\Delta y)^2)\frac{(1 + c\Delta t)^n - 1}{c\Delta t} \\ &\leq e^{cn\Delta t}\tilde{M}(\Delta t + (\Delta x)^2 + (\Delta y)^2), \end{aligned}$$

which proves convergence.

Stability

We use the Von-Neumann technique to investigate stability. This approach is strictly speaking viable only in the case of linear equations with constant coefficients and periodic boundary conditions. Nevertheless, it is often applied to more general problems as a necessary stability condition. In the case of variable coefficients, stability is treated as local phenomenon, whereupon the coefficients are frozen and stability investigated in a particular node.

To this end we suppress the spatial indices and denote the coefficients by a_1, a_2, b_1, b_2 and c. We now alter the notation from chapter 2, and let i designate the *imaginary unit*, i.e. $i = \sqrt{-1}$, and we let r, s be the spatial indices. Replacing $U_{r,s}^n$ by $\lambda^n e^{i(rk_x\Delta x + sk_y\Delta y)}$ in (2.42) in chapter 2 leads to

$$\begin{aligned} \lambda - 1 = {} & b_1\frac{\gamma_1}{2}(e^{ik_x\Delta x} - e^{-ik_x\Delta x}) + b_2\frac{\gamma_2}{2}(e^{ik_y\Delta y} - e^{-ik_y\Delta y}) \\ & + a_1\mu_1(e^{ik_x\Delta x} - 2 + e^{-ik_x\Delta x}) + a_2\mu_1(e^{ik_y\Delta y} - 2 + e^{-ik_y\Delta y}) + \Delta t c. \end{aligned}$$

Exploiting the fact that

$$e^{ik_x\Delta x} + e^{-ik_x\Delta x} - 2 = -4\sin^2(\frac{1}{2}k_x\Delta x),$$

we get

$$\begin{aligned}\lambda \triangleq \lambda(k_x,k_y) = 1 + \Delta tc - 4\left[\mu_1 a_1 \sin^2(\frac{1}{2}k_x\Delta x) + \mu_2 a_2 \sin^2(\frac{1}{2}k_y\Delta y)\right] \\ + i\left[b_1\gamma_1 \sin(k_x\Delta x) + b_2\gamma_2 \sin(k_y\Delta y)\right].\end{aligned}$$

Then

$$\begin{aligned}|\lambda|^2 = \left(1 + \Delta tc - 4\left[\mu_1 a_1 \sin^2(\frac{1}{2}k_x\Delta x) + \mu_2 a_2 \sin^2(\frac{1}{2}k_y\Delta y)\right]\right)^2 \\ + \left(b_1\gamma_1 \sin(k_x\Delta x) + b_2\gamma_2 \sin(k_y\Delta y)\right)^2.\end{aligned}$$

If $\mu_1 a_1 + \mu_2 a_2 \leq \frac{1}{2}$ then the first parenthesis is ≤ 1 (recall that $c \leq 0$), in which case

$$\begin{aligned}|\lambda|^2 &\leq 1 + \left(b_1\gamma_1 + b_2\gamma_2\right)^2 \\ &= 1 + (\Delta t)^2\left(\frac{b_1}{\Delta x} + \frac{b_2}{\Delta y}\right)^2 \\ \Rightarrow |\lambda| &\leq 1 + \frac{1}{2}(\Delta t)^2\left(\frac{b_1}{\Delta x} + \frac{b_2}{\Delta y}\right)^2 + \mathcal{O}((\Delta t)^2)\end{aligned}$$

where the last inequality follows from a Taylor expansion. Moreover,

$$|\lambda| \leq 1 + \mathcal{O}((\Delta t)^2). \tag{A.13}$$

We see that the explicit scheme is conditionally stable.

A.3 Stability of the θ-Scheme

We proceed as above by conducting a Von-Neumann stability analysis on the corresponding equation with frozen coefficients. In one dimension the θ-scheme takes the form

$$\begin{aligned}&\left(1 + \theta\Delta tc + \theta 2a\mu\right)U_j^{n+1} - \theta\left(\frac{b}{2}\gamma + a\mu\right)U_{j+1}^{n+1} + \theta\left(\frac{b}{2}\gamma - a\mu\right)U_{j-1}^{n+1} = \\ &\left(1 - (1-\theta)\Delta tc - (1-\theta)2a\mu\right)U_j^n + (1-\theta)\left(\frac{b}{2}\gamma + a\mu\right)U_{j+1}^n - (1-\theta)\left(\frac{b}{2}\gamma - a\mu\right)U_{j-1}^n.\end{aligned}$$

where $\mu = \frac{\Delta t}{(\Delta x)^2}$ and $\gamma = \frac{\Delta t}{\Delta x}$. Replacing U_j^n by $\lambda e^{ikj\Delta x}$ and rearranging yields

$$|\lambda|^2 \leq \frac{\left(1 - 4(1-\theta)a\mu\sin^2\left(\frac{1}{2}k\Delta x\right)\right)^2 + (1-\theta)^2 b^2\gamma^2\sin^2(k\Delta x)}{\left(1 + 4\theta a\mu\sin^2\left(\frac{1}{2}k\Delta x\right)\right)^2 + \theta^2 b^2\gamma^2\sin^2(k\Delta x)} \tag{A.14}$$

Clearly, for $\theta = \frac{1}{2}$ and $\theta = 1$ we have that $|\lambda| \leq 1 + \mathcal{O}(\Delta t)$.

A.4 Tridiagonal Matrix Algorithm

Consider the tridiagonal system of equations

$$\begin{pmatrix} b_1 & c_1 & & & & 0 \\ a_2 & b_2 & c_2 & & & \\ & \ddots & \ddots & \ddots & & \\ & & \ddots & \ddots & \ddots & \\ & & & a_{n-1} & b_{n-1} & c_{n-1} \\ 0 & & & & a_n & b_n \end{pmatrix} \begin{pmatrix} x_1 \\ x_2 \\ \vdots \\ \vdots \\ x_{n-1} \\ x_n \end{pmatrix} = \begin{pmatrix} d_1 \\ d_2 \\ \vdots \\ \vdots \\ d_{n-1} \\ d_n \end{pmatrix} \tag{A.15}$$

The tridiagonal matrix algorithm solves (A.4) by eliminating the a_i's in a forward sweep followed by back substitution:

$$c_i' = \begin{cases} \frac{c_i}{b_i}, & i = 1 \\ \frac{c_i}{b_i - c_{i-1}' a_i}, & i = 2, ..., n-1 \end{cases}$$

$$d_i' = \begin{cases} \frac{d_i}{b_i}, & i = 1 \\ \frac{d_i - d_{i-1}' a_i}{b_i - c_{i-1}' a_i}, & i = 2, ..., n \end{cases}$$

Back substitution yields

$$\begin{aligned} x_n &= d_n \\ x_i &= d_i' - c_i' x_{i+1}, \quad i = n-1, ..., 1 \end{aligned}$$

A.5 An Application of Cauchy's Integral Formula

The contour integral along γ can decomposed into integrals along small circles around each pole. The Cauchy integral formula states that

$$f(a) = \oint_\gamma \frac{f(z)}{z - a} dz. \tag{A.16}$$

Now, let $\gamma_k,\ k = 1, ..., p$, be circles enclosing the λ_k's. Then

$$\begin{aligned} \oint_\gamma \frac{b(z)e^{zt}}{a(z)} dz &= \sum_{k=1}^{p} \oint_{\gamma_k} \frac{b(z)e^{zt}}{a(z)} dz \\ &= \sum_{k=1}^{p} \oint_{\gamma_k} \frac{\frac{b(z)e^{zt}}{\prod_{j \neq k}(z - \lambda_j)}}{(z - \lambda_k)} dz \\ &= \sum_{k=1}^{p} \frac{b(\lambda_k)e^{\lambda_k t}}{\prod_{j \neq k}(\lambda_k - \lambda_j)} \\ &= \sum_{k=1}^{p} \frac{b(\lambda_k)e^{\lambda_k t}}{a^{(1)}(\lambda_k)}. \end{aligned}$$

A.6 Moment Generating Function of a Poisson Integral

Define $f(s) = e^{-\alpha(T-s)}$ and recall that $dL_s = \int_{\mathbb{R}_0} zN(ds, dz)$. Let

$$\left\{ t = s_0^{(n)} \leq s_1 \leq ... \leq s_{m_n}^{(n)} = \tau \right\}$$

be a partition of $[t, T]$ such that

$$\lim_{n\to\infty} \max_{0\leq i\leq m_n} |s_{i+1}^{(n)} - s_i^{(n)}| = 0.$$

The simple functions are dense in the set of continuous functions, and we can write

$$f(s) = \lim_{n\to\infty} \sum_{j=0}^{m_n-1} f(s_j^{(n)}) \mathbf{1}_{(s_j^{(n)}, s_{j+1}^{(n)}]}(s). \tag{A.17}$$

To ease the notation, let $f_j = f(s_j^{(n)})$ and $\Delta s_j^{(n)} = s_{j+1}^{(n)} - s_j^{(n)}$. By using the dominated convergence theorem repeatedly in conjunction with the independent increment property of Lévy processes, we get

$$\begin{aligned}
E_Q\left[\exp\left(\int_t^T \int_{\mathbb{R}_0} e^{-\alpha(\tau-s)} zN(ds, dz)\right)\right] &= E_Q\left[\exp\left(\int_t^\tau f(s) dL_s\right)\right] \\
&= E_Q\left[\exp\left(\lim_{n\to\infty} \sum_{j=0}^{m_n-1} f_j \int_t^T \mathbf{1}_{(s_j^{(n)}, s_{j+1}^{(n)}]}(s) dL_s\right)\right] \\
&= \lim_{n\to\infty} \prod_{j=0}^{m_n-1} E_Q\left[\exp\left(f_j\left(L_{s_{j+1}^{(n)}} - L_{s_j^{(n)}}\right)\right)\right] \\
&= \lim_{n\to\infty} \prod_{j=0}^{m_n-1} \exp\left(\Delta s_j^{(n)} \psi_L(-if_j)\right) \\
&= \exp\left(\lim_{n\to\infty} \sum_{j=0}^{m_n-1} \psi_L(-if_j)\Delta s_j^{(n)}\right) \\
&= \exp\left(\int_t^T \lim_{n\to\infty} \sum_{j=0}^{m_n-1} \psi_L(-if_j) \mathbf{1}_{(s_j^{(n)}, s_{j+1}^{(n)}]} ds\right) \\
&= \exp\left(\int_t^T \psi_L(-if(s)) ds\right).
\end{aligned}$$

Now, denote by ψ_Z the log-characteristic function of a Gaussian variable with mean a and variance b^2.

$$\begin{aligned}
\exp\left(\int_t^T \psi_L(-if(s))ds\right) &= \exp\left(\int_t^T \int_{\mathbb{R}_0} \left(e^{f(s)z} - 1\right) \phi(z)dz\lambda ds\right) \\
&= \exp\left(\int_t^T e^{\phi_Z(-if(s))}\lambda ds - \lambda(\tau - t)\right) \\
&= \exp\left(\int_t^T \exp\left(af(s) + \frac{b^2}{2}f(s)^2\right)\lambda ds - \lambda(\tau - t)\right) \\
&= \exp\left(\int_t^T \exp\left(ae^{-\alpha(\tau-s)} + \frac{b^2}{2}e^{-2\alpha(\tau-s)}\right)\lambda ds - \lambda(\tau - t)\right).
\end{aligned} \tag{A.18}$$

Appendix B

Matlab Code

B.1 Implicit-Explicit Scheme for Jump-Diffusion

```
function U = SchwartzJD(theta,alpha,lambda,a,b,sigma,Smin,Smax,Ns,Nt,T)
dt = T/Nt;
ds = (Smax-Smin)/Ns;
s = Smin:ds:Smax;
U = s'; Umat = zeros(Ns+1,Nt+1); Umat(:,1) = U;
mu = (sigma/ds)^2; mutilde = 1/alpha*0.5*sigma^2;
%Integral term
nu = zeros(Ns+1,Ns+1);
y = zeros(Ns+1,Ns+1);
for j = 2:Ns+1
    ymax = Smax/s(j);
    dy = ymax/Ns;
    y(j,:) = 0:dy:ymax;
    nu(j,1) = 0.5*(y(j,2)-y(j,1))*lognpdf(y(j,1),a,b);
    nu(j,Ns+1) = 0.5*(y(j,Ns+1)-y(j,Ns))*lognpdf(y(j,Ns+1),a,b);
    for p = 2:Ns
        nu(j,p) = 0.5*(y(j,p+1)-y(j,p-1))*lognpdf(y(j,p),a,b);
    end
end
nu = lambda*nu;
%Tridiagonal matrix
A1 = 0.5*(mu*s(2:Ns).^2-alpha*(mutilde-log(s(2:Ns))).*s(2:Ns)/ds);
A1 = [A1';0;0];
B1 = -(mu*s(2:Ns).^2); B1 = [0;B1';0];
C1 =  0.5*(mu*s(2:Ns).^2+alpha*(mutilde-log(s(2:Ns))).*s(2:Ns)/ds);
C1 = [0;0;C1'];
D = spdiags([A1 B1 C1],[-1 0 1],Ns+1,Ns+1);
for n = 1:Nt
    bnd = [SJDExact(s(1),a,b,sigma,alpha,lambda,n*dt),...
   SJDExact(s(Ns+1),a,b,sigma,alpha,lambda,n*dt)];
```

```
    AU = dt*D*U;
    IU = dt*Ioperator(U,y,nu,s,ds,Ns);
    tmp1 = U+(1-theta)*AU+IU;
    U = SchwartzJDtridiagsolve(tmp1,theta,mu,mutilde,alpha,Smin,Smax,bnd,dt);
    Umat(:,n+1) = U;
end
end

function x = SchwartzJDtridiagsolve(U,theta,mu,mutilde,alpha,Smin,Smax,bnd,dt)
Ns = size(U,1)-1; x = zeros(size(U));
ds = (Smax-Smin)/Ns; s = Smin:ds:Smax;
RHS = U(2:Ns);
%Construct LHS
a = -theta*dt*(0.5*(mu*s(2:Ns).^2-alpha*(mutilde-log(s(2:Ns))).*s(2:Ns)/ds));
b = 1+theta*dt*(mu*s(2:Ns).^2);
c = -theta*dt*(0.5*(mu*s(2:Ns).^2+alpha*(mutilde-log(s(2:Ns))).*s(2:Ns)/ds));
RHS(1) = RHS(1) - a(1)*bnd(1);
RHS(Ns-1) = RHS(Ns-1) - c(Ns-1)*bnd(2);
n = length(RHS); c(1) = c(1) / b(1); RHS(1) = RHS(1) / b(1);
 for i = 2:n-1
    tmp = b(i) - a(i) * c(i-1);
    c(i) = c(i) / tmp;
    RHS(i) = (RHS(i) - a(i) * RHS(i-1))/tmp;
end
RHS(n) = (RHS(n) - a(n) * RHS(n-1))/( b(n) - a(n) * c(n-1));
x(n+1) = RHS(n);
for i = n-1:-1:1
    x(i+1) = RHS(i) - c(i) * x(i+2);
end
x(1) = bnd(1);
x(Ns+1) = bnd(2);
end

function E = SJDExact(svec,a,b,sigma,alpha,lambda,T)
thetahat = 0; n = length(svec); E = zeros(size(svec))';
for i = 1:n
    s0 = svec(i);
    E(i) = (s0)^(exp(-alpha*T))*exp(Simp(@(tau)...
 0.5*sigma^2*exp(-2*alpha*(T-tau))+thetahat*sigma*exp(-alpha*(T-tau)),0,T,10)...
+Simp(@(tau) lambda*xi_func(a,b,alpha,T,tau),0,T,10)-lambda*T);
end
end
```

B.2 Longstaff-Schwartz for CARMA

```
function P = LSCARMApq(p,q,b,alpha,sigma,x,K,r,T,n,m,fhandles,Season)
```

```
S = (Season==1)*CarmaSeason(T)+SimCARMA(p,q,alpha,b,0,0,sigma,x,T,n,m);
S(:,1) = [];
dt = T/n;
d = exp(-r*dt*(1:n))';
Cashflow = max(K-S(:,n),0);
Extime = n*ones(m,1);
Nbasis = length(fhandles);
for i = n-1:-1:1
    Inmoney = find(S(:,i) < K);
    X = zeros(length(Inmoney),Nbasis);
    Sdata = S(Inmoney,i);
    for k = 1:Nbasis
        X(:,k) = feval(fhandles{k},Sdata);
    end
    Y = Cashflow(Inmoney).*d(Extime(Inmoney)-i);
    beta = regress(Y,X);
    Exvalue = max(K-Sdata,0);
    Contvalue = X*beta;
    ind = find(Exvalue > Contvalue);
    Expaths = Inmoney(ind);
    Cashflow(Expaths)= Exvalue(ind);
    Extime(Expaths) = i;
end
P = max(K-b'*x,mean(Cashflow.*d(Extime)));
end
```

B.3 Douglas ADI for CARMA(2,1)

```
function U = Carma21ADI(theta,r,sigma,sigmaeps,...
alpha1,alpha2,beta1,X1min,X1max,X2min,X2max,N1,N2,Nt,T,K)
Season = 1;
dx1 = (X1max-X1min)/N1; dx2 = (X2max-X2min)/N2;
x1 = X1min:dx1:X1max; x2 = X2min:dx2:X2max;
%Initial value (Call at maturity)
U = zeros(N1+1,N2+1);
for i = 1:N1+1
    for j = 1:N2+1
        U(i,j) = max((Season == 1)*CarmaSeason(T)+x1(i)+beta1*x2(j)-K,0);
    end
end
mu1 = (sigmaeps/dx1)^2; mu2 = (sigma/dx2)^2;
%Dirichlet boundaries
bndx1 = zeros(2,N2+1);
bndx2 = zeros(N1+1,2);
for j = 1:N2+1
```

```
    bndx1(1,j) = CarmaEuCall(2,1,[alpha2 alpha1]',...
[1 beta1]',[0 0]',0,sigma,r,0,T,[x1(1) x2(j)]',K,Season);
    bndx1(2,j) = CarmaEuCall(2,1,[alpha2 alpha1]',...
[1 beta1]',[0 0]',0,sigma,r,0,T,[x1(N1+1) x2(j)]',K,Season);
end
for i = 1:N1+1
    bndx2(i,1) = CarmaEuCall(2,1,[alpha2 alpha1]',...
[1 beta1]',[0 0]',0,sigma,r,0,T,[x1(i) x2(1)]',K,Season);
    bndx2(i,2) = CarmaEuCall(2,1,[alpha2 alpha1]',...
[1 beta1]',[0 0]',0,sigma,r,0,T,[x1(i) x2(N2+1)]',K,Season);
end
%Tridiagonal matrix in x1 direction
A1 = 0.5*(mu1-x1(2:N1)/dx1); A1 = [A1';0;0];
B1 = -(mu1+0.5*r)*ones(N1+1,1);
C1 =  0.5*(mu1+x1(2:N1)/dx1); C1 = [0;0;C1'];
D1 = spdiags([A1 B1 C1],[-1 0 1],N1+1,N1+1);
%Tridiagonal matrix in x2 direction
A2 = 0.5*(mu2+alpha1*x2(2:N2)/dx2); A2 = [A2';0;0];
B2 = -(mu2+0.5*r)*ones(N2+1,1);
C2 = 0.5*(mu2-alpha1*x2(2:N2)/dx2); C2 = [0;0;C2'];
D2 = spdiags([A2 B2 C2],[-1 0 1],N2+1,N2+1);
A3 = 0.5*alpha2/dx2*ones(N2-1,1); A3 = [A3;0;0];
B3 = zeros(N2+1,1);
C3 = -0.5*alpha2/dx2*ones(N2-1,1); C3 = [0;0;C3];
D3 = spdiags([A3 B3 C3],[-1 0 1],N2+1,N2+1);
for n = 1:Nt
    Y0 = U+C20A1(U,D1,r,dt)+C20A2(U,D2,D3,x1,r,dt);
    tmp1 = Y0-theta*C20A1(U,D1,r,dt);
    Y1 = tridiagsolve1(tmp1,theta,r,mu1,X1min,...
X1max,X2min,X2max,bndx1,dt);
    tmp2 = Y1-theta*C20A2(U,D2,D3,x1,r,dt);
    U = tridiagsolve2(tmp2,theta,r,mu2,alpha1,...
alpha2,X1min,X1max,X2min,X2max,bndx1,bndx2,dt);
end
end


function x = tridiagsolve1(A,theta,r,mu1,X1min,X1max,X2min,X2max,bndx1,dt)
N1 = size(A,1)-1; N2 = size(A,2)-1; x = zeros(size(A));
dx1 = (X1max-X1min)/N1; dx2 = (X2max-X2min)/N2;
x1 = X1min:dx1:X1max; x2 = X2min:dx2:X2max;
for j = 2:N2
    RHS = A(2:N1,j);
    %Construct RHS
    a = -theta*0.5*dt*(mu1-x1(2:N1)/dx1);
    b = 1-theta*(-dt)*(mu1+0.5*r)*ones(N1-1,1);
    c = -theta*0.5*dt*(mu1+x1(2:N1)/dx1);
    RHS(1) = RHS(1) - a(1)*bndx1(1,j);
```

```
    RHS(N1-1) = RHS(N1-1) - c(N1-1)*bndx1(2,j);
    n = length(RHS);
    c(1) = c(1) / b(1);
    RHS(1) = RHS(1) / b(1);
     for i = 2:n-1
        tmp = b(i) - a(i) * c(i-1);
        c(i) = c(i) / tmp;
        RHS(i) = (RHS(i) - a(i) * RHS(i-1))/tmp;
    end
    RHS(n) = (RHS(n) - a(n) * RHS(n-1))/( b(n) - a(n) * c(n-1));
    x(n+1,j) = RHS(n);
    for i = n-1:-1:1
        x(i+1,j) = RHS(i) - c(i) * x(i+2,j);
    end
end
x(1,:) = bndx1(1,:);
x(N1+1,:) = bndx1(2,:);
end


function x = C20tridiagsolve2(A,theta,...
r,mu2,alpha1,alpha2,X1min,X1max,X2min,X2max,bndx1,bndx2,dt)
N1 = size(A,1)-1; N2 = size(A,2)-1; x = zeros(size(A));
dx1 = (X1max-X1min)/N1; dx2 = (X2max-X2min)/N2;
x1 = X1min:dx1:X1max; x2 = X2min:dx2:X2max;
for i = 2:N1
    RHS = A(i,2:N2);
    %Construct LHS
    a = -theta*(0.5*dt)*(mu2+alpha1*x2(2:N2)/dx2+alpha2*x1(i)/dx2);
    b = 1-theta*(-dt)*(mu2+0.5*r)*ones(N2-1,1);
    c = -theta*(0.5*dt)*(mu2-alpha1*x2(2:N2)/dx2-alpha2*x1(i)/dx2);
    RHS(1) = RHS(1) - a(1)*bndx2(i,1);
    RHS(N2-1) = RHS(N2-1) - c(N2-1)*bndx2(i,2);
    n = length(RHS);
    c(1) = c(1) / b(1);
    RHS(1) = RHS(1) / b(1);
    for j = 2:n-1
        tmp = b(j) - a(j) * c(j-1);
        c(j) = c(j) / tmp;
        RHS(j) = (RHS(j) - a(j) * RHS(j-1))/tmp;
    end
    RHS(n) = (RHS(n) - a(n) * RHS(n-1))/( b(n) - a(n) * c(n-1));
    x(i,n+1) = RHS(n);
    for j = n-1:-1:1
        x(i,j+1) = RHS(j) - c(j) * x(i,j+2);
    end
end
x(1,:) = bndx1(1,:);
```

```
x(N1+1,:) = bndx1(2,:);
x(:,1) = bndx2(:,1);
x(:,N2+1) = bndx2(:,2);
end
```

B.4 Brennan-Schwartz for CAR(1)

```
function U = AmCAR1(theta,r,sigma,alpha1,X1min,X1max,N1,dt,T,K)
Season = 1;
dx1 = (X1max-X1min)/N1; x1 = X1min:dx1:X1max;
%Initial value
U = max(0, K-((Season==1)*CarmaSeason(T)+x1))';
U0 = U;
Umat = zeros(N1+1,Nt+1); Umat(:,Nt+1) = U;
LSmat = zeros(N1+1,Nt+1); LSmat(:,Nt+1) = U;
mu1 = (sigma/dx1)^2;
%Boundaries
lsm = zeros(size(u));
warning 'off'
for i = 1:N1+1
    lsm(i) = LSCARMApq(1,0,[1]',[alpha1]',sigma,...
[x1(i)]',K,r,T,10,100,{@(x)ones(length(x),1), @(x)x, @(x)x.^2},Season);
end
bndx1 = [lsm(1);lsm(N1+1)];
%Tridiagonal matrix in x1 direction
A1 = 0.5*(mu1+alpha1*x1(2:N1)/dx1); A1 = [A1';0;0];
B1 = -(mu1+r)*ones(N1+1,1);
C1 =  0.5*(mu1-alpha1*x1(2:N1)/dx1); C1 = [0;0;C1'];
D1 = spdiags([A1 B1 C1],[-1 0 1],N1+1,N1+1);
for n = 1:Nt
    AU = dt*D1*U;
    Y0 = U+AU;
    tmp1 = Y0-theta*AU;
    [U Ex] = Amtridiagsolve1(tmp1,theta,r,mu1,alpha1,X1min,X1max,bndx1,dt,U0);
    Umat(:,Nt+1-n) = U;
end
end
```

```
function x = Amtridiagsolve1(A,theta,r,mu1,alpha1,X1min,X1max,bndx1,dt,f)
N1 = size(A,1)-1; x = zeros(size(A));
dx1 = (X1max-X1min)/N1; x1 = X1min:dx1:X1max;
RHS = A(2:N1);
%Construct LHS
a = -theta*0.5*dt*(mu1+alpha1*x1(2:N1)/dx1);
b = 1-theta*(-dt)*(mu1+r)*ones(N1-1,1);
c = -theta*0.5*dt*(mu1-alpha1*x1(2:N1)/dx1);
```

```
RHS(1) = RHS(1) - a(1)*bndx1(1,1);
RHS(N1-1) = RHS(N1-1) - c(N1-1)*bndx1(2,1);
n = length(RHS);
c(1) = c(1) / b(1);
RHS(1) = RHS(1) / b(1);
 for i = 2:n-1
    tmp = b(i) - a(i) * c(i-1);
    c(i) = c(i) / tmp;
    RHS(i) = (RHS(i) - a(i) * RHS(i-1))/tmp;
end
RHS(n) = (RHS(n) - a(n) * RHS(n-1))/( b(n) - a(n) * c(n-1));
x(n+1) = max(RHS(n),f(n+1));
for i = n-1:-1:1
    x(i+1) = max(RHS(i) - c(i) * x(i+2),f(i+1));
end
x(1) = bndx1(1,1);
x(N1+1) = bndx1(2,1);
end
```

B.5 Composite Simpson's Rule

```
function I = Simp(f,a,b,n)
h = (b-a)/n;
S = 0;
for i = 1:2:n-1;
    S = S+4*f(a+i*h);
end
for i = 2:2:n-2
      S = S+2*f(a+i*h);
end
I = h/3*(f(a)+S+f(b));
end
```

B.6 CARMA Functions

```
function Lambda = CarmaSeason(t)
Lambda = 6.3750+0.0001*t+10.4411*cos(2*pi*(t+165.7591)/365);
```

```
function C = CarmaEuCall(p,q,alpha,b,sigma,r,tvec,T,x,K,Season)
n = length(tvec);C = zeros(1,n);
for i = 1:n
    t = tvec(i);
    A = full(spdiags([0;ones(p-1,1)],1,p,p));
    A(p,:) = -alpha;
```

```
    ep = zeros(p,1); ep(p,1) = 1;
    Lambda = (Season == 1)*CarmaSeason(T);
    m = Lambda+b'*expm(A*(T-t))*x;
    Sigma = sqrt(Simp(@(u) (b'*expm(A*(T-u))*ep*sigma)^2,t,T,10));
    d = (m-K)/Sigma; Psi = d*normcdf(d)+normpdf(d);
    C(i) = exp(-r*(T-t))*Sigma*Psi;
end
end
```

```
function Y = SimCARMA(p,alpha,b,sigma,x,T,n,m)
dt = T/n;
X = zeros(m,n+1,p);
Y = zeros(m,n+1);
for i = 1:m
    X(i,1,:) = x;
    Y(i,1) = b'*x;
end
A = spdiags([0;ones(p-1,1)],1,p,p);A(p,:) = -alpha;
ep = zeros(p,1); ep(p,1) = 1;
Sigma = sigma*sqrt(Simp(@(u) (expm(A*u)*ep*ep'*expm(A'*u)),0,dt,10));
Sigma = diag(Sigma);
for i = 1:m
    for j = 1:n
      Xn = shiftdim(X(i,j,:));
      X(i,j+1,:)= expm(A*dt)*Xn+Sigma.*randn(p,1);
      Y(i,j+1) = b'*shiftdim(X(i,j+1,:));
    end
end
end
```